10-6-1995

Geochemistry of the Boring Lava along the West Side of the Tualatin Mountains and of Sediments from Drill Holes in the Portland and Tualatin Basins, Portland, Oregon

Michelle Lynn Barnes
Portland State University

THESIS APPROVAL

The abstract and thesis of Michelle Lynn Barnes for the Master of Science in Geology were presented October 6, 1995, and accepted by the thesis committee and the department.

COMMITTEE APPROVALS: [redacted]

Marvin H. Beeson, Chair

[redacted]

Richard E. Thoms

[redacted]

Ansel G. Johnson

[redacted]

Trevor D. Smith
Representative of the Office of Graduate Studies

DEPARTMENT APPROVAL: [redacted]

Marvin H. Beeson, Chair
Department of Geology

* *

ACCEPTED FOR PORTLAND STATE UNIVERSITY BY THE LIBRARY

by [redacted] on 27 December 1995

ABSTRACT

An abstract of the thesis of Michelle Lynn Barnes for the Master of Science in Geology presented October 6, 1995.

Title: Geochemistry of the Boring Lava along the West Side of the Tualatin Mountains and of Sediments from Drill Holes in the Portland and Tualatin Basins, Portland, Oregon.

Instrumental Neutron Activation Analysis (INAA) was used to identify geochemical groups in Boring Lava along the west side of the Tualatin Mountains, and in sediments of the Portland and Tualatin basins. Samples of Boring Lava were obtained from TriMet drill core collected during planning of the tunnel alignment for the Westside Light Rail line. Additional samples of Boring Lava were collected from outcrops along the west side of the Tualatin Mountains. Samples of sediment from the Tualatin and Portland basins were obtained from drill core collected during an Oregon Department of Geology and Mineral Industries (DOGAMI) Earthquake Hazards Mapping project.

INAA of Boring Lava samples resulted in the identification of three geochemical groups. Additional data sets, including x-ray fluorescence geochemistry, magnetic polarity, and age dates, allowed for the distinction of three Boring Lava units. The Boring Lava of Barnes Road is a young, normal unit, the Boring Lava of Sylvan Hill is an older normal unit, and the Boring Lava of Cornell Mountain is the oldest, reversed unit. The surface distribution, identified using topography and outcrop geochemistry, is consistent with the subsurface distribution, identified using boring logs and core geochemistry. Volcanic vent locations are proposed at topographic highs within the identified surface distribution of the Boring Lava of Barnes Road.

INAA of sediment samples resulted in the identification of seven groups: (1) Columbia River source sediments, (2) lower Troutdale Formation, (3) Reed Island ashes, (4) young Columbia River sediments, (5) high-alumina basalt sediments, (6) episodic Cascadian volcanic sediments, and (7) Columbia River Basalt Group (CRBG) sediments. Only the CRBG sediments group was identified in the Tualatin basin, while all seven groups were identified in the Portland basin. This appears to demonstrate that the sediment packages in the two basins are different.

Finally, each sediment group can be placed into one of three broad geochemical categories: Columbia River source sediments and lower Troutdale Formation represent a Columbia River or continental source; Reed Island ashes, young Columbia River sediments, high-alumina basalt sediments, and episodic Cascadian volcanic sediments represent a Cascadian or local source; and CRBG sediments represent residual soils or sediments overlying Columbia River basalt flows.

GEOCHEMISTRY OF THE BORING LAVA
ALONG THE WEST SIDE OF THE TUALATIN MOUNTAINS
AND OF
SEDIMENTS FROM DRILL HOLES
IN THE PORTLAND AND TUALATIN BASINS,
PORTLAND, OREGON

by

MICHELLE LYNN BARNES

A thesis submitted in partial fulfillment of the
requirements for the degree of

MASTER OF SCIENCE
in
GEOLOGY

Portland State University
1995

ACKNOWLEDGEMENTS

First, I'd like to thank my parents. As I was growing up, they were forever reminding me that I could choose to be whatever I wanted, and that I could accomplish anything. They have supported, wholeheartedly, my endeavors as a geologist since high school.

Second, I'd like to thank everyone who took part in this project: Dr. Marv Beeson, my advisor; Brian Peterson and Steve Hay, excellent rock crushers; Dody Orendurff and Sheryl Zinsle, eager-to-learn undergraduate students; Guy Weisenbach, the CAD-guy; and Sara Havnar, word processing genius. I'd also like to thank TriMet, the Oregon Department of Transportation, and the Oregon Department of Geology and Mineral Industries (DOGAMI) for supplying core and chip samples for analysis, and DOGAMI for supporting my research during the summer of 1993. In addition, a big THANKS goes to the Reed College Nuclear Reactor Staff for their prompt attention to my requests.

Finally, I'd like to give an extra special thank you to my husband-to-be, Brian Peterson. He has been unbelievably helpful and patient during the final "hours" of this project.

TABLE OF CONTENTS

PAGE

LIST OF TABLES vi

LIST OF FIGURES vii

INTRODUCTION 1

PREVIOUS WORK 4

LOCAL GEOGRAPHY 6

Tualatin Mountains 6

Portland and Tualatin Basins 9

LOCAL STRATIGRAPHY 11

METHOD OF INVESTIGATION 16

Introduction 16

Choice of Method 16

General Theory of Activation Analysis 17

Sample Location 18

Sample Description 27

Irradiation 93D
Irradiation 93E
Irradiation 93G
Irradiation 94A

Sample Preparation 29

Analysis Procedure 30

DATA AND RESULTS 33

BORING LAVA INTERPRETATION 37

Introduction 37

Age Dates 37

Magnetic Polarity 38

XRF Geochemistry 38

INAA Geochemistry 39

Statistical Analysis 50

Discussion 51

SEDIMENT GEOCHEMISTRY AND INTERPRETATION 55

Introduction 55

Shallow Sediment and Miscellaneous Samples....... 55

High-Alumina Basalt Sediments
CRBG Sediments
Reed Island Ashes
Young Columbia River Sediments
Columbia River Source Sediments

Portland International Airport Drill Hole 77

Young Columbia River Sediments
Episodic Cascadian Volcanic Sediments
Lower Troutdale Formation

Hillsboro Airport Drill Hole 85

Statistical Analysis 96

Discussion 99

CONCLUSIONS 107

FUTURE WORK 110

REFERENCES 112

APPENDICES

A Geochemical Data for the Boring Lava 116

B Geochemical Data for the Shallow Sediment and Miscellaneous Samples 127

C Geochemical Data for the Hillsboro Airport Drill Hole (HBD1) 138

D Geochemical Data for the Portland International Airport Drill Hole (MTD1) 145

E Geochemical Data for Standards Used in Irradiations 93D, 93E, 93G, and 94A 151

F Statistical Analysis Tables 154

LIST OF TABLES

TABLE		PAGE
I	Comparison of five key stratigraphic interpretation	12
II	Age dates and sample numbers for the Boring Lava	35
III	Magnetic polarity and sample numbers for the Boring Lava	35
IV	X-ray fluorescence data for selected Boring Lava samples	36
V	Approximate ages of the five samples that have age dates	38
VI	Magnetic polarity and selected INAA data for the four samples along the tunnel alignment which have age dates	45
VII	Comparison of the depth of occurrence of volcanic or hyaloclastite materials in wells examined by Hoffstetter (1984) and Swanson (1986) near MTD1	102

LIST OF FIGURES

FIGURE		PAGE
1	Geography of the Portland, Oregon area	7
2	Approximate location of the tunnel alignment through the Tualatin Mountains ...	8
3	TriMet drill core sample locations	20
4	Locations of DOGAMI drill holes sampled for this project	22
5	Location of outcrop samples and two chip/core samples collected along the west side of the Tualatin Mountains	23
6	Approximate location of Boring Lava samples collected by Dr. Marvin H. Beeson	24
7	Approximate location of the David Hill Well	25
8	Approximate location of the samples collected from Reed Island	26
9	Boring Lava Scatter Plot Scandium vs. Cerium	40
10	Boring Lava Scatter Plot Iron vs. Chromium	41
11	Boring Lava Scatter Plot Lanthanum vs. Scandium	42
12	Surface distribution of Boring Lava (road map)	46
13	Surface distribution of Boring Lava (topographic map)	47
14	Distribution of Boring Lava along the west end of Line Section 5A of the TriMet tunnel alignment	48

FIGURE PAGE

15 Shallow Sediments Scatter Plot
Iron vs. Hafnium 57

16 Shallow Sediments Scatter Plot
Hafnium vs. Thorium 58

17 Shallow Sediments Scatter Plot Closeup
Hafnium vs. Thorium 59

18 Shallow Sediments Scatter Plot
Cobalt vs. Hafnium 60

19 Shallow Sediments Scatter Plot
Lanthanum/Samarium vs. Iron 61

20 Shallow Sediments Scatter Plot
Lanthanum/Samarium vs. Hafnium 62

21 Shallow Sediments Chondrite Plot
High-Alumina Basalt Sediments 65

22 Shallow Sediments Chondrite Plot
Samples from TriMet drill hole B563 67

23 Shallow Sediments Chondrite Plot
Samples from TriMet drill hole B565 68

24 Shallow Sediments Chondrite Plot
Reed Island Ashes and BVD4-91.4 Sample 70

25 Shallow Sediments Chondrite Plot
Young Columbia River Sediments 72

26 Shallow Sediments Chondrite Plot
Columbia River Source Sediments 75

27 Shallow Sediments Chondrite Plot
Columbia River Source Sediments 76

28 Portland International Airport Drill Hole
Sediments Scatter Plot
Hafnium vs. Chromium 79

29 Portland International Airport Drill Hole
Sediments Scatter Plot
Hafnium vs. Thorium 80

FIGURE PAGE

30 Portland International Airport Drill Hole Sediments Chondrite Plot Episodic Cascadian Volcanic Sediments 82

31 Portland International Airport Drill Hole Sediments Chondrite Plot Lower Troutdale Formation 83

32 Portland International Airport Drill Hole Sediments Chondrite Plot Lower Troutdale Formation 84

33 Shallow and Portland International Airport Drill Hole Sediments Scatter Plot Cobalt vs. Hafnium 86

34 Shallow and Portland International Airport Drill Hole Sediments Scatter Plot Hafnium vs. Thorium 87

35 Shallow and Portland International Airport Drill Hole Sediments Scatter Plot Lanthanum/Samarium vs. Hafnium 88

36 Hillsboro Airport Drill Hole Sediments Scatter Plot Lanthanum/Samarium vs. Iron 90

37 Hillsboro Airport Drill Hole Sediments Scatter Plot Cobalt vs. Hafnium 91

38 Hillsboro Airport Drill Hole Sediments Chondrite Plot CRBG Sediments and the ash layer @ 760′ 92

39 Shallow, Portland, and Hillsboro Drill Hole Sediments Scatter Plot Lanthanum/Samarium vs. Iron 93

40 Shallow, Portland, and Hillsboro Drill Hole Sediments Scatter Plot Hafnium vs. Thorium 94

41 Shallow, Portland, and Hillsboro Drill Hole Sediments Scatter Plot Iron vs. Hafnium 95

INTRODUCTION

The Quaternary and late Tertiary geologic history of the Portland, Oregon area is rich with complexity. It involves many processes, including (1) eruption of a local volcanic unit, the Boring Lava, (2) the deposition and erosion of sedimentary units including the Troutdale Formation, Sandy River Mudstone, Portland Hills Silt (glacial loess), and catastrophic flood sediments, and (3) structural deformation resulting from regional stress regimes (Beeson and others, 1989; Yeats and others, 1991), the locally identified Portland Hills structural zone (Balsillie and Benson, 1971; Beeson and others, 1989), and related, local, parallel structural zones (Yelin and Patton, 1991; Madin and others, 1993).

This mix of constructive and destructive geologic processes has produced a complex stratigraphy to study. Though much work has been completed by many geologists on a range of scales (i.e. Treasher, 1942; Trimble, 1963; Hart and Newcomb, 1965; Schlicker and Deacon, 1967; Allen, 1975; Beeson and others, 1989; Madin, 1990; Squier Associates, 1992; Blakely and others, 1995), there still remain many unanswered questions concerning (1) the origin of the Boring Lava, (2) the effect of the presence/absence of the incipient Tualatin Mountains on deposition of the Columbia River Basalt Group (CRBG) and sediments, (3) the distribution of catastrophic flood materials, and (4) the stratigraphy of the Portland and Tualatin basins.

This study focuses on the geochemistry of post-CRBG volcanic and sedimentary rocks, specifically the Boring Lava, Sandy River Mudstone, Troutdale Formation, Portland Hills Silt, and Missoula Floods deposits. Geochemical analyses of the Troutdale Formation and Sandy River Mudstone in the Portland basin (Swanson, 1986) have been completed as part of a previous study by a Portland State University graduate student. Aside from this thesis, however, few geochemical data exist for the above mentioned units. Geochemical data, when used in combination with other data sets (magnetic polarity, x-ray fluorescence, field/core/hand samples, and age dates) allow realistic hypotheses to be suggested for problems relating to stratigraphy, structure, age, and provenance.

The information presented in this study is two-fold. The first portion of the study addresses the geochemistry of the Boring Lava along the west side of the Tualatin Mountains. The second portion addresses the geochemistry of Portland and Tualatin basin sediments, as represented in drill holes located in the two basins and along the tunnel alignment in the Tualatin Mountains. Although the same method was used to obtain data for both parts of the study, each is discussed separately. Conclusions for both sections are presented at the end of the study.

PREVIOUS WORK

The first detailed mapping of the Portland, Oregon area was done by Treasher (1942). He is credited with naming the Boring Lava for its occurrence near the town of Boring, Oregon. Following Treasher, Trimble (1963) published a detailed map and geologic report that is still used as a reference today. In it he defines a detailed stratigraphic column for the Tualatin Mountains and the Portland basin.

During the next 30 years, reports were published on the stratigraphy, groundwater, and engineering geology of both the Tualatin and Portland basins (i.e. Schlicker and others, 1964; Hart and Newcomb, 1965; Hogenson and Foxworthy, 1965; Schlicker and Deacon, 1967; Frank and Collins, 1978; Yeats and others, 1991). Typically, geologists examined either one basin or the other in their reports, not both.

In the 1970's, geologists began to recognize important structural features, particularly the Portland Hills-Clackamas River structural zone and its association with the Tualatin Mountains (Balsillie and Benson, 1971; Allen, 1975; Beeson and others, 1975). In the 1980's, the stratigraphy of the CRBG was presented by Hooper (1982), and a series of papers was published examining that stratigraphy and its relationship to the evolution of the Portland basin, the location of ancestral Columbia River channels, and the deposition of the Sandy River Mudstone and the Troutdale Formation (Tolan and Beeson, 1984; Beeson and others, 1985; Beeson and others, 1989).

In 1990, Madin revisited Trimble's (1963) map area to assess potential earthquake hazard areas. Small revisions were made in the geology in some locations and the stratigraphic column was simplified. Some of the most recently published work includes a geologic map of the Portland Quadrangle by Beeson and others (1991), the Westside Light Rail Tunnel Project Technical Report completed by Squier Associates (1992), and an aeromagnetic survey map by Blakely and others (1995).

LOCAL GEOGRAPHY

TUALATIN MOUNTAINS

The Tualatin Mountains, commonly known as the Portland Hills or the West Hills, are aligned with the Portland Hills-Clackamas River fault zone, a northwest-trending structure identified by Beeson and others (1989) as the western boundary of a pull-apart basin. Tolan and Reidel (1989) and Yelin and Patton (1991) identify an eastern boundary to this pull apart basin; Tolan and Reidel (1989) called it the Lacamas Lake-Sandy River fault zone while Yelin and Patton (1991) called it the Frontal Fault zone. As Tolan and Reidel (1989) first identified it, the name they chose will be used herein. Portland is located within this pull-apart basin (Figure 1).

The Tualatin Mountains were a critical area of study for the current project of extending the light rail system to the west side of the Portland area. The new light rail line has been designed to pass through the Tualatin Mountains via a tunnel (Figure 2). Large amounts of drill core and new geologic information were produced during the studies conducted to choose a tunnel alignment.

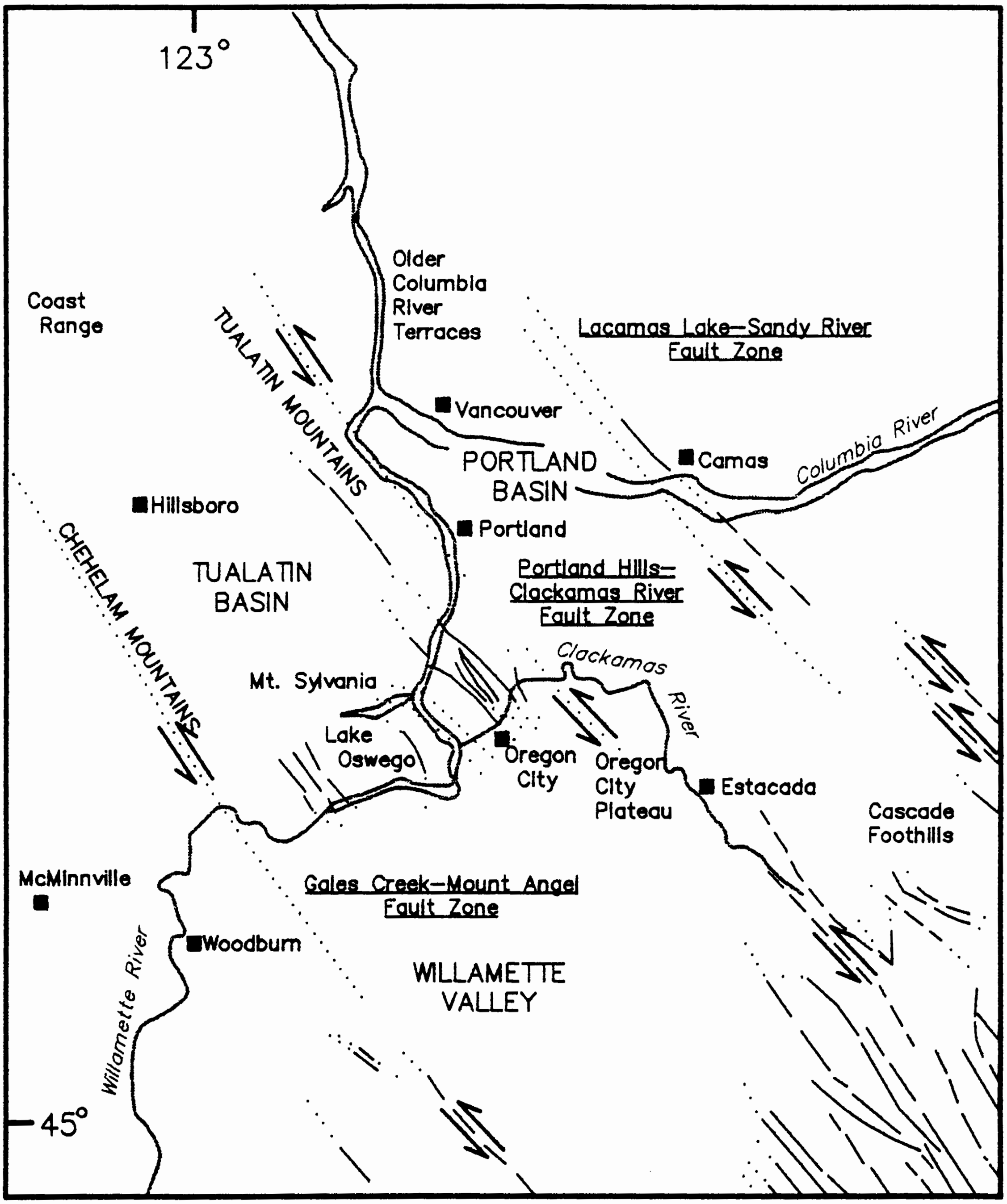

Figure 1. Geography of the Portland, Oregon area. Modified from Tolan and Reidel (1989).

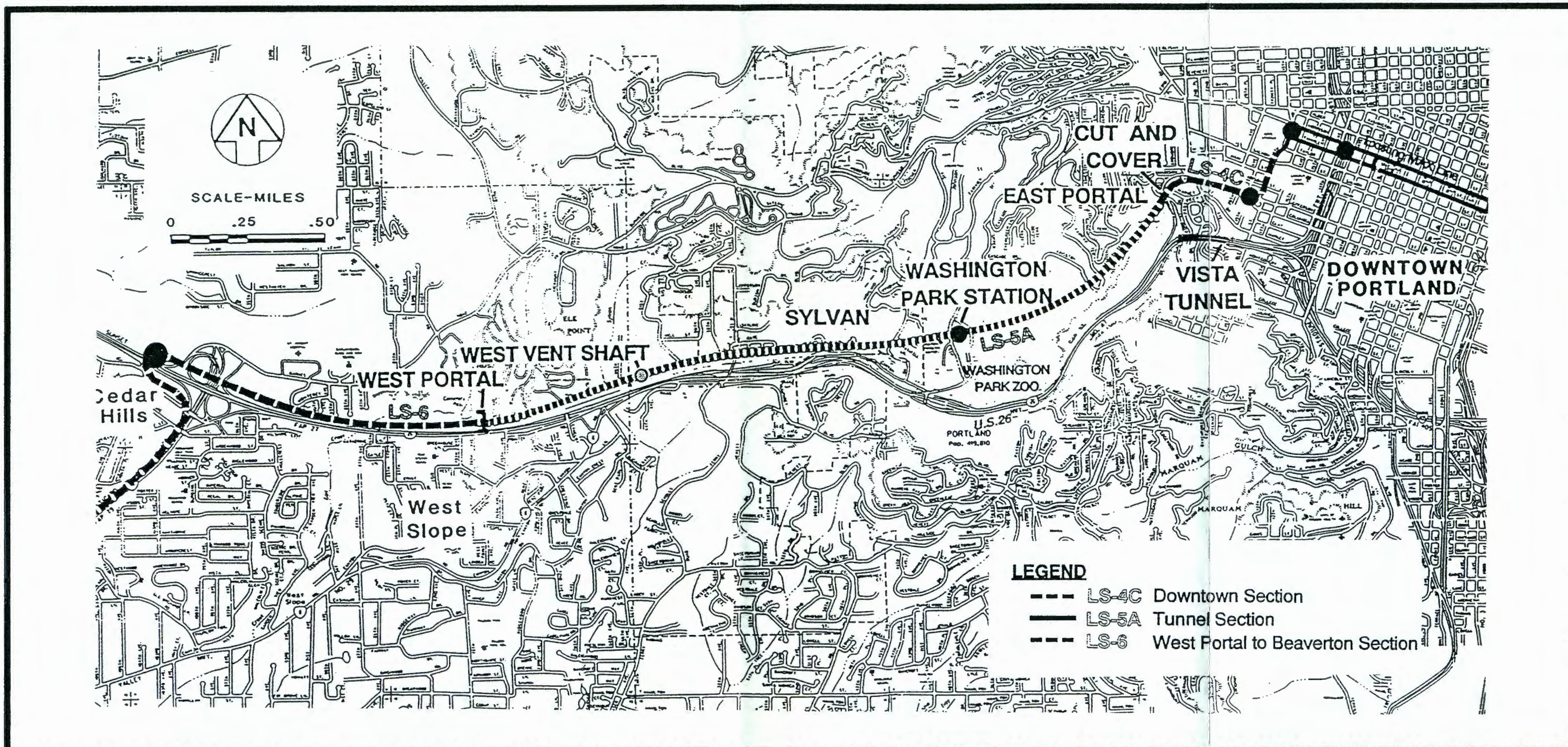

Figure 2. Approximate location of the tunnel alignment through the Tualatin Mountains. The west portion of Line section 5A, from Sylvan to the West Portal, was examined for this study.

PORTLAND AND TUALATIN BASINS

The Tualatin Mountains separate the Portland pull apart basin, or the Portland basin, on the east, from the Tualatin basin on the west (Figure 1). The Portland basin is that area between the Tualatin Mountains and Portland Hills-Clackamas River fault zone on the west, the Oregon City plateau on the south, the foothills of the Cascades on the south and southeast, the Lacamas Lake-Sandy River fault zone on the east and northeast, and old Columbia River terraces on the north. The Tualatin basin is that area between the Chehalem Mountains on the west, Mt. Sylvania and Lake Oswego on the south, the Tualatin Mountains on the east and northeast, and the Coast Range on the north and northwest.

Each basin contains a thick sequence of sediments overlying the CRBG. Prior to the development of the Portland Hills, the two basins may have received similar depositional materials. The rise of the Portland Hills likely altered the distribution of materials into each basin, which should have resulted in unique stratigraphic sequences for each basin.

The Oregon Department of Geology and Mineral Industries (DOGAMI) has undertaken a study in the Portland area, to identify geographic areas overlying sediments that could potentially liquefy during an earthquake. To accomplish this, DOGAMI has completed numerous drill holes in both the Portland and Tualatin basins, to identify and log the sediments. The study will result in the publication of new earthquake hazard maps for the Portland area. Maps for the Portland, Lake Oswego, Gladstone, and Beaverton 7.5 minute Quadrangles are currently available.

LOCAL STRATIGRAPHY

The primary focus of this study is the geochemistry of post-CRBG units in the Portland area. As such, the interpretations presented in this study will be primarily based on the geochemical data. However, previous interpretations of the stratigraphy have not used geochemistry as a basis for describing stratigraphic units. Consequently, several interpretations, proposed by previous authors, must be considered. The following is a review of five key interpretations as presented by Hart and Newcomb (1965), Schlicker and Deacon (1967), Trimble (1963), Madin (1990), Tolan and Beeson (1993).

Table I shows a comparison of five interpretations of Portland area stratigraphy. The two left-hand columns are interpretations of Tualatin basin stratigraphy and the three right-hand columns are interpretations of Portland basin stratigraphy.

Each of the previous authors have recorded similar interpretations of the stratigraphy. In fact, from the CRBG through the Boring Lava, the only differences among the five columns are the presence of the Sandy River Mudstone and the Rhododendron Formation in the Portland basin stratigraphic columns (Trimble, 1963; Tolan and

Table I. A comparison of five stratigraphic interpretations (from left to right: Hart & Newcomb, 1965; Schlicker & Deacon, 1967; Trimble, 1963; Madin, 1990; Tolan & Beeson, 1993). Columns modified after above authors; not to scale.

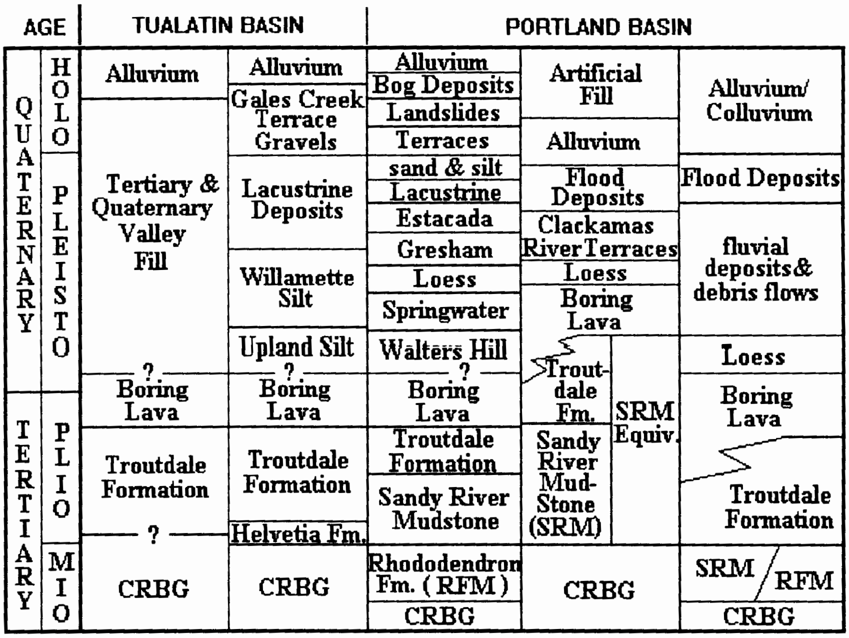

Beeson, 1993) and the addition of the Helvetia Formation in the Tualatin basin stratigraphic column (Schlicker and Deacon, 1967). Madin (1990) identifies a sedimentary unit in the Tualatin basin (SRM equivalent) that he interprets to include the Troutdale Formation, the equivalent to the Sandy River Mudstone of the Portland basin, and the Helvetia Formation of Schlicker and Deacon (1967). Madin (1990) and Tolan and Beeson (1993) identify Troutdale Formation deposits interfingered with Boring Lava.

By far the largest discrepancies occur in the columns during Pleistocene times. Much of this has to do with the interpretation of field evidence that likely represents the remains of catastrophic flood sediments, periodically released from Lake Missoula in western Montana during the last Ice Age. In the Tualatin basin, the Tertiary and Quaternary Valley Fill of Hart and Newcomb (1965), and the Willamette Silt, lacustrine deposits, and terrace gravels of Gales Creek of Schlicker and Deacon (1967) are most probably deposits of the Missoula Floods. In the Portland basin, Trimble (1963) presented a detailed interpretation for the Pleistocene epoch. Madin (1990) examined the Quaternary stratigraphy for both basins and suggested the following simplifications:

Catastrophic flood deposits

Includes the terrace, sand and silt, and lacustrine deposits of Trimble (1963), and the lacustrine deposits and Willamette Silt of Schlicker and Deacon (1967).

Clackamas River terraces

Includes the Estacada Formation of Trimble (1963).

Loess

Includes the upland silt of Schlicker and Deacon (1965).

Troutdale Formation

Includes the Gresham and Walters Hill Formation of Trimble (1963).

Madin (1990) also added artificial fill as a stratigraphic unit due to the nature of his study.

The final interpretation listed (Tolan and Beeson, 1993) generally agrees with that suggested by Madin (1990). The unit identified as fluvial deposits and debris flows by Tolan and Beeson (1993) likely represents materials similar to the Clackamas River terraces of Madin (1990), and would include materials deposited by the Clackamas River, or volcanic materials that flowed down the Clackamas River channel.

The interpretations presented by Madin (1990), and Tolan and Beeson (1993), represent some of the most updated information regarding Portland area stratigraphy. A new interpretation will not be presented as a part of

A new interpretation will not be presented as a part of this study. The units to be defined during this study will be placed into the existing stratigraphic framework. As such, the description of the units mapped in the Portland and Tualatin basins will not change, and are not presented here. For descriptions of each unit, please refer to the appropriate reference as listed in the above table.

METHOD OF INVESTIGATION

INTRODUCTION

The primary method of investigation used for this study was Instrumental Neutron Activation Analysis (INAA). Magnetic polarity of basalt samples was also measured using a fluxgate magnetometer. Additional data sets were available for the Boring Lava samples and include geochemical analyses by x-ray fluorescence (XRF) and age dates obtained using K-Ar dating methods.

CHOICE OF METHOD

Unpublished INAA and XRF data (Beeson, 1993; personal communication) indicated that trace elements could be useful in differentiating Boring Lava units. Sediments made up of differing source materials should have differing trace element concentrations as well (Piper, 1974; McLennan and Taylor, 1980; Bhatia and Taylor, 1981; Kadri and others, 1983). Thus, INAA was chosen as the primary method of investigation because of its ability to detect a wide range of trace elements, and its availability at Portland State University.

GENERAL THEORY OF ACTIVATION ANALYSIS

Activation analysis is based on the principle that radioactive isotopes of different elements have distinct radioactive decay patterns. Bombarding a sample with neutrons in a nuclear reactor produces unstable isotopes or radioisotopes. As the radioisotopes decay, they emit gamma rays (electromagnetic radiation) of specific energies. These gamma rays can be observed by a high purity Germanium detector. When a gamma ray of a specific energy is observed by the detector, one "count" for the gamma ray of that energy, is recorded by an analyzing unit connected to the detector. Based on the energy of each observed gamma ray, the analyzing unit stores gamma ray "counts" into data files. Each time a gamma ray of a specific energy is detected and recorded, the number of counts for that gamma ray increases by one in that data file. For each sample analyzed, a range of gamma ray energies, in the form of a spectrum of gamma ray energy peaks, is produced by the elements present in that sample. Several standards having known elemental concentrations determined by a variety of independent analytical techniques, are also included in the data set. Comparison of the sample spectra to the standard spectra, allow the elemental concentrations for each sample to be calculated (Muecke, 1980).

SAMPLE LOCATION

A total of 163 samples were analyzed for this study from two main sources:

1. Drill core taken by TriMet for studies conducted to locate a suitable tunnel alignment through the Tualatin Mountains for extension of the light rail line to the Tualatin Valley. The drill hole numbers and depth at which each sample was collected is shown on Figure 3.
2. Drill core taken by DOGAMI in the Portland and Tualatin basins for their Relative Earthquake Hazards Mapping Project. Approximately 20 shallow drill holes (50-300 feet) are located throughout the two basins. One deep drill hole is located near the center of each basin: HBD1 at the Hillsboro Airport in the Tualatin basin (1095 feet), and MTD1 at the Portland International Airport in the Portland basin (1523 feet). Figure 4 shows the approximate locations of the sampled drill holes.

Nineteen samples were obtained from sources other than the two mentioned above. Additional sources include:

3. Ten outcrop samples of the Boring Lava located along the west side of the Tualatin Mountains as shown on Figure 5. Two core/chip samples were also obtained from the same area and are also shown on Figure 5.
4. Three outcrop samples of Boring Lava, collected previously by Dr. Marvin Beeson, from Mt. Sylvania and Cookes Butte as shown on Figure 6.
5. One sample obtained from a commercial bag of bentonite drilling mud.
6. One sample of pre-CRBG sediment collected by Doyle Wilson, from the David Hill well at the western edge of the Tualatin basin. The well is believed to be located in Section 22, Township 1 North, Range 4 West of the Willamette Meridian on the Gales Creek Quadrangle (Figure 7).
7. Two volcanic ash samples collected from Reed Island in the Columbia River east of the Sandy River Delta. Both samples were collected from the south side of the island, in Section 22, Township 1 North, Range 4 East of the Willamette Meridian on the Washougal Quadrangle (Figure 8).

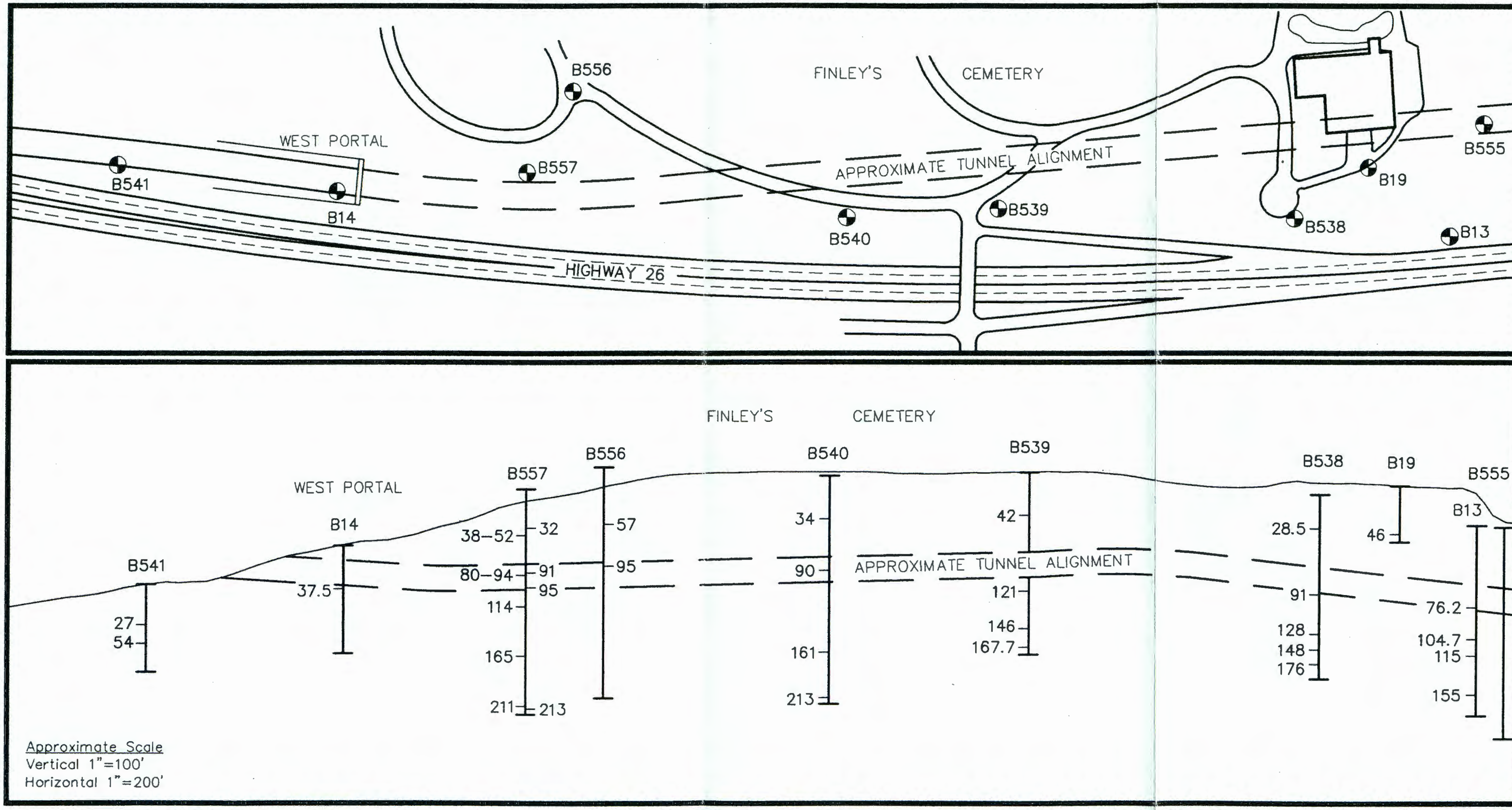

Figure 3. TriMet drill core sample locations. Modified after Squier Associates (1992).

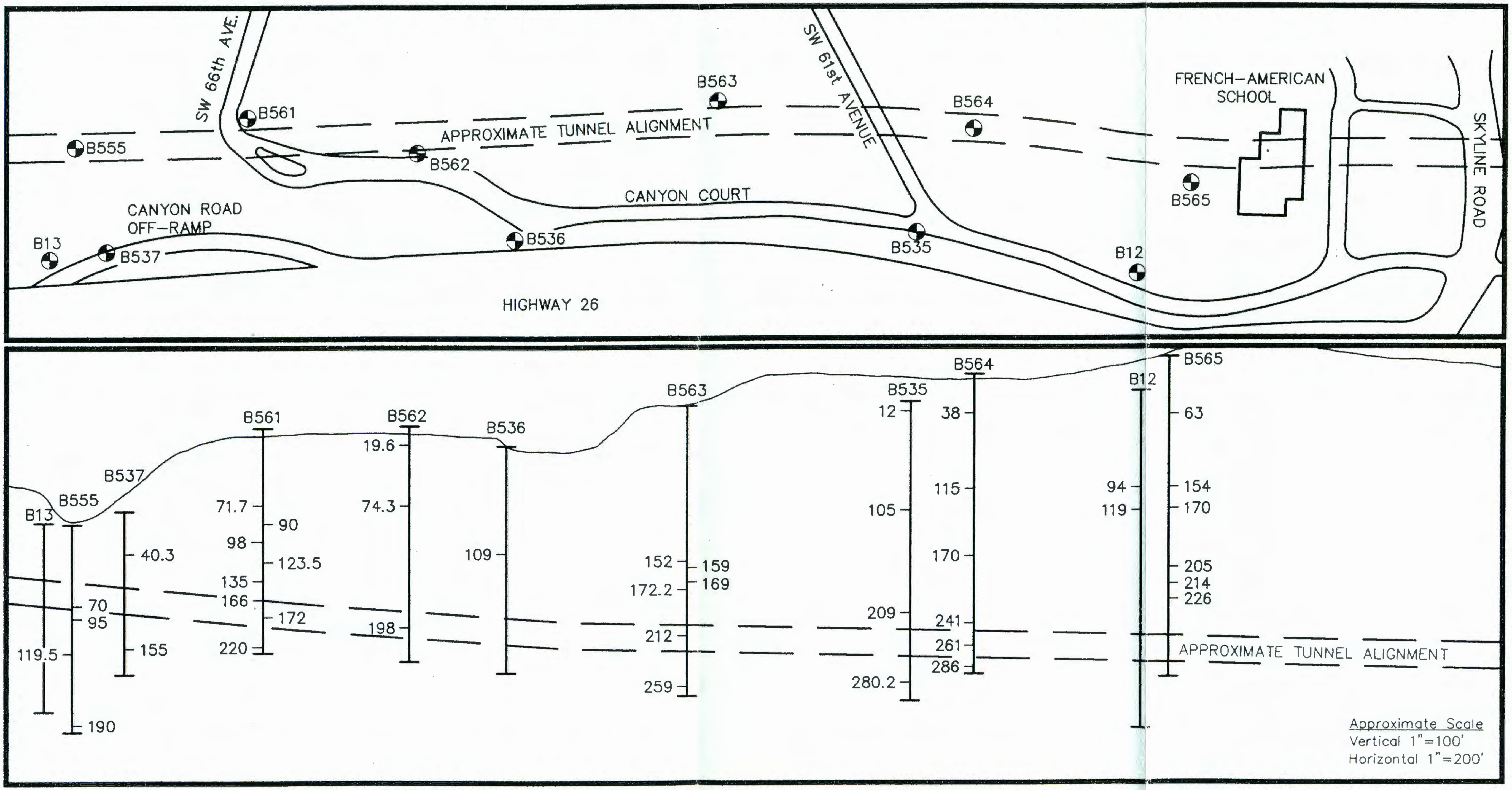

Figure 3 continued.

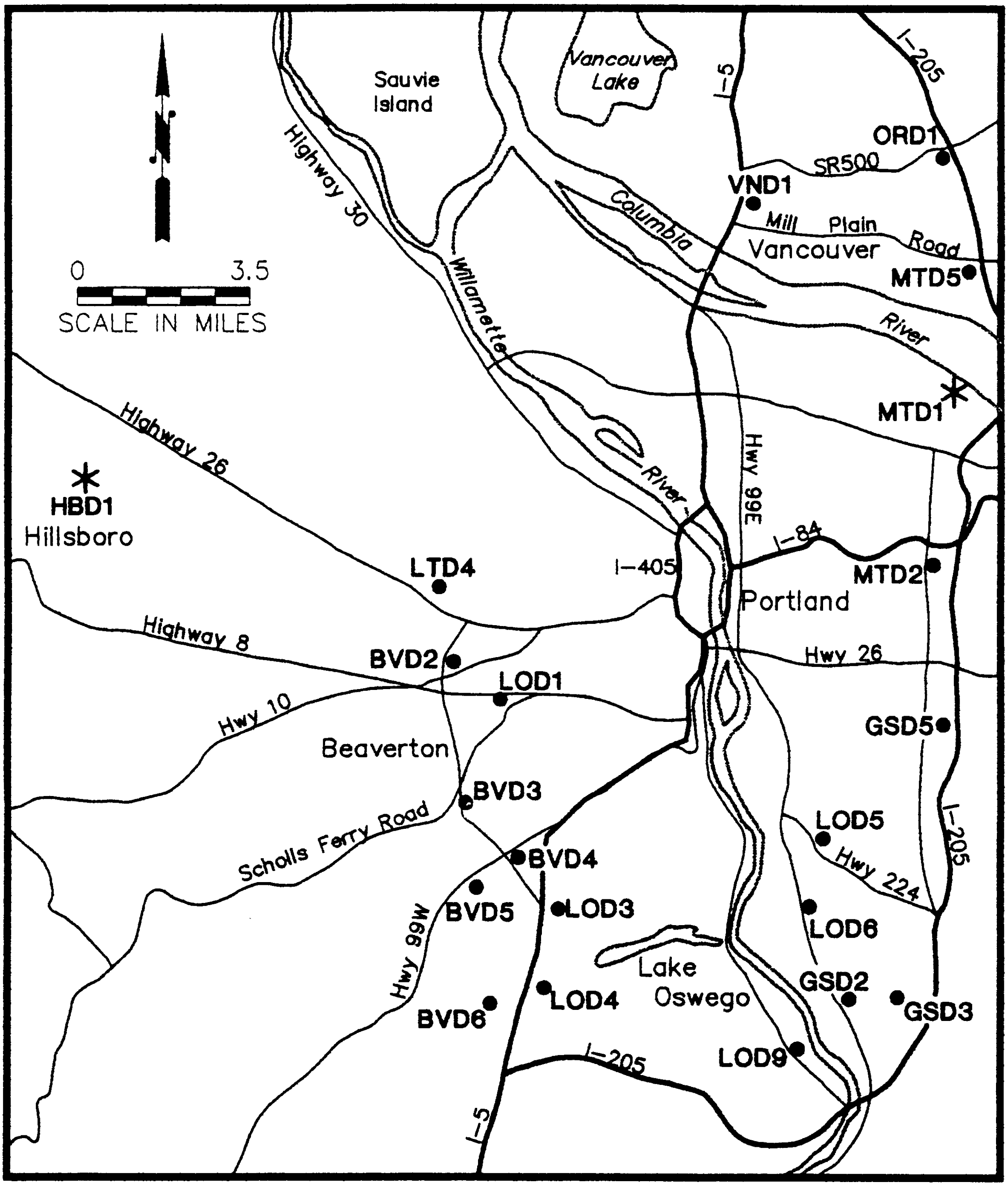

Figure 4. Locations of DOGAMI drill holes sampled for this project. Stars represent the two deep drill hole locations.

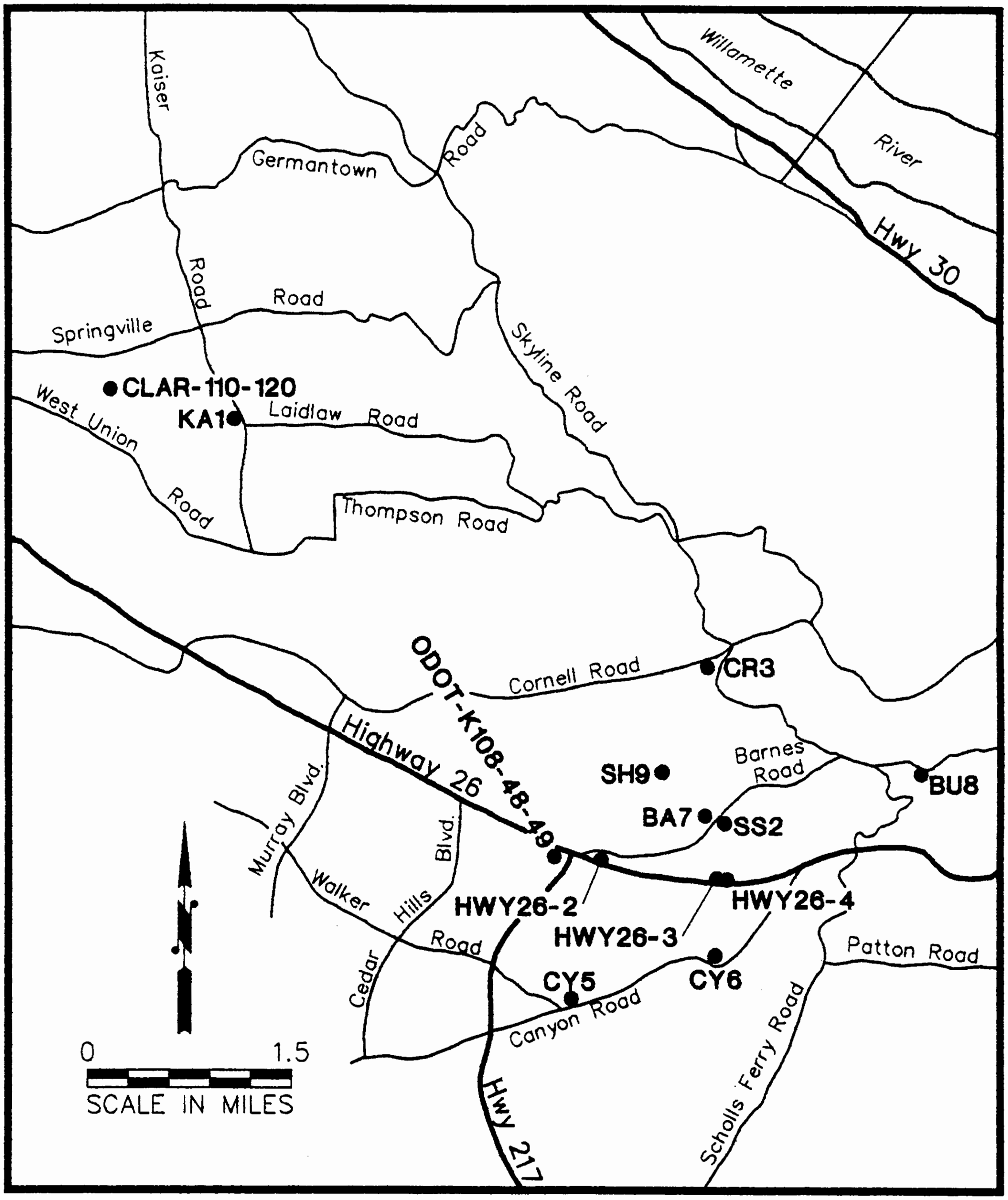

Figure 5. Location of outcrop samples and the two chip/core samples collected along the west side of the Tualatin Mountains.

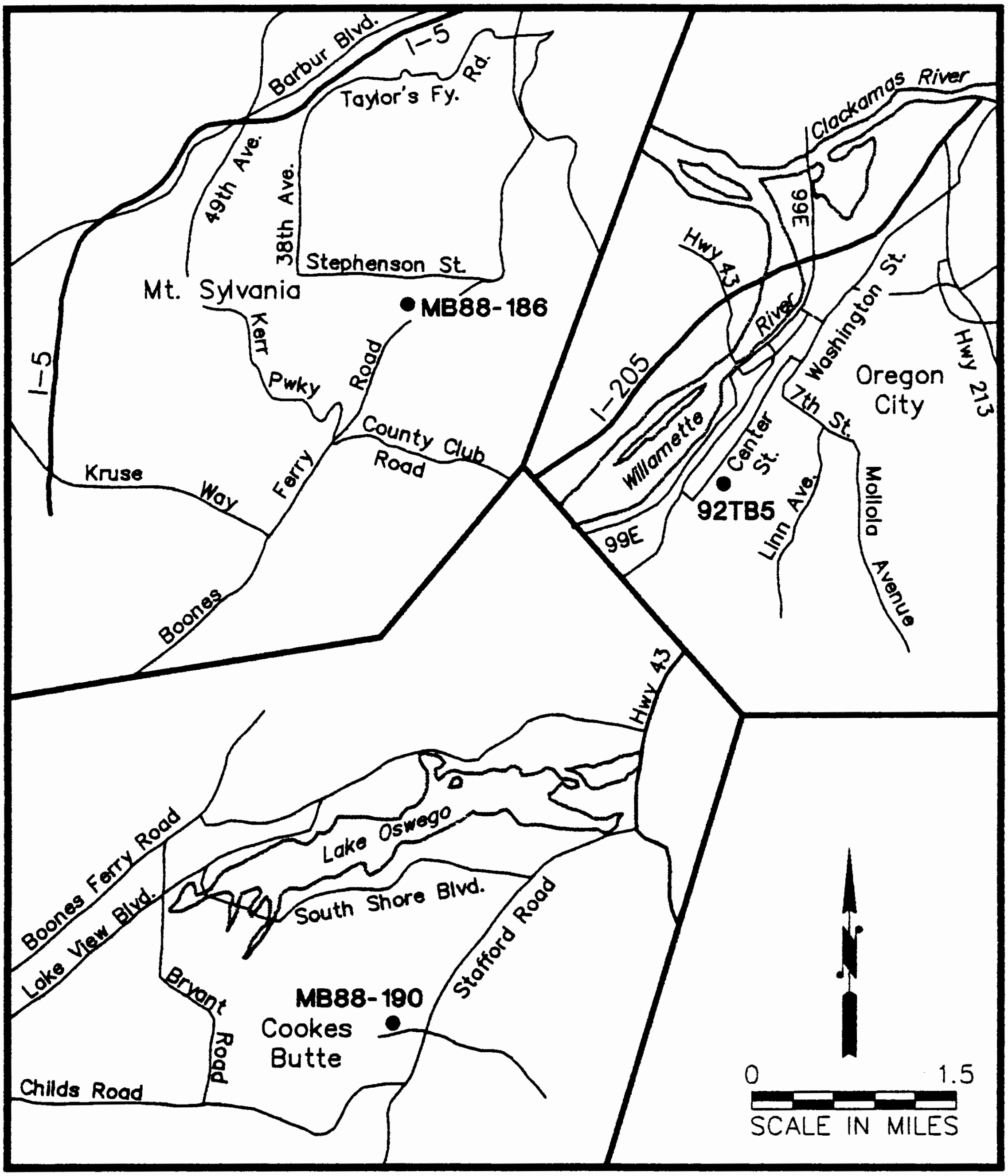

Figure 6. Approximate location of Boring Lava samples collected by Dr. Marvin Beeson.

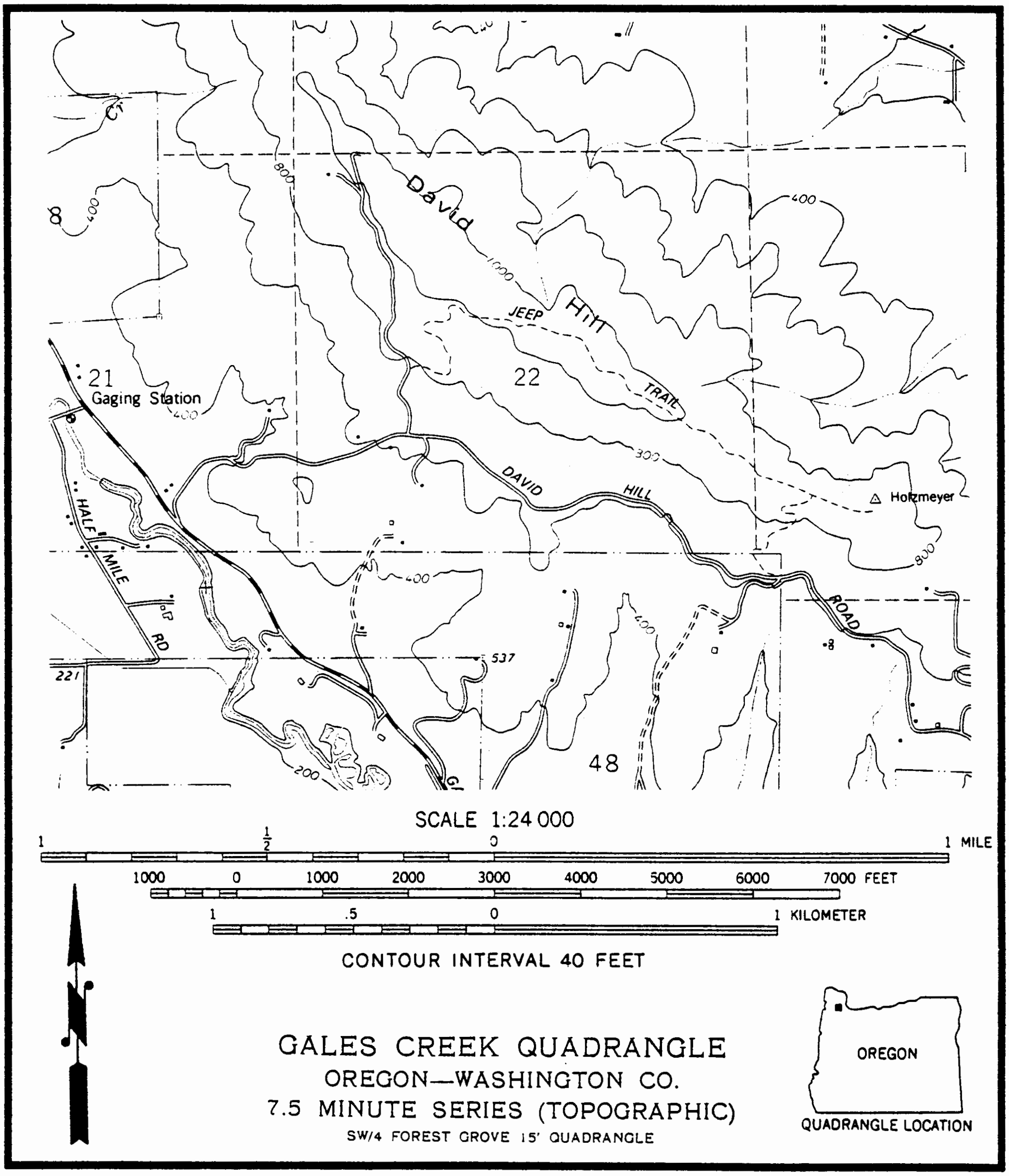

Figure 7. Approximate location of the David Hill Well, near the western edge of the Tualatin basin (Section 22, T1N, R4W).

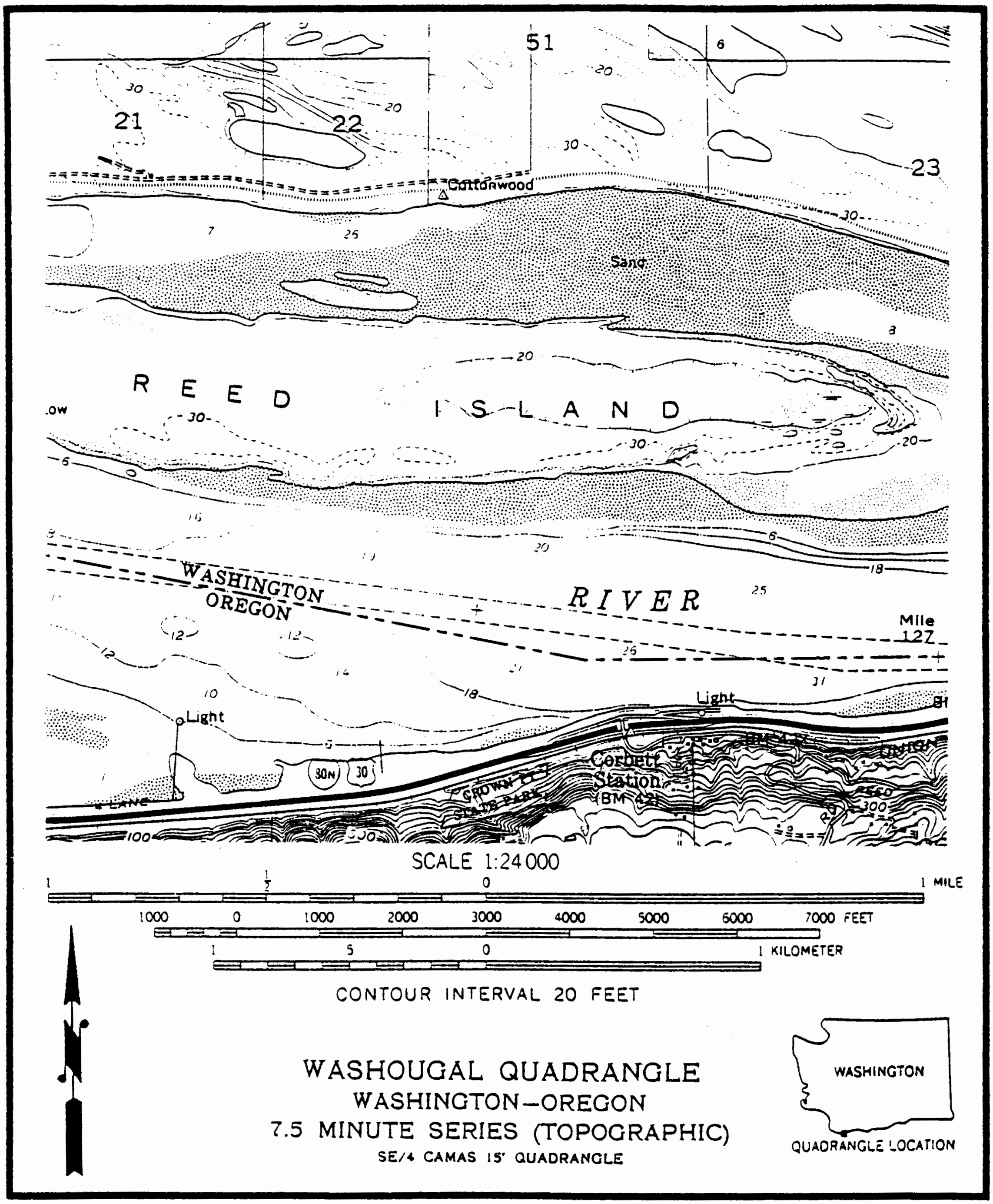

Figure 8. Approximate location of the two volcanic ash samples collected from Reed Island (Section 22, T1N, R4E).

The names assigned to each outcrop sample include a letter/number combination to identify the outcrop location and the total number of outcrop samples collected to date. The names assigned to the core/chip samples include the name of the drill hole followed by the depth from which the sample was taken. As both DOGAMI and TriMet used English units (feet) to indicate depth on the drill hole logs, the samples collected for this study are also labeled by using the depth of the sample in feet.

SAMPLE DESCRIPTION

Four irradiations (93D, 93E, 93G, and 94A) were completed for this study. The standards included with the irradiation are as follows: CFA(1633a), Coal Fly Ash; BCR1, Columbia River basalt (Grande Ronde Basalt); and MAG-1, Marine Mud.

Irradiation 93D

Boring Lava and sediment samples were collected from TriMet drill core by the Spring 1993, Advanced Geochemistry Class at Portland State University for a class project. Thirty-nine samples were analyzed: 21 Boring Lava, 15 sediments, 3 standards (CFA, BCR1, and MAG-1).

Irradiation 93E

Boring Lava samples were collected from TriMet drill core and from outcrops located along the west side of the Tualatin Mountains. Thirty-nine samples were analyzed: 37 Boring Lava, 2 standards (BCR1 and CFA).

Irradiation 93G

Sediment samples were collected from TriMet drill core and from DOGAMI drill hole HBD1 located in the Tualatin basin. Thirty-nine samples were analyzed: 10 TriMet core, 26 HBD1 core, 3 standards (CFA, BCR1, and MAG-1).

Irradiation 94A

Sediment samples were collected from DOGAMI drill core taken from numerous shallow holes in the Portland and Tualatin basins, and from DOGAMI drill hole MTD1 located in the Portland basin. Miscellaneous samples include one sample of bentonite drilling mud, two volcanic ash samples, one pre-CRBG sediment sample, and the three Boring Lava samples previously collected by Dr. Marvin Beeson. Fifty-seven samples were analyzed: 48 sediments, 2 volcanic ash, 1 drilling mud, 3 Boring Lava, 3 standards (CFA, BCR1, and MAG-1).

SAMPLE PREPARATION

All samples and standards were prepared and analyzed in accordance with the Portland State University Radiation Safety Program (PSU, 1987). Three irradiations of 39 samples, and one irradiation of 57 samples were analyzed.

Each Boring Lava sample to be analyzed was prepared using the following procedure: A mechanical rock crusher was used to break the outcrop or core sample into pieces small enough to crush using a mortar and pestle. Clean, unweathered chips from the outcrop samples were powdered by hand using a mortar and pestle of hardened steel. To remove any drilling mud, clean, unweathered chips from core samples were cleaned ultrasonically for one to two minutes, then rinsed with tap water followed by distilled water, and dried prior to powdering with the mortar and pestle.

Each sediment sample to be analyzed was prepared using the following procedure: The sediment samples containing moisture were placed in an oven at approximately 75°C until dry. A mechanical rock crusher was used to break the samples into pieces small enough to crush using a mortar and pestle. Due to their fissility, sediment samples were not ultrasonically cleaned. Once dry, the sediment samples were also powdered by hand using a mortar and pestle of hardened steel. When all of the samples to be analyzed for each irradiation had been powdered, the samples were placed into containers appropriate for the irradiation process. Approximately one gram of each powdered sample was weighed and put into individual 1/2 dram polyvials. The 1/2 dram polyvials were heat sealed to contain all material, and then rinsed in isopropyl alcohol to clean the surface. Once dry, the 1/2 dram polyvials were put, one each, into a 2 dram polyvial for the first three irradiations (93D, 93E, and 93G). For the last irradiation (94A), two 1/2 dram polyvials were placed into the 2 dram polyvial to allow for more samples to be irradiated at one time.

ANALYSIS PROCEDURE

Samples were irradiated at the Reed College Nuclear Reactor for 1 hour at approximately 250 kilowatts. Following irradiation, samples were left at the reactor for five days to allow the highly active, short-lived isotopes (Al-28, Mn-56, and Na-24) to decay to safe levels. On the sixth day, the samples were transported to Portland State University for analysis.

An EG&G Solid State Photon Detector with a high-purity Germanium crystal was used for all analyses. Because different radioisotopes decay at different rates, information can be obtained for different elements by counting irradiated samples at several times after irradiation. The first analysis, or "first counts", for each irradiation was completed 5-7 days after irradiation in the nuclear reactor. Data were obtained for K, Na, As, U, La, and Sm. The second analysis, or "second counts", for each irradiation was completed 18-27 days after irradiation in the nuclear reactor. Data were obtained for Rb, Cs, Sr, Ba, Fe, Sc, Cr, Co, Zr, Hf, Ta, Th, Zn, Ce, Nd, Eu, Tb, Yb, and Lu.

Geochemical data were entered into a computer spreadsheet. Numerous plots were generated in order to interpret the geochemical data and to identify and define geochemical groups. Scatter plots were generated using element concentrations and/or ratios of element concentrations. Chondrite plots were generated using the rare earth element (REE) concentrations normalized to the C1 Chondrite, and the position of the REE on the periodic table. C1 Chondrite values were taken from Ekambarum and others (1984). Both types of graphs aid in identifying geochemical groups by allowing patterns in the data to be more easily observed.

Hand drawn boundaries on the scatter plots show the differences and similarities between the identified geochemical groups. Hand drawn lines, connecting the points representing the REE normalized concentrations of each sample presented on a chondrite plot, also show the differences and similarities between the identified geochemical groups. The dashed lines on the chondrite plots represent the interpreted path of lines to and from those elements not having a calculated concentration.

As this study deals primarily with the geochemistry of rock and sediments, the scatter plots and chondrite plots were the primary tools used in the interpretation of the data. However, a brief visual inspection of hand samples was conducted both to aid in the interpretation of the geochemistry, and to confirm what the geochemistry indicated. The geographical location from which the sample was collected was also noted to aid in the interpretation of the geochemical data.

Once geochemical groups were recognized, cross sections, stratigraphic columns, and distributions of geologic units, were constructed using all of the available data (geochemistry, magnetic polarity, lithology, and radiometric age). Basic statistical tests (F and T tests) were also conducted on the identified geochemical groups.

DATA AND RESULTS

Trace element geochemical data were obtained for all 163 samples analyzed using INAA. Data were collected for the following elements:

Na, K, Rb, Cs, Sr, Ba
Fe, Sc, Cr, Co, Zr, Zn
Hf, Ta, Th, U
As, Sb
La, Ce, Nd, Sm, Eu, Tb, Yb, Lu

Due to human error made during analysis, samples b557-38-52, b557-80-94, b541-27, and LOD6-95-110 do not have complete data sets. The locations from which b557-38-52, b557-80-94, and b541-27 were collected, were re-sampled. LOD6 was not re-sampled and has only a partial data set. Additionally, some samples do not have complete data sets as there was not sufficient information obtained from the detector with which to calculate concentrations for some elements.

Those elements having less than ten percent counting error are considered the most reliable data and include Ba, Ce, Co, Cr, Cs, Eu, Fe, Hf, La, Na, Sc, Sm, Tb, and Th. Many of these elements were very useful in defining geochemical groups. Most of the remaining elements have counting errors greater than ten percent, and were generally not useful in defining geochemical groups. A complete listing of geochemical data is contained in Appendices A through E.

Additional data sets are available for the Boring Lava samples. The data sets include age dates, magnetic polarity, and XRF geochemistry (Tables II-IV).

The number and type of data sets available for the Boring Lava (XRF and INAA geochemistry, age dates, and magnetic polarity) allowed for the distinction of three Boring Lava units. The XRF data and the age dates obtained prior to this study indicated that there were two, and possibly three units. The magnetic polarity and INAA data confirmed that there were three units. The elements Sc, La, Ce, Cr, Eu, and Co, were the most useful in distinguishing the three units. Geochemical data for the Boring Lava samples are presented in Appendix A.

The data available for the sediment samples include the INAA geochemistry, and the location and depth from which the sample was collected. Seven geochemical groups of sedimentary materials were identified. The useful elements for distinguishing the sediment groups included Hf, La, Sm, Th, Fe, Cr, and Co. Geochemical data for the sediment samples is presented in Appendices B through E.

Table II. Age dates and sample numbers for the Boring Lava (Data from Rick Conrey. Sample 92TB5 was also dated by the United States Geological Survey).

Sample Number	Age Date
B14-37.5	0.26 +/- .11 Ma
B12-119	0.96 +/- .03 Ma
B12-94	0.86 +/- .04 Ma
B537-155	0.97 +/- .14 Ma
92TB5	2.44 - 2.6 Ma

Table III. Magnetic polarity and sample numbers for the Boring Lava.

NORMAL Magnetic Polarity

b538-28.5	SS2	B13-76.2
b539-42	CY5	B13-104.7
b540-34	CY6	B19-46
b556-57	BA7	B535-105
b556-95	BU8	B538-91
b557-165	SH9	B541-27
b557-211	HWY26-2	B557-32
b557-213	HWY26-3	B557-63
b561-98	HWY26-4	B557-93.5
b561-135	ODOT-K108-48-49	B561-71.7
b564-115		B561-90
		B561-123.5
		B562-74.3
		B562-198.5

REVERSE Magnetic Polarity

b538-176	CR3	B13-155
b539-167.7	92TB5	B535-209
b540-213	MB88-186	B537-40.3
b561-166	MB88-190	B555-70
b561-172		B555-119.5
b564-170		B565-154

Table IV. X-ray fluorescence data for selected Boring Lava samples (Data from Marvin Beeson; samples analyzed at Washington State University).

Sample Number	B12-94	B12-119	B538-91	B555-70	B561-90	B562-198
	Normalized Results (Weight %)					
SiO_2	52.04	52.43	54.60	52.77	52.10	51.80
Al_2O_3	16.91	17.86	17.11	17.82	17.40	16.75
TiO_2	1.30	1.31	1.29	1.32	1.40	1.33
FeO^*	8.16	8.24	7.80	8.05	8.25	8.14
MnO	0.13	0.14	0.13	0.14	0.13	0.13
CaO	8.91	8.67	7.72	8.55	8.38	8.76
MgO	7.31	6.41	5.86	6.23	7.01	7.72
K_2O	1.18	0.71	0.98	0.77	1.19	1.21
Na_2O	3.71	3.97	4.17	4.09	3.74	3.81
P_2O_5	0.36	0.27	0.32	0.27	0.39	0.35
	Trace Elements (ppm)					
Ni	158	109	108	109	156	149
Cr	251	162	165	153	258	235
Sc	20	24	22	28	23	27
V	172	188	147	184	197	187
Ba	293	197	298	228	343	339
Rb	15	6	10	5	15	15
Sr	1024	655	776	721	966	1028
Zr	159	139	155	144	170	160
Y	15	24	19	23	19	16
Nb	13	9	9	9	13	14
Ga	18	18	20	18	23	18
Cu	54	50	50	57	67	49
Zn	76	75	94	77	83	73
Pb	2	1	2	3	5	1
La	38	13	28	15	28	23
Ce	48	29	41	42	72	65
Th	3	2	1	2	4	4

* Total Fe is expressed as FeO.

BORING LAVA INTERPRETATION

INTRODUCTION

Four separate data sets were used to examine the Boring Lava along the west side of the Tualatin Mountains, near Highway 26. XRF geochemical data and age dates were obtained from previous studies. INAA geochemical data were obtained during this study. Magnetic polarity data were obtained both during previous work and during this study.

AGE DATES

Five of the samples analyzed by INAA, were dated using a K-Ar dating method (Conrey, 1995; personal communication). The five dates are listed in Table II. Three general dates are established and presented below in Table V. The locations of the dated samples are shown on Figures 3 and 6.

Table V. Approximate ages of the five samples that have age dates.

Approximate Date (years)	Radiometric Date (Ma)	Sample Number
250,000	0.26 +/- .11	B14-37.5
750,000 to 1,000,000	0.96 +/- .03	B12-119
	0.86 +/- .04	B12-94
2,500,000	0.97 +/- .14	B537-155
	2.44 - 2.6	92TB5

MAGNETIC POLARITY

Magnetic polarity data were recorded for each sample collected for this study (Table IV). Magnetic polarities for TriMet drill core were recorded at the time the drill core was extracted by TriMet personnel. Magnetic polarities for outcrop samples were recorded at the time of collection using a fluxgate magnetometer.

XRF GEOCHEMISTRY

XRF data (Beeson, 1993; personal communication) reveal at least two different geochemical groups as seen in both major and trace element geochemistry (Table IV).

As mentioned previously, XRF data for the trace elements showed that INAA would also be useful in differentiating between Boring Lava units.

INAA GEOCHEMISTRY

Geochemical data for the Boring Lava are presented in Appendix A. Scatter plots of INAA data generally show two to three recurring groups (Figures 9, 10, and 11). These groups are most clearly defined on Figure 9 (Scandium vs. Cerium). Samples at the edges of the groups, which may plot away from the main cluster, tend to represent pyroclastic material associated with the eruption of that unit, or may represent weathered flow boundaries.

Several exceptions are obvious on Figure 9, and are visible on Figures 10 and 11 as well. Sample KA1 was collected from the northern-most section of the Boring Lava considered for this study. The outcrop is weathered, bleached, and very rubbly. The geochemistry of this sample is no doubt obscured by weathering effects. Thus, it always plots away from the above three groups.

Sample CLAR-110-120 was collected previous to this study from drill cuttings taken from a water well at the Claremont Golf Course. Though the chips appear to be of Boring Lava, the powdered sample does not look like other powdered Boring Lava samples. It too tends to plot away

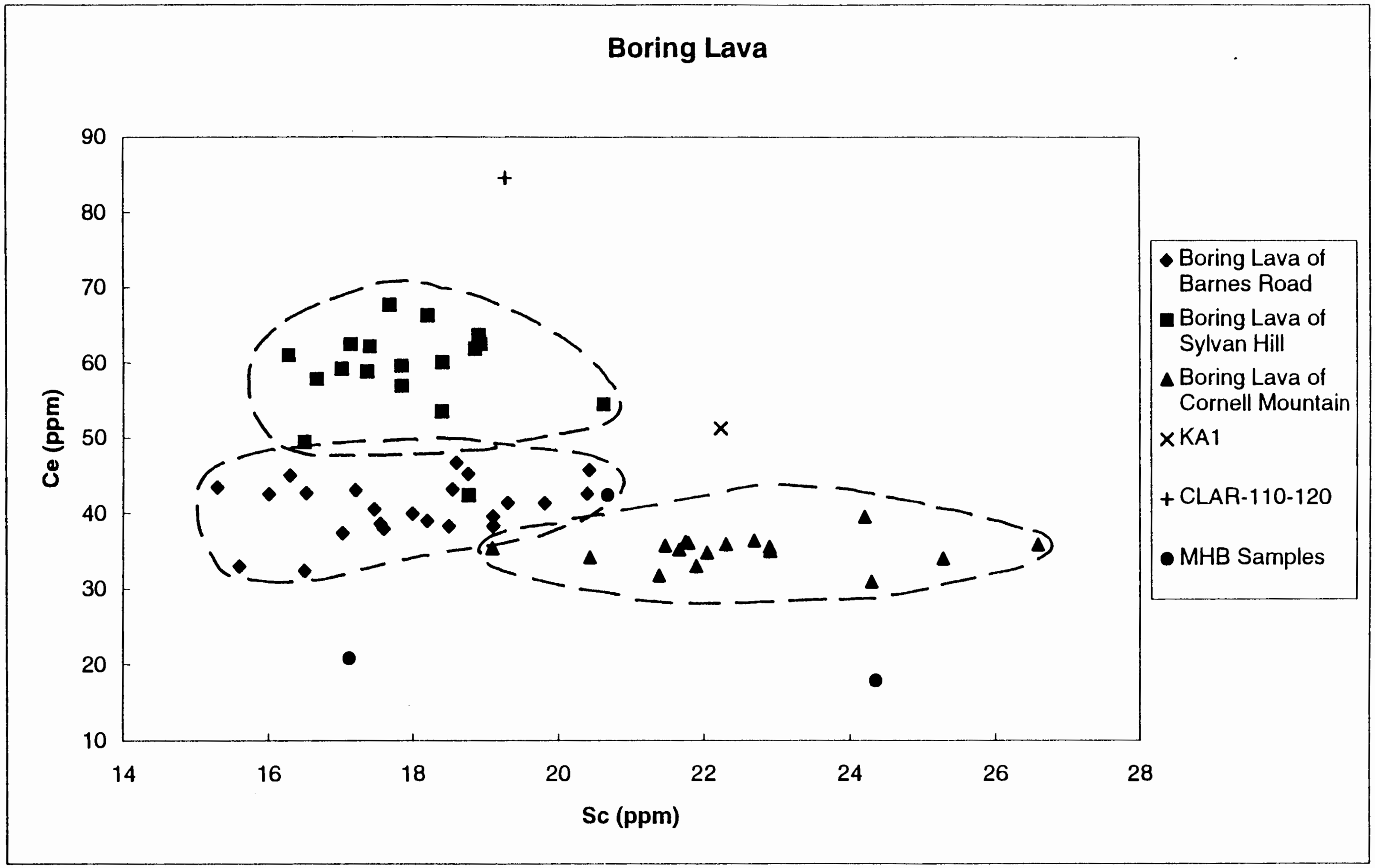

Figure 9. Boring Lava Scatter Plot (Scandium vs. Cerium).

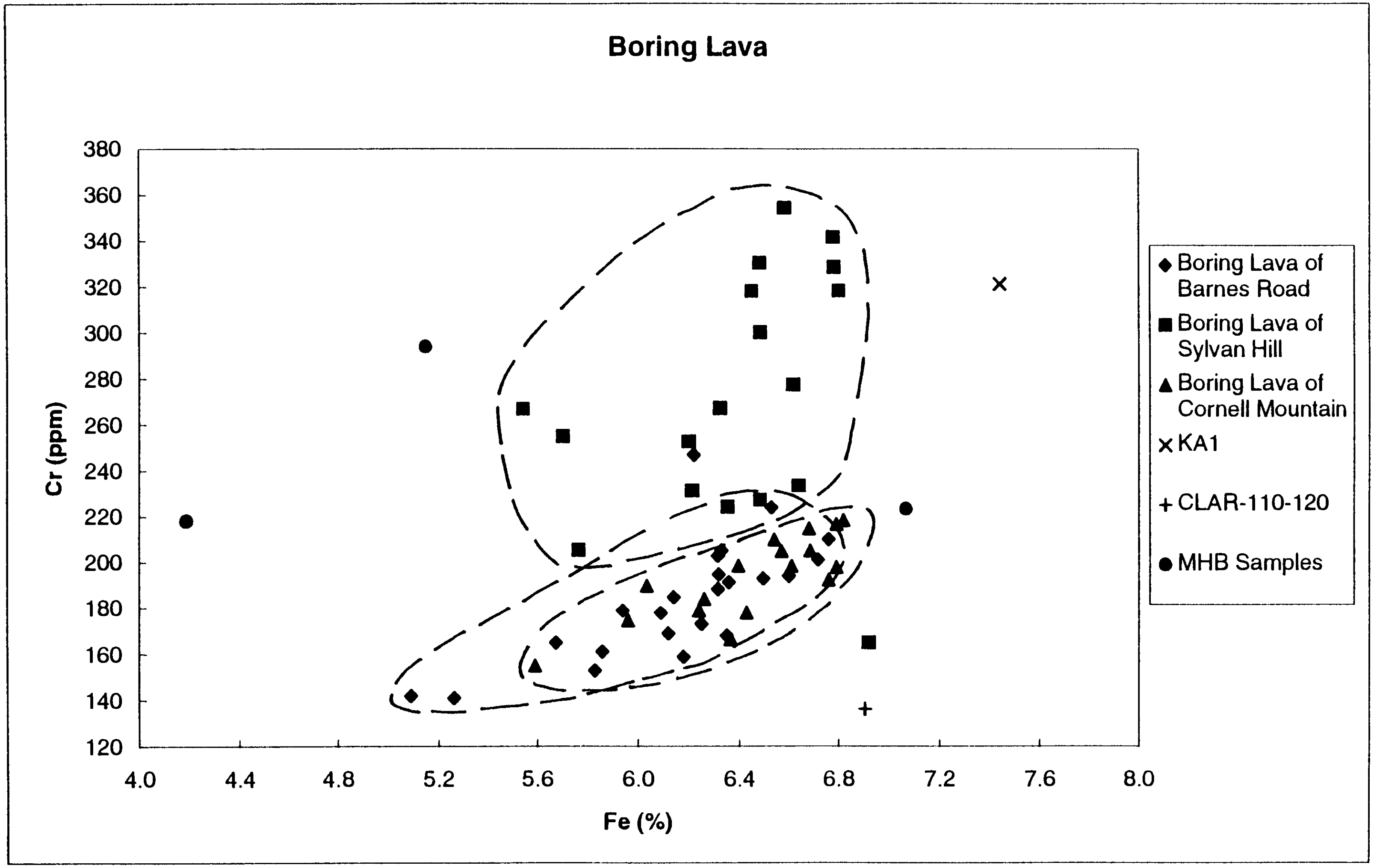

Figure 10. Boring Lava Scatter Plot (Iron vs. Chromium).

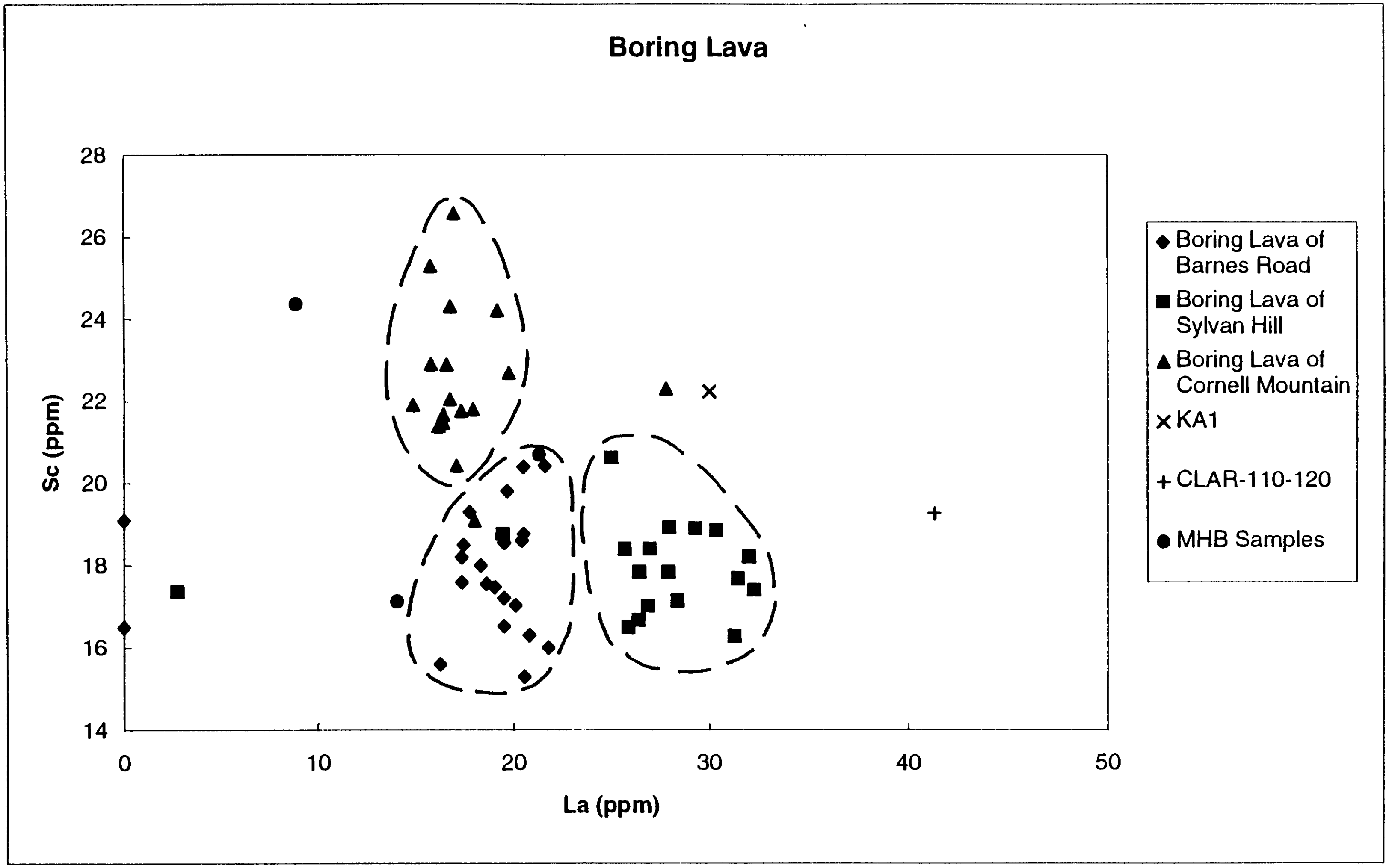

<u>Figure 11.</u> Boring Lava Scatter Plot (Lanthanum vs. Scandium).

from or on the margins of the above three groups, and may represent a separate geochemical group.

Samples MB88-186, MB88-190, and 92TB5 are outcrop samples from Mt. Sylvania, Cookes Butte, and the Oregon City plateau, respectively, collected previous to this study (labeled as MHB samples on Figure 9-11). They are interpreted to have erupted from separate vents and do not consistently plot with the other groups.

Table VI presents age, magnetic polarity, and selected INAA data for the four samples along the light rail tunnel alignment which have age dates. From these data, three Boring Lava units are identified along the west side of the Tualatin Mountains near Highway 26: the Boring Lava of Barnes Road, the Boring Lava of Sylvan Hill, and the Boring Lava of Cornell Mountain. The names chosen for the three units are based primarily on the identified surface distribution, and the relation of each unit to a geographic or cultural feature, as shown in Figures 12 and 13.

Using all available data, differentiating between the three Boring Lava units is straightforward. The Boring Lava of Sylvan Hill and the Boring Lava of Cornell Mountain both yield approximately the same radiometric age. However, they have different magnetic polarities and are chemically distinct from one another. The difference in magnetic polarity is attributed to the last major magnetic reversal, which occurred approximately 0.80 Ma years ago. The Boring Lava of Barnes Road, though it is chemically similar to the Boring Lava of Cornell Mountain, has a normal magnetic polarity and is approximately 0.50 Ma younger. Knowing these differences, geographic distribution and stratigraphic position of the three Boring Lava units was determined in the southern portion of the study area using both the drill hole and outcrop sample locations (Figures 12, 13 and 14).

Because there is very little surface exposure of Boring Lava along the west side of the Tualatin Mountains, the pictured distributions of the three Boring Lava units are based primarily on the existing topography. A topographic map showing the same Boring Lava distributions is presented in Figure 13. Figure 14 shows the subsurface distribution of the three Boring Lava units along the tunnel alignment. The contacts and the resulting, apparent structures shown in Figure 14 are based on the geochemistry, radiometric age, magnetic polarity, and the boring logs presented in Squier Associates (1992). The dark, solid colors (blue, red, and green) on Figure 14 indicate solid rock while shaded areas of the same color represent rubbly or weathered zones. As CRBG units were not addressed in this study, the CRBG units and the structures within them and bounding them, on Figure 14, are presented as they are shown in Squier Associates (1992).

Table VI. Magnetic polarity and selected INAA data for the four samples along the tunnel alignment which have age dates.

Sample Number	B12-94	B12-119	B14-37.5	B537-155
Age (Ma)	0.86+.04	0.96+.03	0.26+.11	0.97+.14
Magnetic Polarity	NORMAL	REVERSE	NORMAL	REVERSE
Selected INAA trace element concentrations (ppm)				
Sr	1005	860	788	789
Cr	319	205	205	217
Co	41	37	30	36
Th	3.7	1.6	1.9	1.8
La	28.4	16.3	20.6	18.0
Ce	62.5	35.7	43.5	35.4
Sm	5.94	4.34	5.18	4.49
Eu	1.92	1.58	1.70	1.53
Lu	0.25	0.50	0.28	0.39

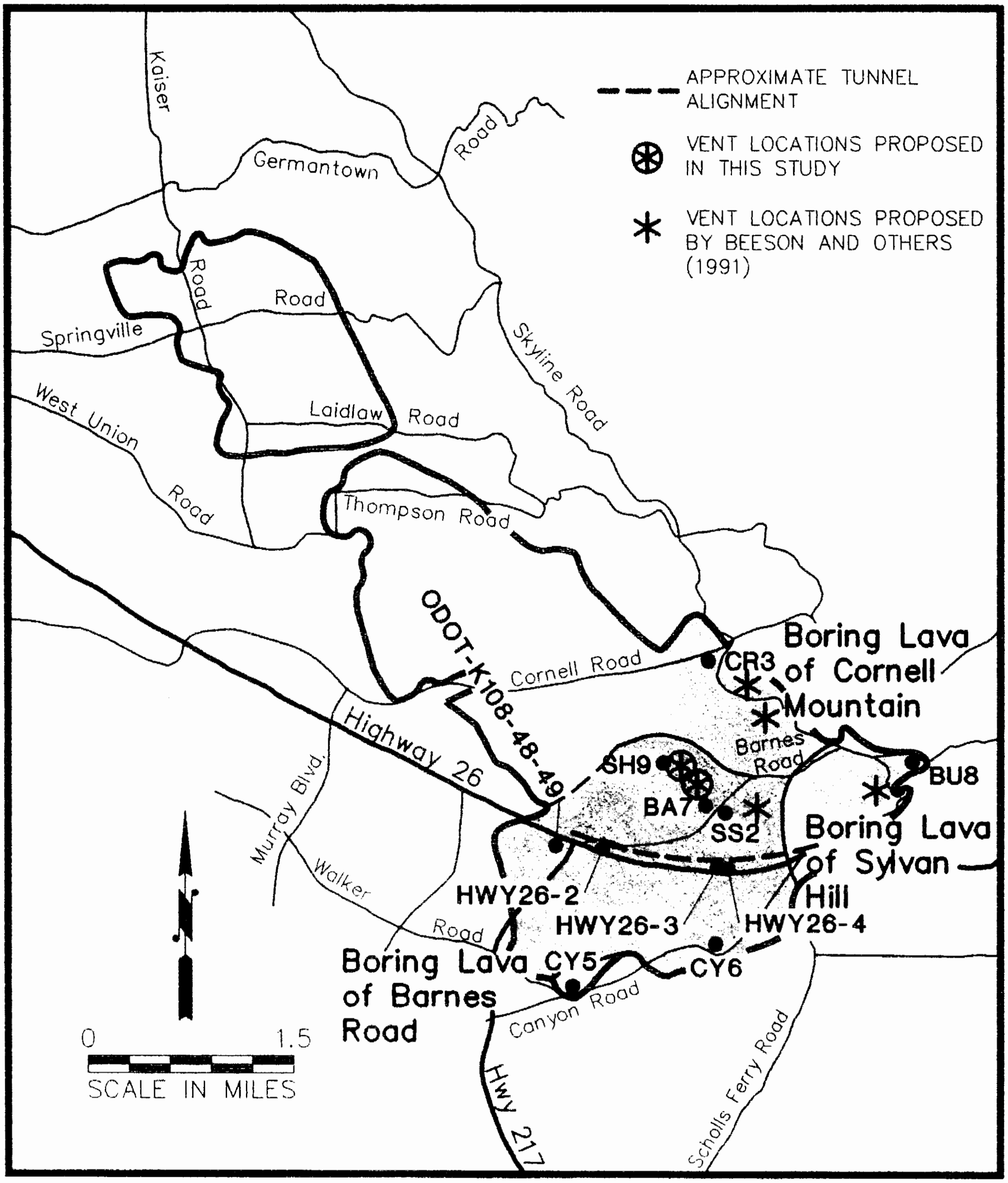

Figure 12. Surface distribution of Boring Lava (road map). Boring Lava outline from Trimble (1963).

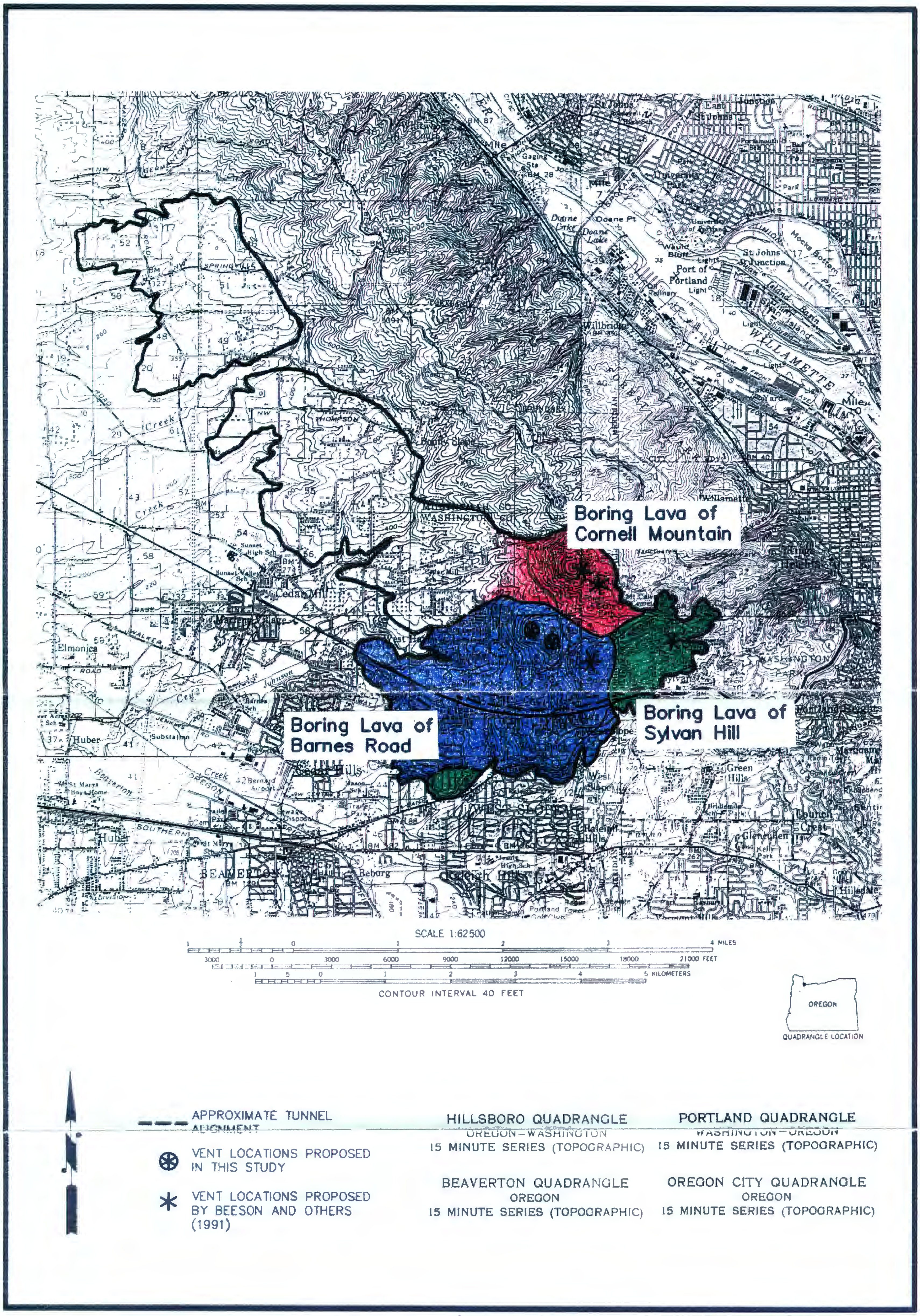

Figure 13. Surface distribution of Boring Lava (topographic map). Boring Lava outline from Trimble (1963).

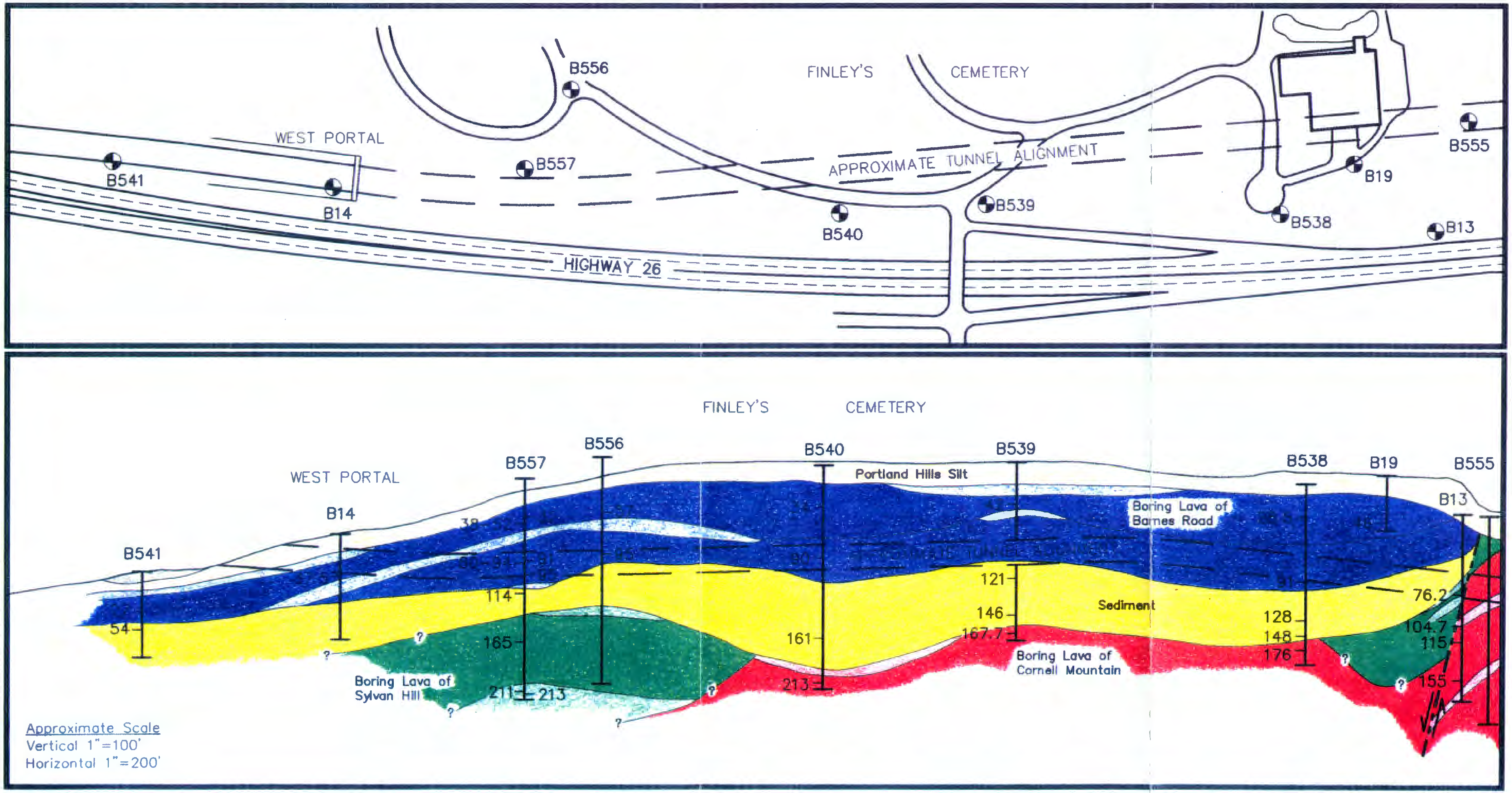

Figure 14. Distribution of Boring Lava along the west end of Line Section 5A of the TriMet tunnel alignment. Modified after Squier Associates (1992).

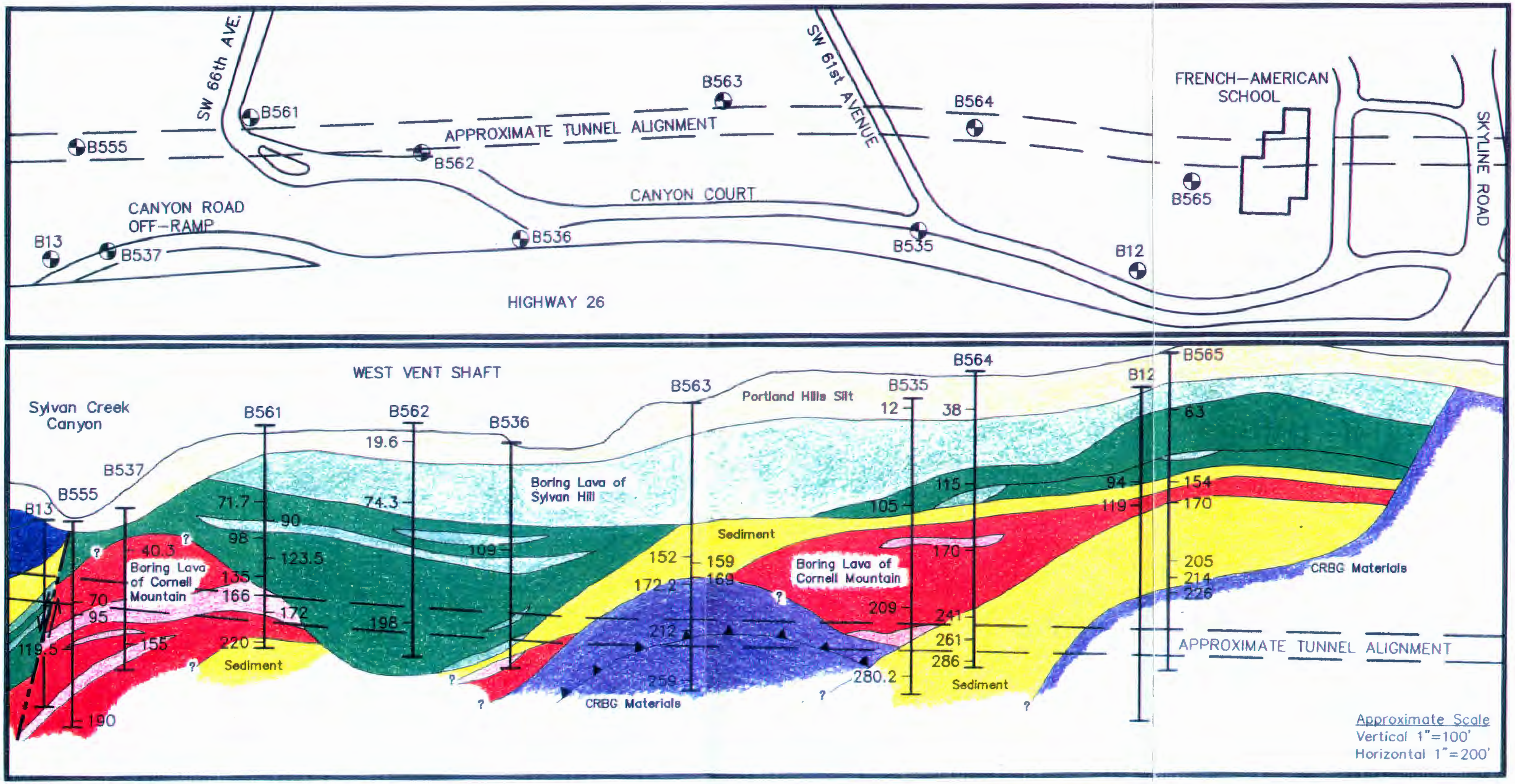

Figure 14 continued.

STATISTICAL ANALYSIS

Basic statistical analysis was completed for the three geochemical groups, which were chosen based on geochemistry, age, and magnetic polarity. The statistical analysis was completed to show that the chosen geochemical groups are indeed distinguishable from one another. F tests were completed initially to examine the equality of the variances between the groups. Where the F test failed to reject the equality of the variances, T tests were conducted to compare the means of the groups. Statistical analysis is presented in Appendix F.

Complete data sets were not available for all of the analyzed samples. As a result, only those samples having complete data sets were used to calculate the mean for that group. In addition, not all elements that had geochemical data available were used in the comparisons. Element choice was based on the counting error and the completeness of the data. Those elements having less than ten percent counting error and complete data sets were used in the statistical analysis. The elements used were Na, Cs, Ba, Fe, Sc, Cr, Co, Hf, Th, La, Ce, Sm, Eu, and Tb.

Based on the results of the F tests, run using a 5% level of significance, the equality of the variances was rejected for each set of Boring Lava units compared. No T tests were necessary. Thus, the three, previously discussed groups, can be considered separate, distinct geochemical groups.

DISCUSSION

Figures 12, 13, and 14, show the distribution of the Boring Lava both stratigraphically and geographically, and suggest a particular sequence of events. The radiometric age, magnetic polarity, and location of the Boring Lava of Cornell Mountain indicate that it erupted first, and flowed south and southwest. Based on the existing topography, it also likely flowed west and northwest, although there are few geochemical data to support this hypothesis. Two vent locations were proposed by Beeson and others (1991).

Based on radiometric age and magnetic polarity, the Boring Lava of Sylvan Hill erupted shortly after the Boring Lava of Cornell Mountain, from a vent located to the southeast of the area from where the Boring Lava of Cornell Mountain erupted. The vent location for the Boring Lava of Sylvan Hill was proposed by Beeson and others (1991). The Boring Lava of Sylvan Hill also appears to have flowed primarily south and southwest, although small amounts appear to extend to the north and east. A small tongue of the Boring Lava of Sylvan Hill is tentatively identified near the southwestern-most corner of the study area, near the intersection of Highway 217 and Walker Road (Figures 12 and 13).

Based on radiometric age alone, the Boring Lava of Barnes Road erupted most recently. There are three vent locations from which the Boring Lava of Barnes Road erupted, located to the west of the eruption points of the other two Boring Lava units. One of the three vent locations was proposed by Beeson and others (1991). Two of the vent locations are proposed based on the information obtained from this study, specifically, outcrop and core geochemistry and topography. The identified distribution of the Boring Lava of Barnes Road is the most extensive, covering much of the west flank of the Tualatin Mountains on either side of Highway 26 (Figures 12 and 13).

In the subsurface, the same sequence is observed (Figure 14). The Boring Lava of Cornell Road underlies the Boring Lava of Sylvan Hill and the Boring Lava of Barnes Road throughout the entire area shown in the cross section. In TriMet drill holes B13 and B561, at depths of approximately 105 and 140 feet respectively, the Boring Lavas of Cornell Mountain and Sylvan Hill are in contact with one another where the Boring Lava of Cornell Mountain directly underlies the Boring Lava of Sylvan Hill. In the eastern half of the cross section, a sediment layer separates the two older Boring Lava units. Based on the radiometric ages and magnetic polarities of the two older Boring Lava units, this sediment layer must have been deposited around the time of the most recent magnetic reversal (approximately 0.80 Ma).

Based on the contacts presented in Figure 14, it appears that a period of deformation/structural activity took place between the time of the eruption of the Boring Lavas of Cornell Mountain and Sylvan Hill, and the Boring Lava of Barnes Road. The difference in the ages of the two older Boring Lava units and the younger Boring Lava unit would provide approximately 0.50 Ma years for uplift and erosion, deposition of sediments, and structural deformation to occur. The upper surface of the two older Boring Lava units appears rather undulatory, and both of the older Boring Lava units are cut by a fault.

The youngest unit, the Boring Lava of Barnes Road, is present only in the western half of the cross section, which agrees with its identified surface distribution. It overlies both a sediment layer and the two older Boring Lava units. Because the ages of the Boring Lava units bounding this sediment layer are known, the age of the sediment layer in the western half of the cross section, is constrained to between approximately 0.25 Ma and 1 Ma.

Based on the presented cross section, the Boring Lava of Barnes Road is not cut by the fault that cuts the older Boring Lavas of Sylvan Hill and Cornell Mountain.

The fault shown on Figure 14, in association with the Sylvan Creek Canyon near the middle of the cross section, is not shown on the surface maps in Figures 12 and 13. The fault would be located near the contact of the Boring Lavas of Barnes Road and Sylvan Hill along the TriMet tunnel alignment on Figures 12 and 13. Beeson and others (1991) inferred a fault in this area. However, no field observations were made as a part of this study. The contacts shown are chosen based primarily on the existing topography and outcrop geochemistry. The result is that only one point exists on the surface maps that has information available (i.e. boring logs, magnetic polarity, and geochemistry) to suggest that a fault might exist. As such, no line could be drawn from this point to other such points to indicate where a fault might be located.

SEDIMENT GEOCHEMISTRY AND INTERPRETATION

INTRODUCTION

Interpretation of the sediment geochemistry is not as straightforward as the interpretation of the Boring Lava geochemistry. Many factors can control the nature of sediment deposition. Particle size, shape, and density, water and/or wind velocity, load of the transporting medium (water vs. wind), local and/or regional volcanic activity, and plant/animal interaction are only a few. The deposition of sediments in the Portland area has likely been affected by all of the listed variables, and more. Nevertheless, it has been possible to identify several groupings among the analyzed samples. In particular, it is the amount of volcanic material in the samples analyzed, that has played a key role in the interpretation of the geochemical data.

SHALLOW SEDIMENT AND MISCELLANEOUS SAMPLES

Geochemical data for the shallow sediment and miscellaneous samples are presented in Appendix B. Shallow sediment samples include samples taken from TriMet core and DOGAMI shallow drill holes. The top 250 feet of the Portland International Airport Drill Hole (MTD1) is included in the analysis of this data set, but is listed in a separate appendix (Appendix D). Miscellaneous samples include two volcanic ash samples collected from Reed Island in the Columbia River east of the Sandy River Delta, a sample of pre-CRBG sediment collected from the western edge of the Tualatin basin, a sample of bentonite drilling mud, and three samples of sediment, one each of Sandy River Mudstone, Portland Hills Silt, and Missoula Flood sediments, collected from type localities or areas where positive identification of that type of sediment was achieved.

The bentonite drilling mud was analyzed to examine its geochemistry in order to identify and evaluate the potential contamination effects of drilling mud remaining on core samples when they were analyzed using INAA. Although the sample of drilling mud was determined to have very high concentrations of Th (up to 36 ppm), none of the other analyzed sediment samples plotted in groups that appeared skewed toward the position of the bentonite drilling mud sample. Thus, it does not appear that any drilling mud remaining on the analyzed samples significantly affected sample geochemistry.

Scatter plots generally show several broad groups (Figures 15-20). Sample geochemistry was compared with

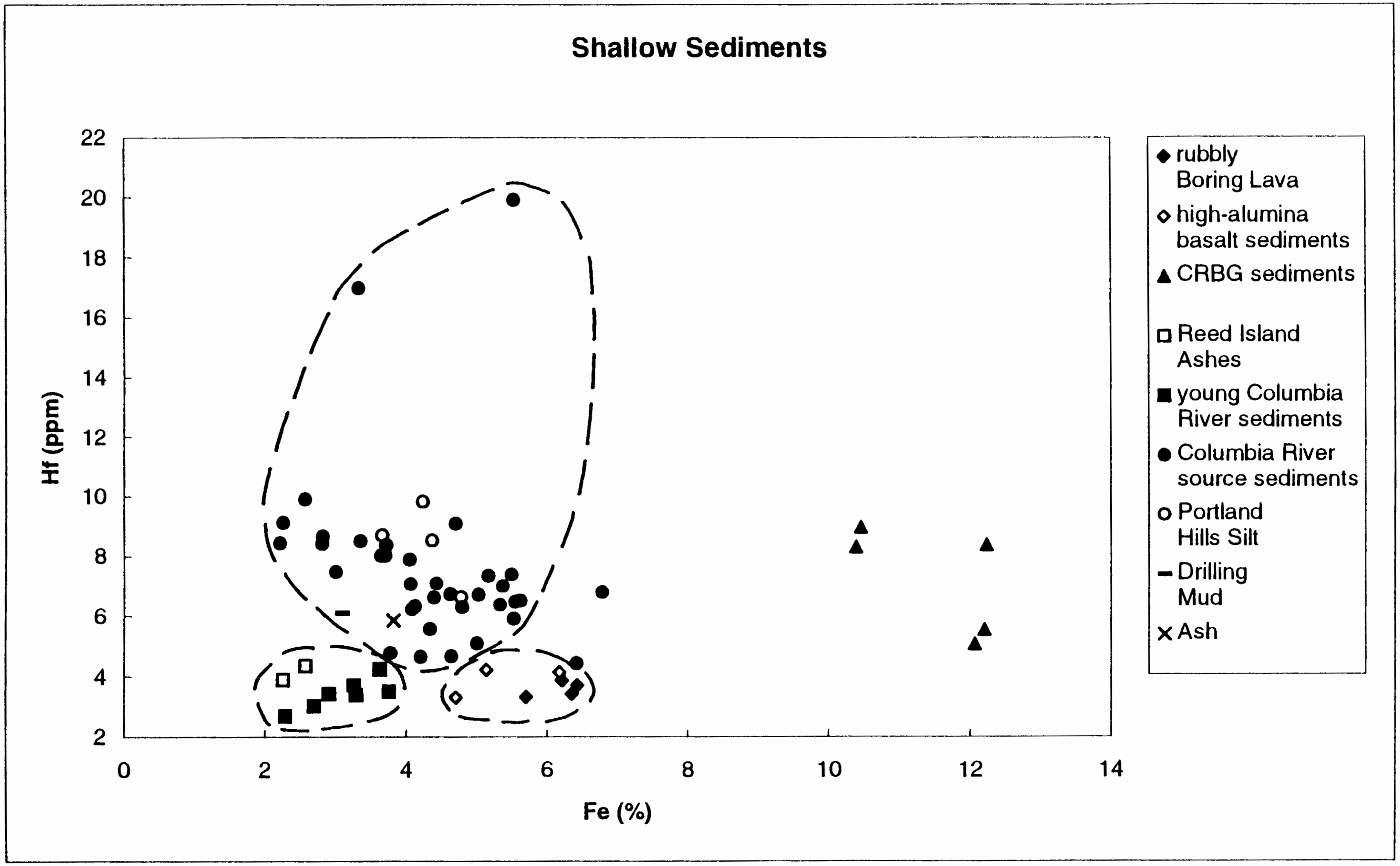

Figure 15. Shallow Sediments Scatter Plot (Iron vs. Hafnium).

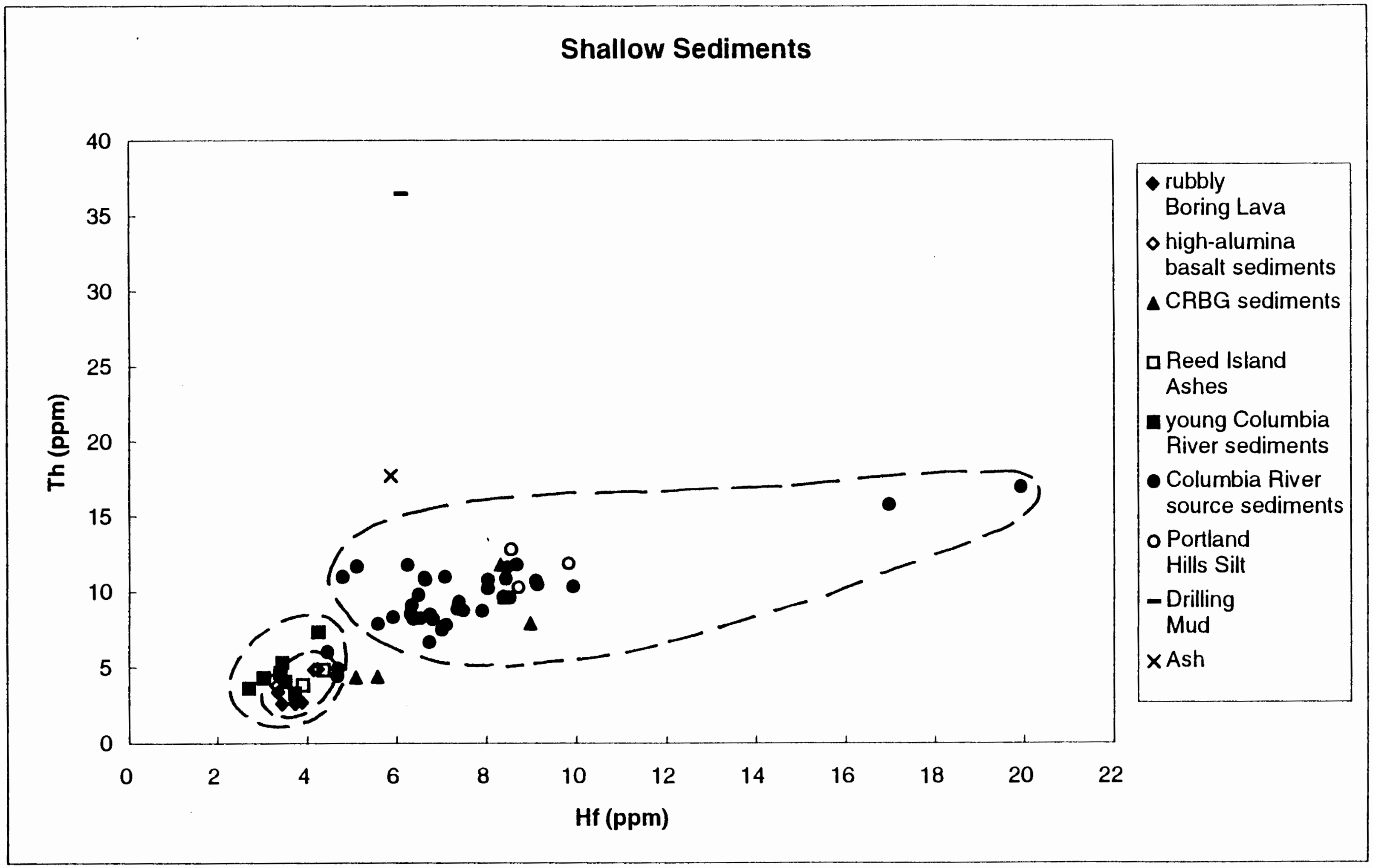

Figure 16. Shallow Sediments Scatter Plot (Hafnium vs. Thorium).

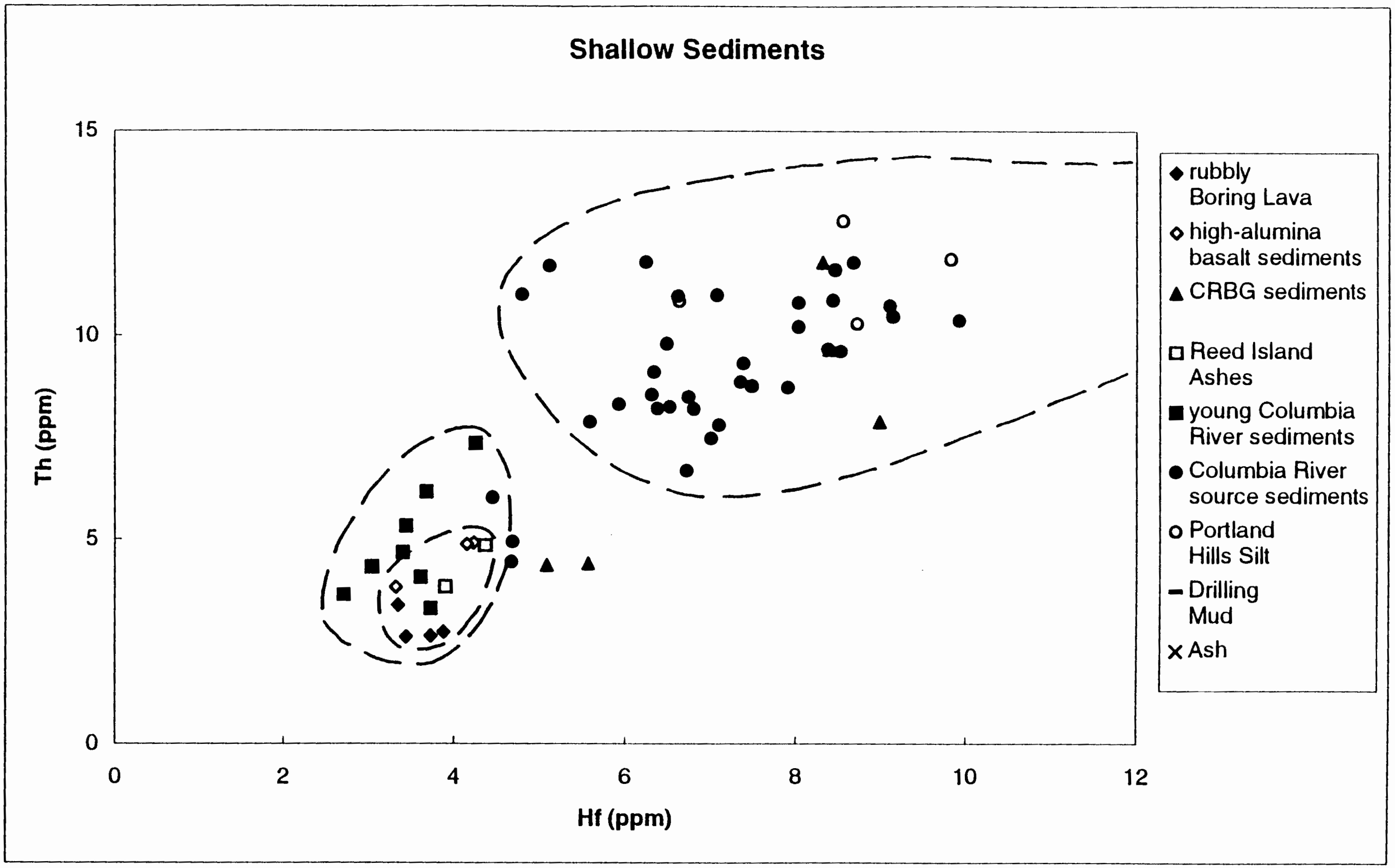

Figure 17. Shallow Sediments Scatter Plot Closeup (Hafnium vs. Thorium).

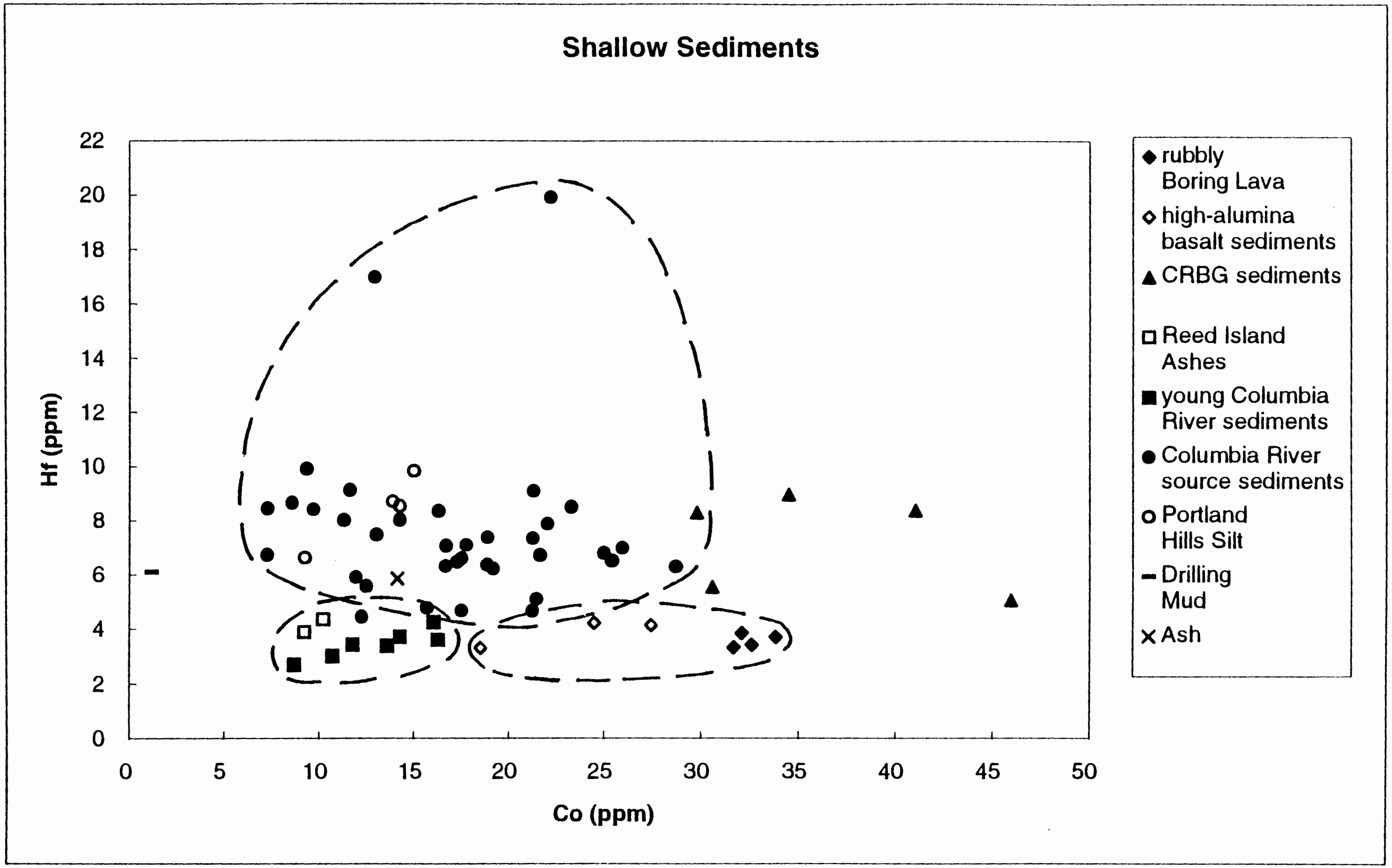

Figure 18. Shallow Sediments Scatter Plot (Cobalt vs. Hafnium).

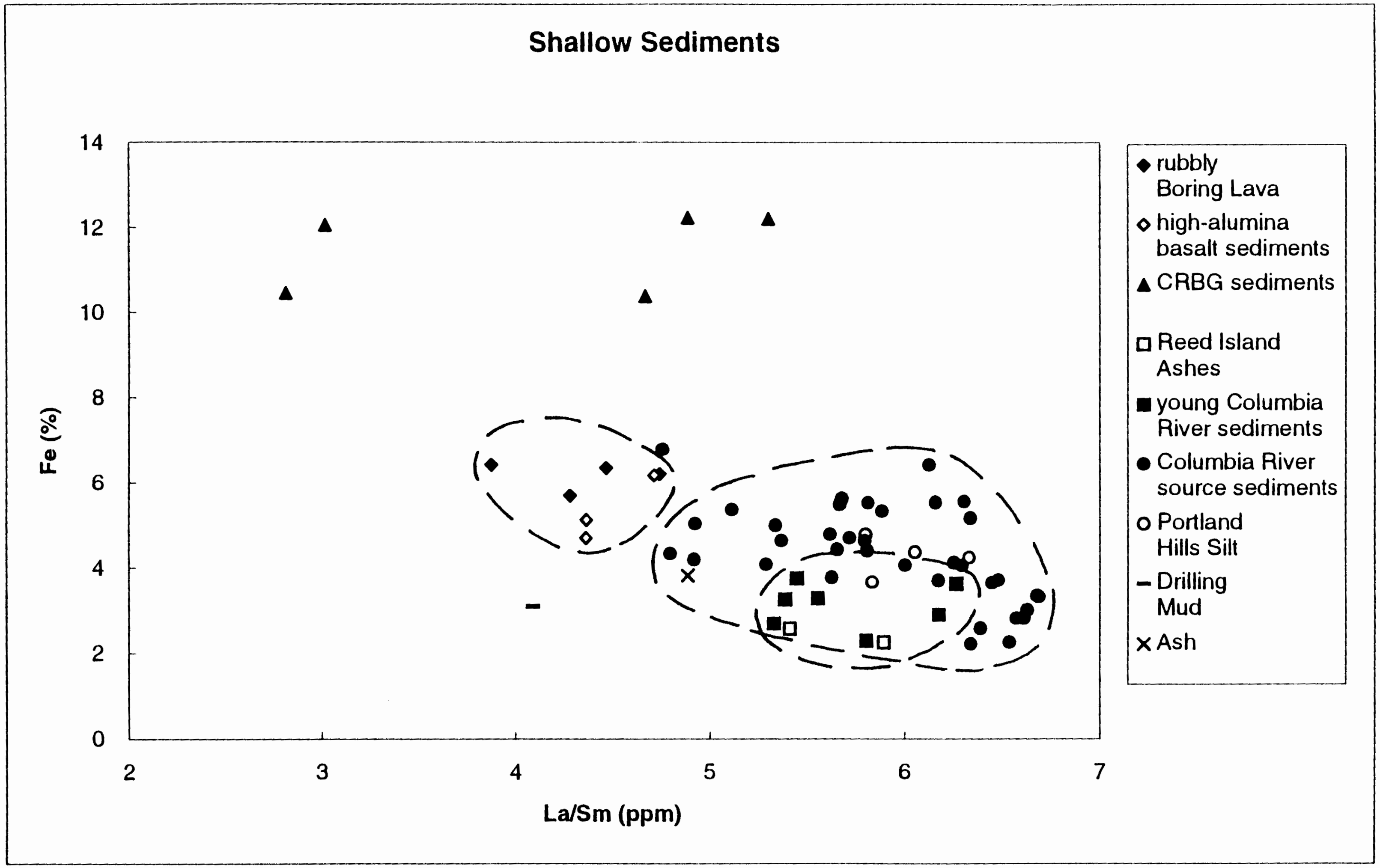

Figure 19. Shallow Sediments Scatter Plot (Lanthanum/Samarium vs. Iron).

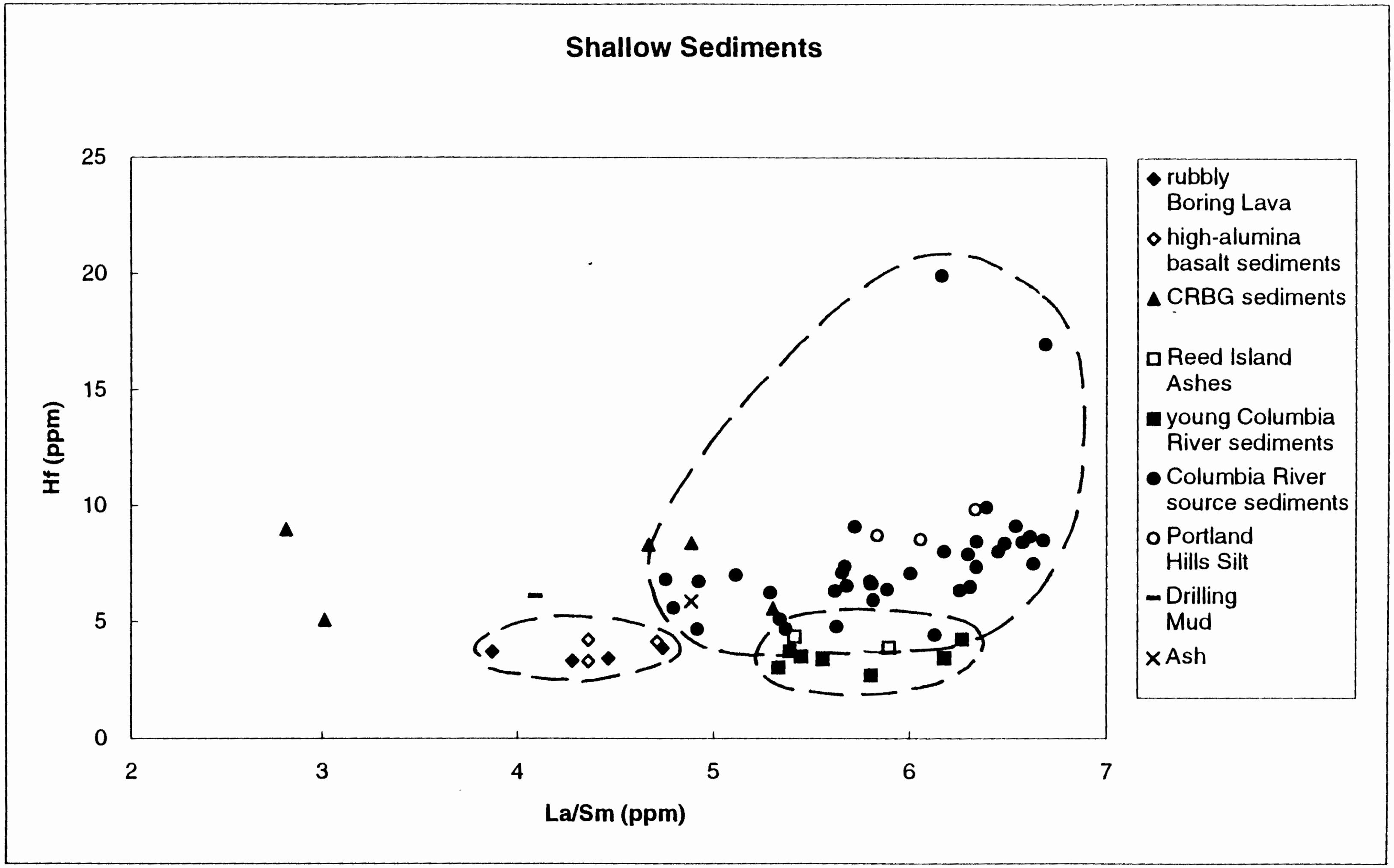

<u>Figure 20.</u> Shallow Sediments Scatter Plot (Lanthanum/Samarium vs. Hafnium).

hand sample examination and geographic location to establish five geochemical groups. Scatter plots of Fe vs. Hf and Hf vs. Th (Figures 15, 16, and 17) most clearly show these five groups, which are:

1. high-alumina basalt sediments,
2. CRBG sediments,
3. Reed Island ashes,
4. young Columbia River sediments,
5. Columbia River source sediments.

The above five geochemical groups were identified by comparing the geochemistry of the shallow and miscellaneous sediment samples, to the geochemistry of the following samples: (1) the three known sediment samples of Sandy River Mudstone, Portland Hills Silt, and Missoula Flood sediments, (2) the CRBG standard analyzed with each irradiation, and (3) the four rubbly Boring Lava samples previously identified in Squier Associates (1992) as Sandy River Mudstone Equivalent.

High-Alumina Basalt Sediments

During the initial investigation of the Boring Lava along the tunnel alignment by a Portland State University Advanced Geochemistry class (PSU, 1993), four samples of TriMet drill core (b557-211, b557-213, b561-135, and b561-172) were collected from material identified as Sandy River Mudstone Equivalent by Squier Associates (1992).

Both hand sample examination and INAA showed that four samples collected as Sandy River Mudstone Equivalent, were primarily rubbly, scoriacious Boring Lava, with minor micaceous silts worked in. On scatter plots, the four samples consistently plotted together (Figure 15-20).

These four rubbly Boring Lava samples aided in the identification of three samples collected from three shallow DOGAMI drill holes (VND1-25-30, GSD2-10-15, and GSD5-75-95) as having a similar geochemistry. Figure 4 presents the location of the DOGAMI drills holes in the Portland and Tualatin basins.

The three DOGAMI samples consistently plot near the four rubbly Boring Lava samples (Figures 15-20). Visual inspection of the three DOGAMI samples showed volcanic sands. A chondrite plot of these three volcanic sand samples with three non-volcanic sediment samples collected from the TriMet drill core show a slight difference in the slopes of the lines from Nd to Eu (Figure 21). The non volcanic sediment samples show steep, straight, negative slopes from Nd to Eu, whereas the volcanic sand samples show a decrease in the slope angle from Sm to Eu.

While one of these three samples is located near a Boring Lava source (Mt. Scott), the other two samples are not. According to Tolan and Beeson (1984), The Boring Lava and High Cascade volcanics are "... chemically,

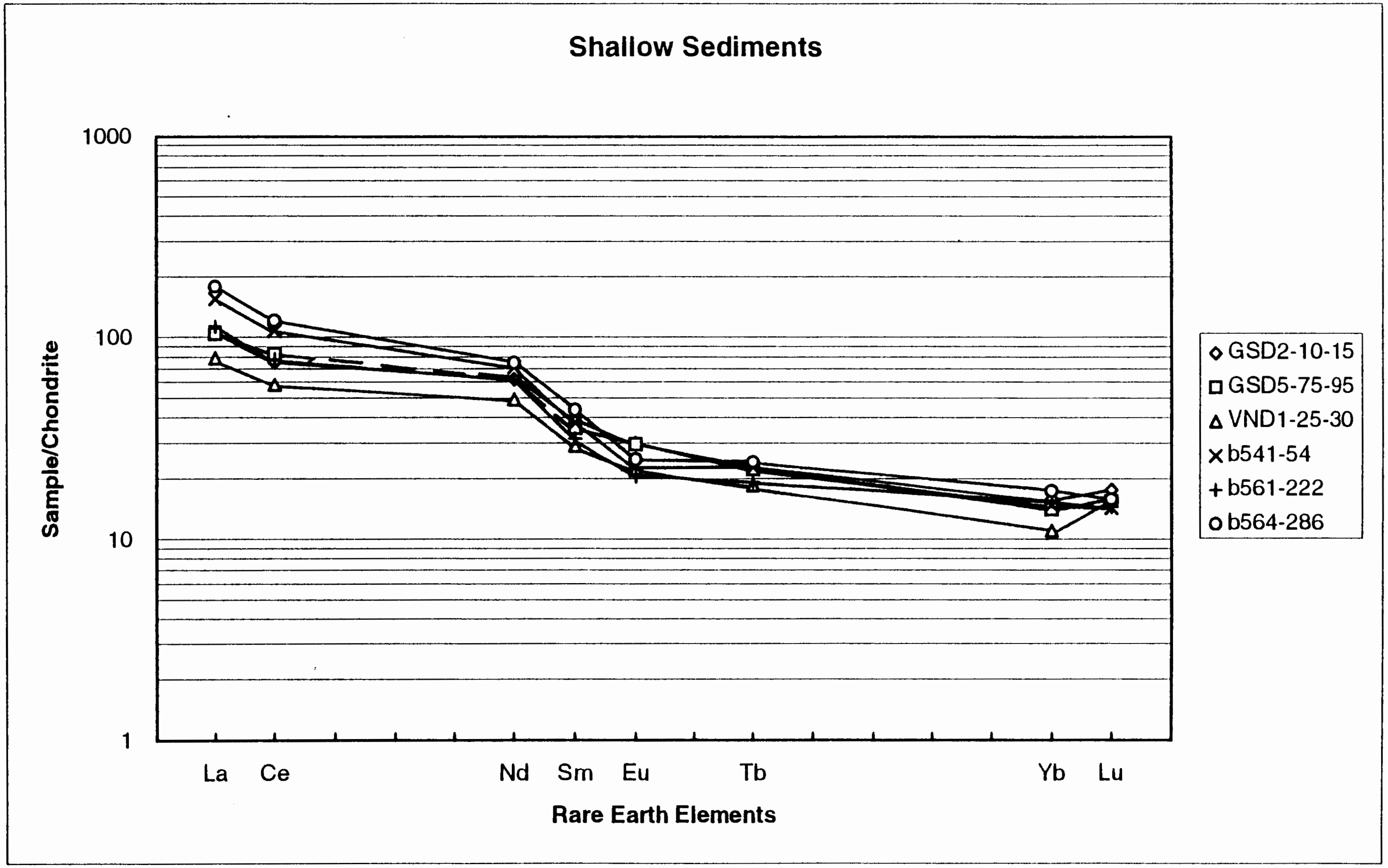

Figure 21. Shallow sediments Chondrite Plot (High-Alumina Basalt Sediments).

lithilogically, and temporally similar." The similarity in geochemistry and the position of the other two DOGAMI sediment samples near rivers carrying Cascadian materials indicates a High Cascadian type of sediment. Tolan and Beeson (1984) used the term "high-alumina basalts" to describe both the Boring Lava and the High Cascade volcanics, as major oxide analyses indicated that both units are high-alumina basalts. On this basis, the term "high-alumina basalt sediments" is the name chosen to describe these three shallow DOGAMI sediment samples.

CRBG Sediments

This group of sediments was identified by using the CRBG standard analyzed in each irradiation. Five samples (b563-172.2, b563-212, b563-259, B565-226, and BVD4-36.5) consistently plot near the CRBG standard. Figures 3 and 4 show these sample locations. Additionally, all five samples were collected from layers overlying solid CRBG rock. Higher concentrations of Fe, Co, Zn, Eu, and Hf typically characterize these sediments. Unique patterns on the chondrite plots also distinguish the CRBG sediments from the overlying sediments (Figures 22 and 23). Figure 22 presents the chondrite plot for all samples collected from TriMet drill hole B563. Figure 23 presents the chondrite plot for all samples collected from TriMet drill hole B565. Both the CRBG sediments and non volcanic

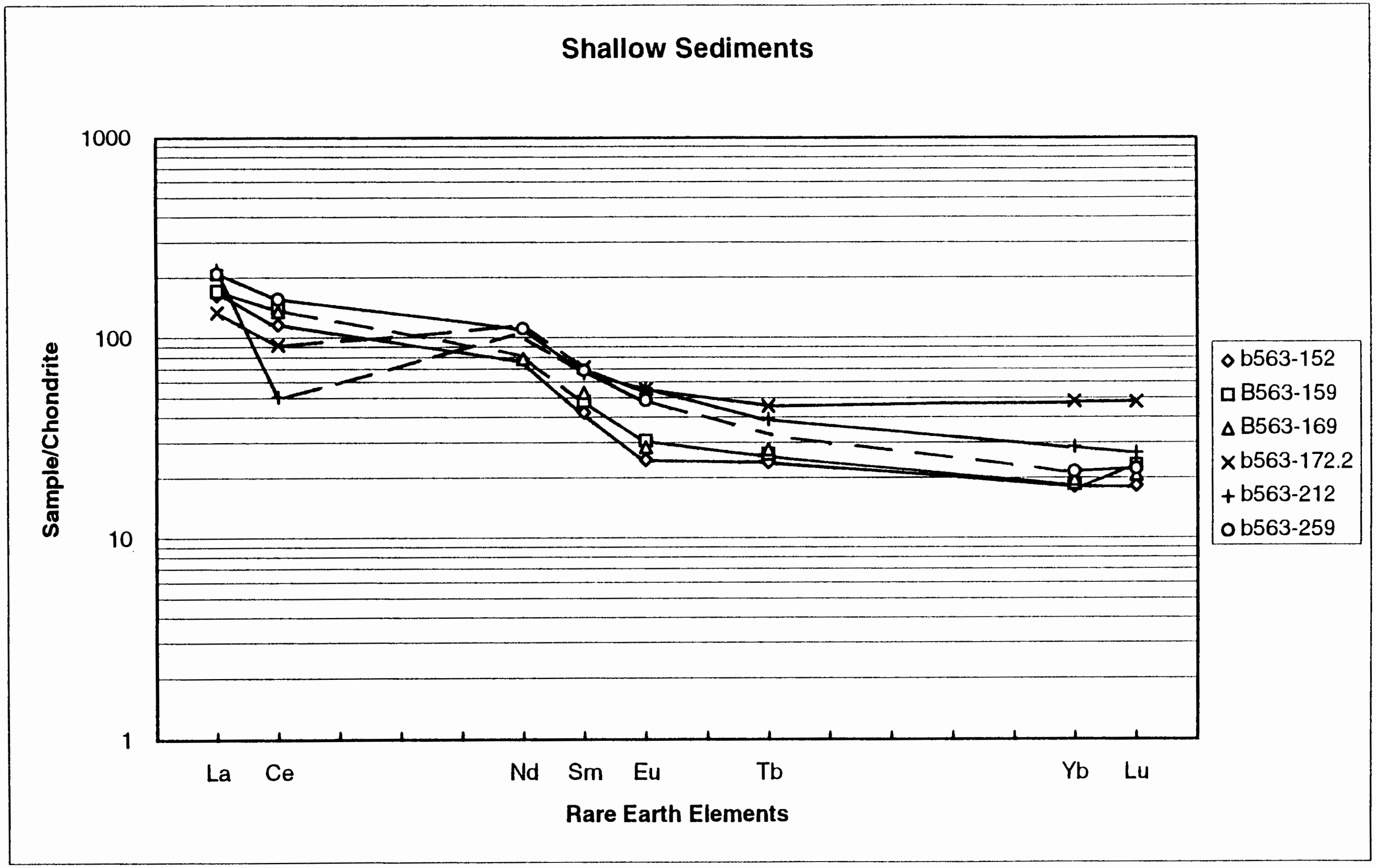

Figure 22. Shallow sediments Chondrite Plot (Samples from TriMet Drill Hole B563).

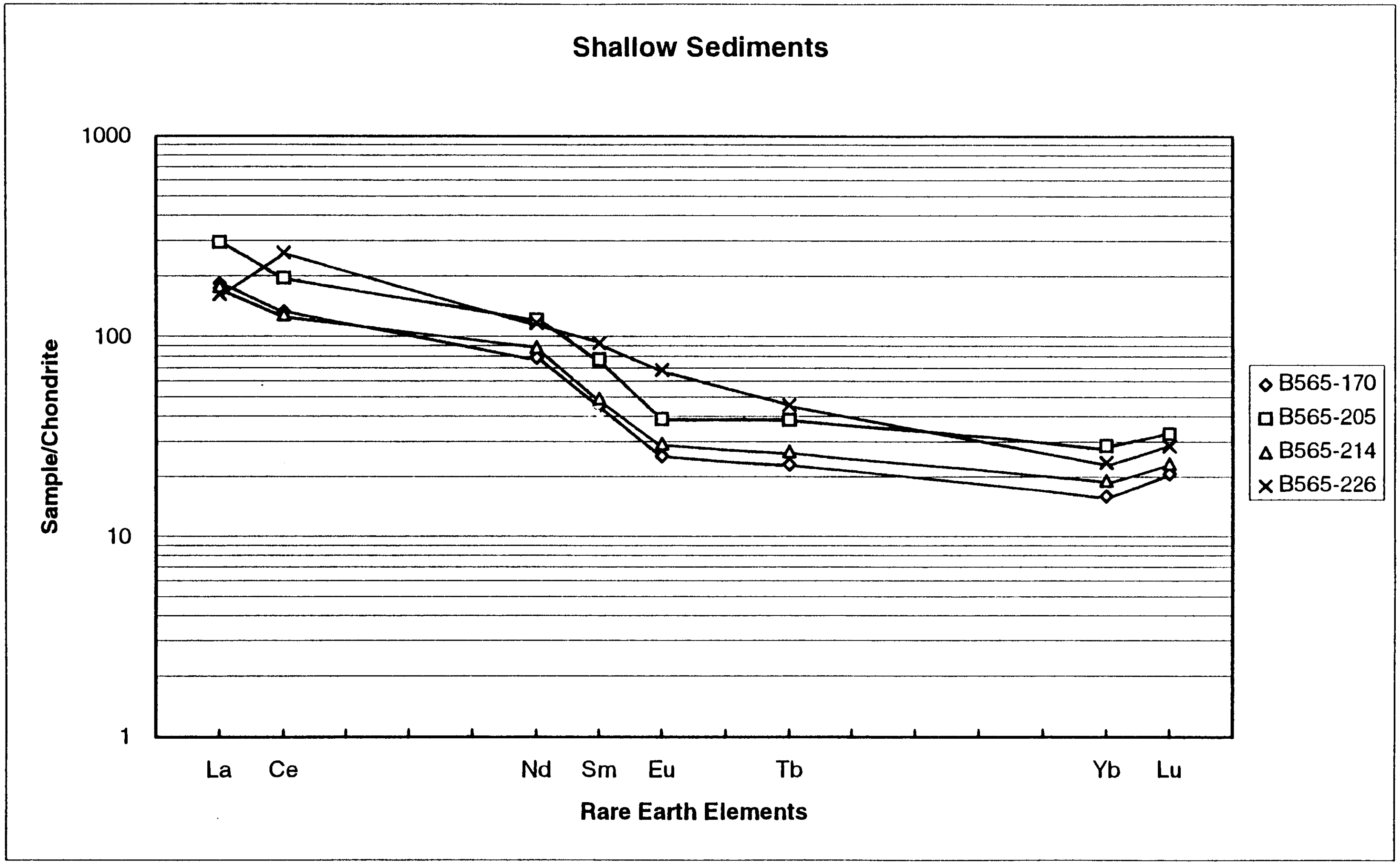

Figure 23. Shallow Sediments Chondrite Plot (Samples from TriMet Drill Hole B565).

sediment samples collected from each hole are included on the chondrite plots. In both plots, the non volcanic sediment samples show steep, straight, negative slopes from Nd to Eu, and an almost zero slope from Eu to Tb. The CRBG sediments show a more gentle, negative slope from Nd all the way to Tb.

The CRBG sediments are easily distinguished from the rubbly Boring Lava and high-alumina basalt sediments. The rubbly Boring Lava and high-alumina basalt sediments have overall lower element concentrations than do the CRBG sediments.

Reed Island Ashes

Two samples of volcanic ash (SR-3-JS and Sample #7) were collected on Reed Island in the Columbia River east of the Sandy River Delta (Figure 8). Though these samples were collected for a separate project under Dr. Curt Peterson, they were irradiated and analyzed as part of this study due to their location in the Columbia River.

Visual inspection showed light-weight, powdery, ashy material. One sample is noted to be an impure ash sample in the notes taken by the sample collector (John Siskowic). The two volcanic ash samples have similar patterns on the chondrite plots, showing a negative slope from Nd to Tb (Figure 24). Another volcanic ash sample and three non-volcanic sediment samples are also shown in

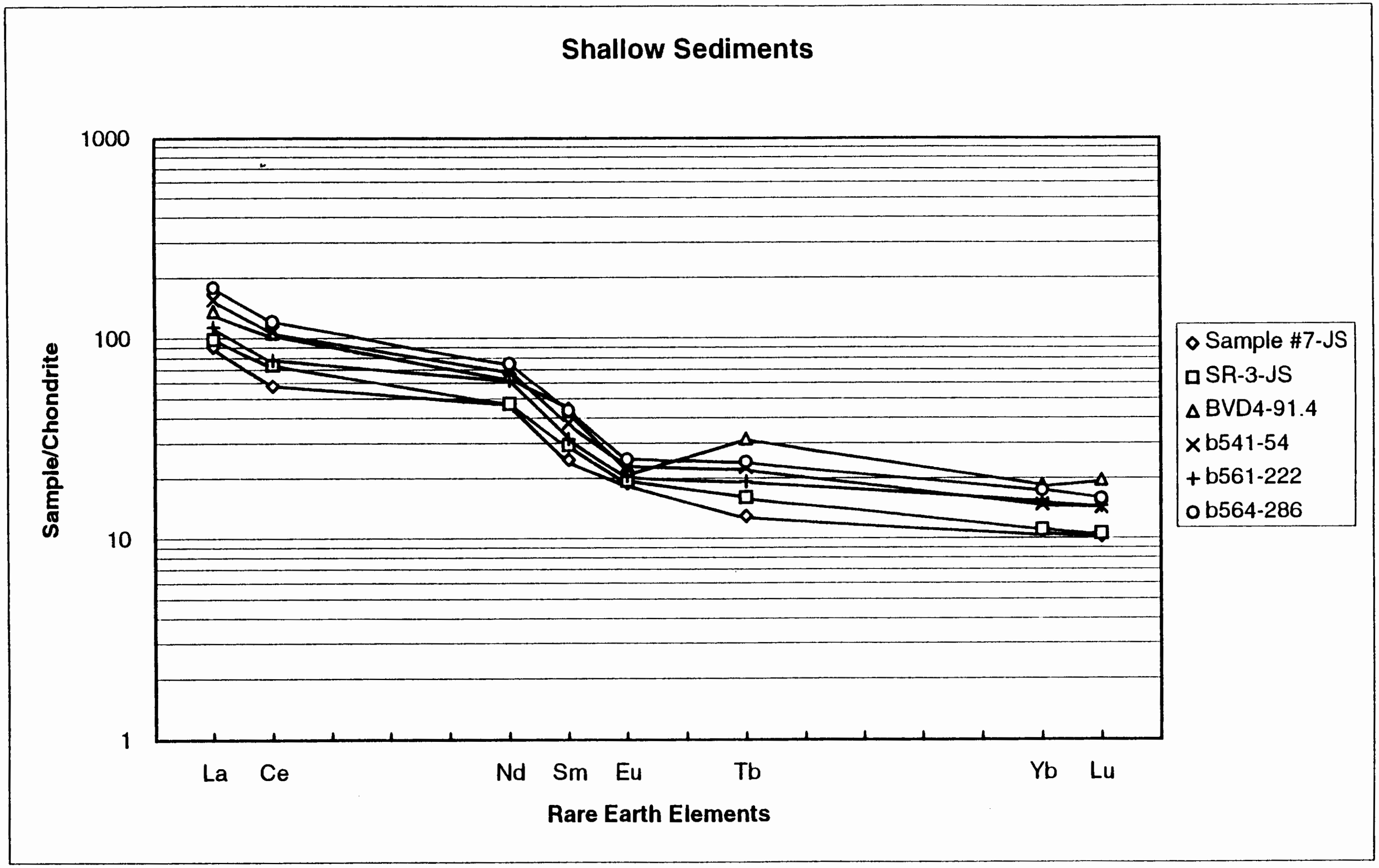

Figure 24. Shallow Sediments Chondrite Plot
(Reed Island Ashes and BVD4-91.4 Sample).

Figure 24. On scatter plots, the two volcanic ash samples tend to plot together (Figures 15-20). The location of the Reed Island ash samples in the Columbia River and their shallow depth (exposed in outcrop on Reed Island during the summer) indicate that these ashes are likely to be local, relatively recent Cascadian ashes. In addition, they consistently plot away from all sediment groups except the young Columbia River sediments (to be discussed in the next section). The Reed Island ashes do not compare with other volcanic ash samples analyzed for this study.

Young Columbia River Sediments

This group is identified primarily using scatter plots. On all but a few plots, six of seven samples (MTD1-30-40, MTD1-50-55, MTD1-105-110, MTD1-155-165, MTD1-225, and MTD2-145-155) plot together in a tight group. The chondrite plot of these samples shows very similar negative slopes from Nd to Tb (Figure 25). These samples also typically have coarse sand to granule size gravel grains including large mica flakes and numerous lithic grains (basalt, quartzite, granite, and andesite). Sample ORD1-19.6 (Figure 4) is a light brown, micaceous sand containing some coarse, black gravelly grains of basalt. It doesn't visually appear to be the same as the above samples and it tends to wander on the scatter plots. The

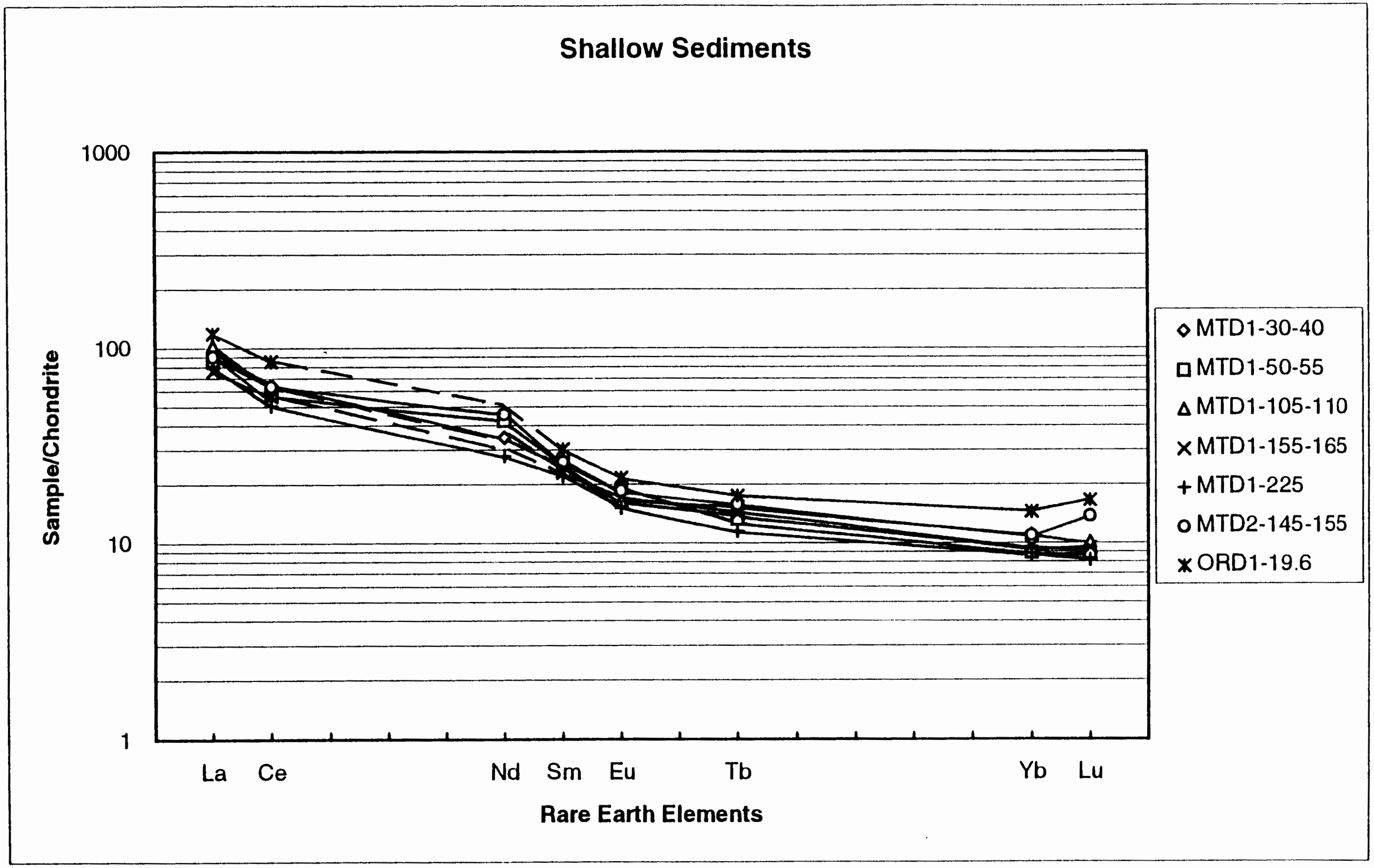

Figure 25. Shallow Sediments Chondrite Plot (Young Columbia River Sediments).

slope of the line for this sample on the chondrite plot compares closely with the above six samples (Figure 25). Thus, it is included in the young Columbia River sediment group.

The geographic location (very near the Columbia River) and stratigraphic position (upper 250 feet of MTD1) of the young Columbia River sediments samples suggest that they represent relatively recent Columbia River channel materials. The position of this group on the scatter plots (Figures 15-20) compares well with the positions of the high-alumina basalt sediments and the rubbly Boring Lava on scatter plots. In particular, on Figures 16 and 17, the young Columbia River sediments and the high-alumina basalt sediments plot in one tight group that does not significantly overlap with the Columbia River source sediments (to be discussed in the next section). This indicates the young Columbia River sediments contain a significant component of younger Cascadian-type materials.

Columbia River Source Sediments

This group is a large and broad representation of the sediments deposited by the Columbia River (Sandy River Mudstone and Missoula Flood deposits), or wind-blown sediment from the Columbia River source area (i.e. the Portland Hills Silt). Though each sediment type may have been deposited under different conditions, they all came from the same general source area; thus their geochemistry is quite similar. None of the samples analyzed in this group were identified on DOGAMI boring logs as Troutdale Formation sediments.

Portland Hills Silt samples are identified only because of sampling location and positive identification of hand samples. The scatter of the four Portland Hills Silt data points within the Columbia River source sediment group shows that they appear to be indistinguishable from the other samples of the Columbia River source sediment group (Figures 15-20).

The chondrite plots of the Columbia River source sediment group show steep, negative slopes from Nd to Eu, then a zero or slightly positive slope from Eu to Tb (Figures 26 and 27). When Columbia River source sediment chondrite plots are compared with volcanic chondrite plots (either CRBG sediments, or high-alumina basalt sediments), the difference in slopes between the groups (sedimentary vs. volcanic) is clearly visible (Figures 21-23).

Two other samples within the Columbia River source sediment should be discussed. First is a sample of pre-CRBG sediment collected from 330 feet of depth in the David Hill Well (DHW-330), located on the western edge of the Tualatin basin (Figure 7). This sample is presumed to have been deposited by the Columbia River prior to the

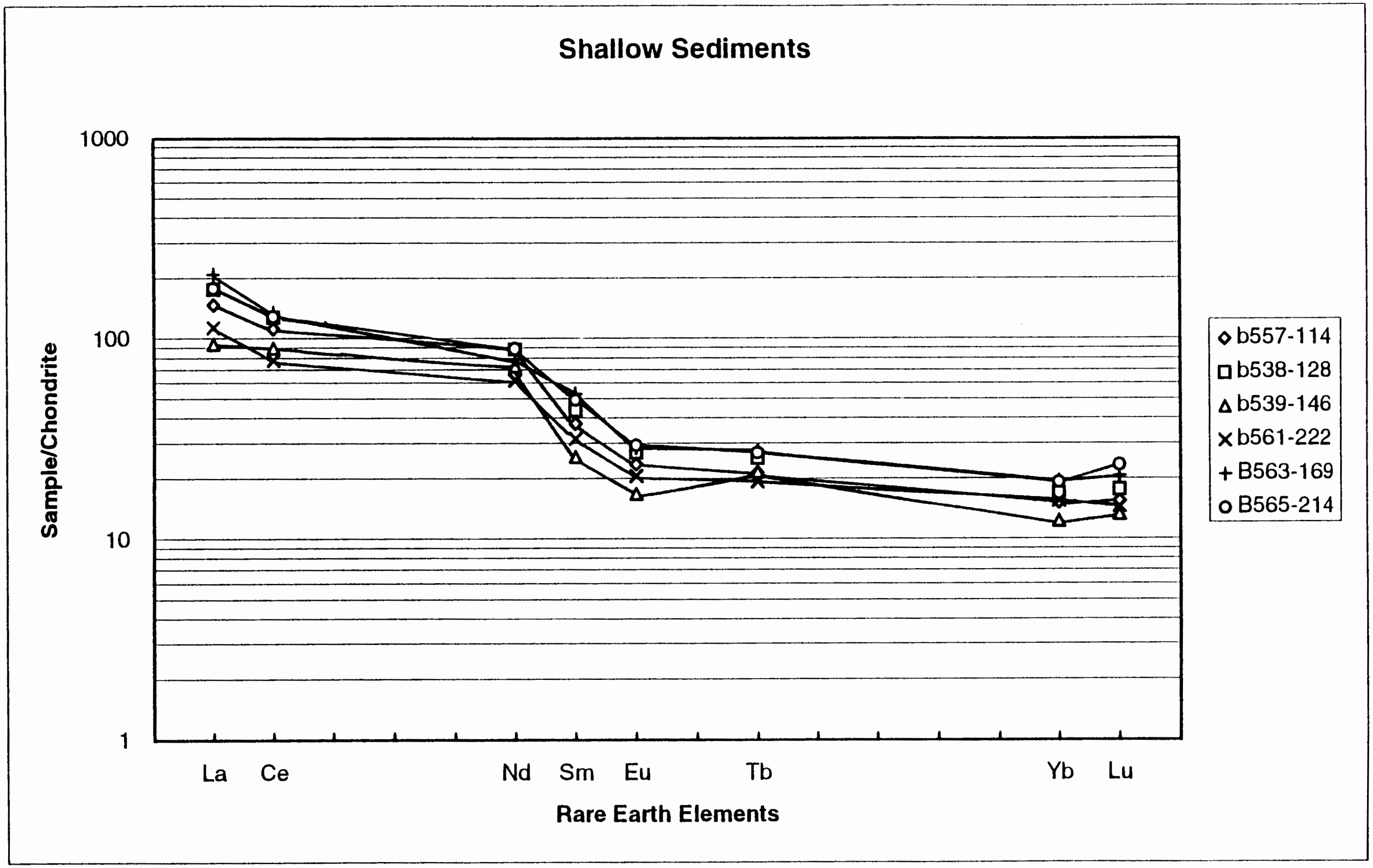

Figure 26. Shallow Sediments Chondrite Plot (Columbia River Source Sediments).

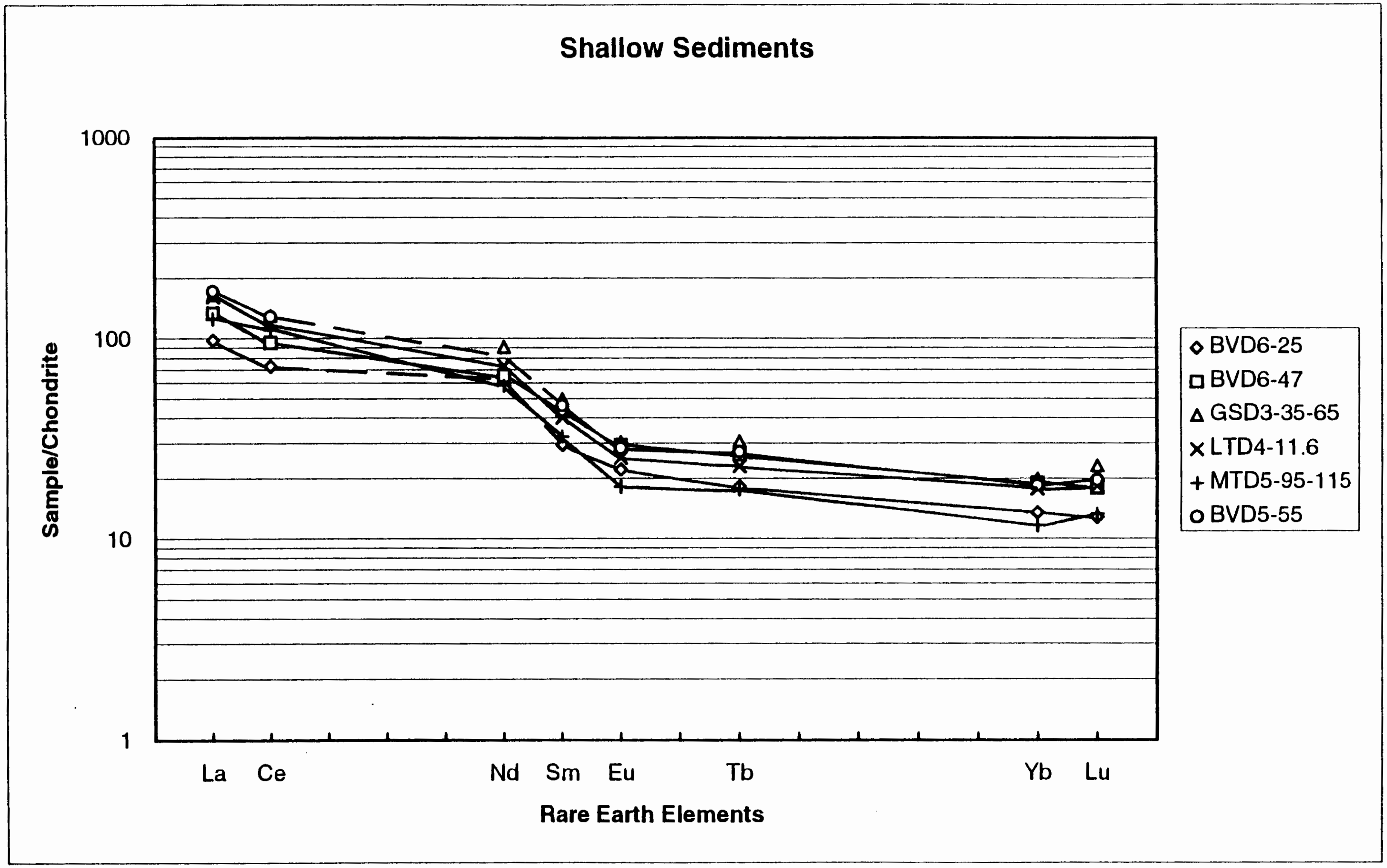

Figure 27. Shallow Sediments Chondrite Plot (Columbia River Source Sediments).

deposition of the CRBG. Consequently, this sample plots with the other Columbia River source sediment samples, and no separate symbol denotes it on the scatter plots.

Second, a thin layer of volcanic ash is identified in BVD4 at 91.4 feet of depth (Figure 4). In hand sample, it is a white, fine-grained, and light-weight material. Though it tends to plot with the Columbia River source sediment group (marked with an X on scatter plots, Figures 15-20), its chondrite plot is noticeably different from the other sediments (Figure 24). A steep, negative slope from Nd to Eu is shown for all of the plotted samples. However, the volcanic ash sample has a positive slope from Eu to Tb, whereas the sediments have zero or continued negative slopes.

PORTLAND INTERNATIONAL AIRPORT DRILL HOLE

The sediment samples collected from the Portland International Airport Drill Hole (MTD1, 1523 feet) represent the materials transported by the Columbia River, into the Portland basin, during and after the eruption and emplacement of the CRBG. Sample geochemistry was compared with hand sample examination to establish geochemical groups. The large amount of volcanic material in many samples made the separation of geochemical units unexpectedly straightforward. Three units are identified and shown on scatter plots of Hf vs. Cr and Hf vs. Th (Figures 28 and 29):

1. young Columbia River sediments,
2. episodic Cascadian volcanic sediments,
3. lower Troutdale Formation.

Young Columbia River Sediments

The arguments for the distinction of the young Columbia River sediment are the same as those presented in the previous section discussing the shallow sediment and miscellaneous samples. One additional sample from the Portland basin sediments is added to the young Columbia River sediment group. MTD1-295-300 was not included in the shallow sediment and miscellaneous sample data set as its depth was greater than 250 feet. However, it does fall neatly into the young Columbia River sediment group on the scatter plots, and has a chondrite plot very similar to the other samples included in that unit.

Episodic Cascadian Volcanic Sediments

This group consists of all samples located between 400 and 800 feet, with the exception of one sample at 575 feet. This group was identified initially by the hand samples, all of which are primarily dark in color. Some samples may even display primary volcanic features and

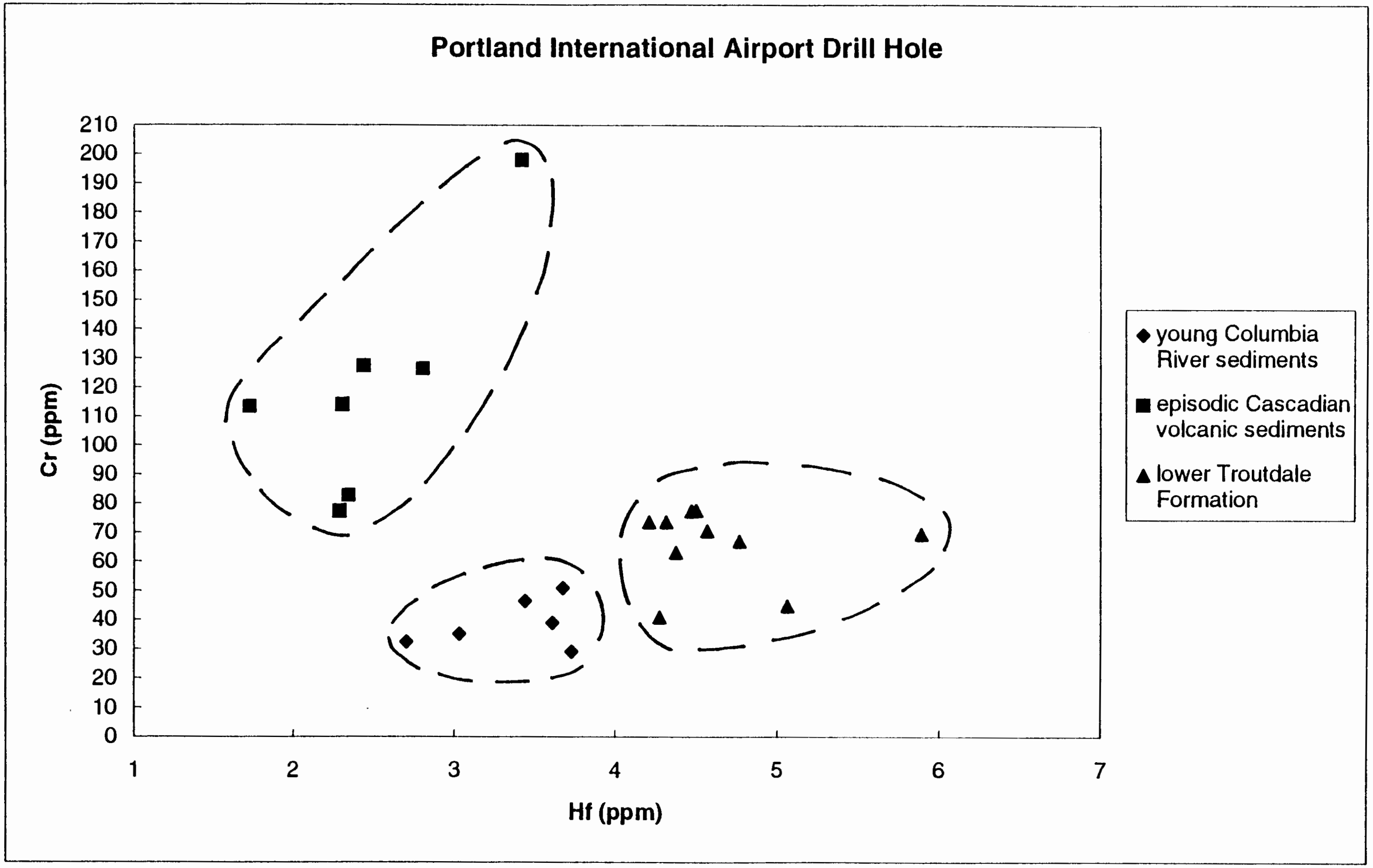

Figure 28. Portland International Airport Drill Hole Scatter Plot (Hafnium vs. Chromium).

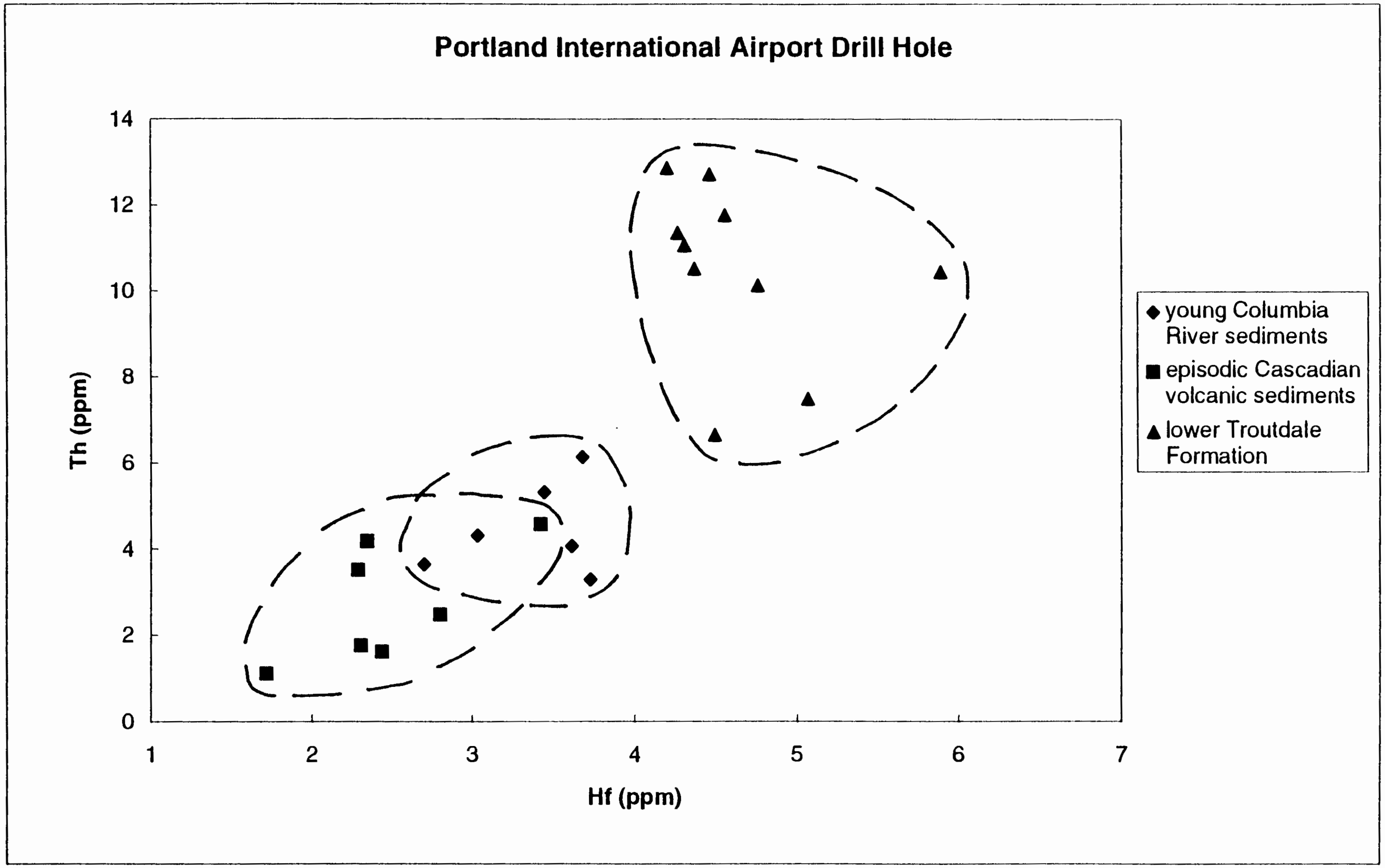

Figure 29. Portland International Airport Drill Hole Scatter Plot (Hafnium vs. Thorium).

textures. The scatter plots confirmed what was visible in the hand samples. The chondrite plots also show that these samples are geochemically similar (Figure 30). Positive slopes from Ce to Nd, negative slopes from Nd to Sm, and zero slopes from Sm to Eu all help to define this particular unit.

The choice of name for this group was based on depth, proximity to the Cascades, and the presence of a non-volcanic sediment layer at 575 feet, indicating at least two episodes in the depositional history. In addition, its geochemistry does not compare with the high-alumina basalt sediments or the CRBG sediments on scatter plots (see Figures 33-35).

Lower Troutdale Formation

This group includes primarily the deeper samples collected from MTD1. The samples from 800 feet of depth and below are considered to be part of the lower Troutdale Formation. Two shallow samples (350-358 feet and 575 feet) are also included in this group, as they generally plot with the other deeper samples on both the scatter and chondrite plots (Figures 28 and 29, and Figures 31 and 32, respectively). This group is identified as the lower Troutdale Formation based on, hand sample inspection, geographic and stratigraphic position, and the description of the lower Troutdale Formation as presented by Tolan and

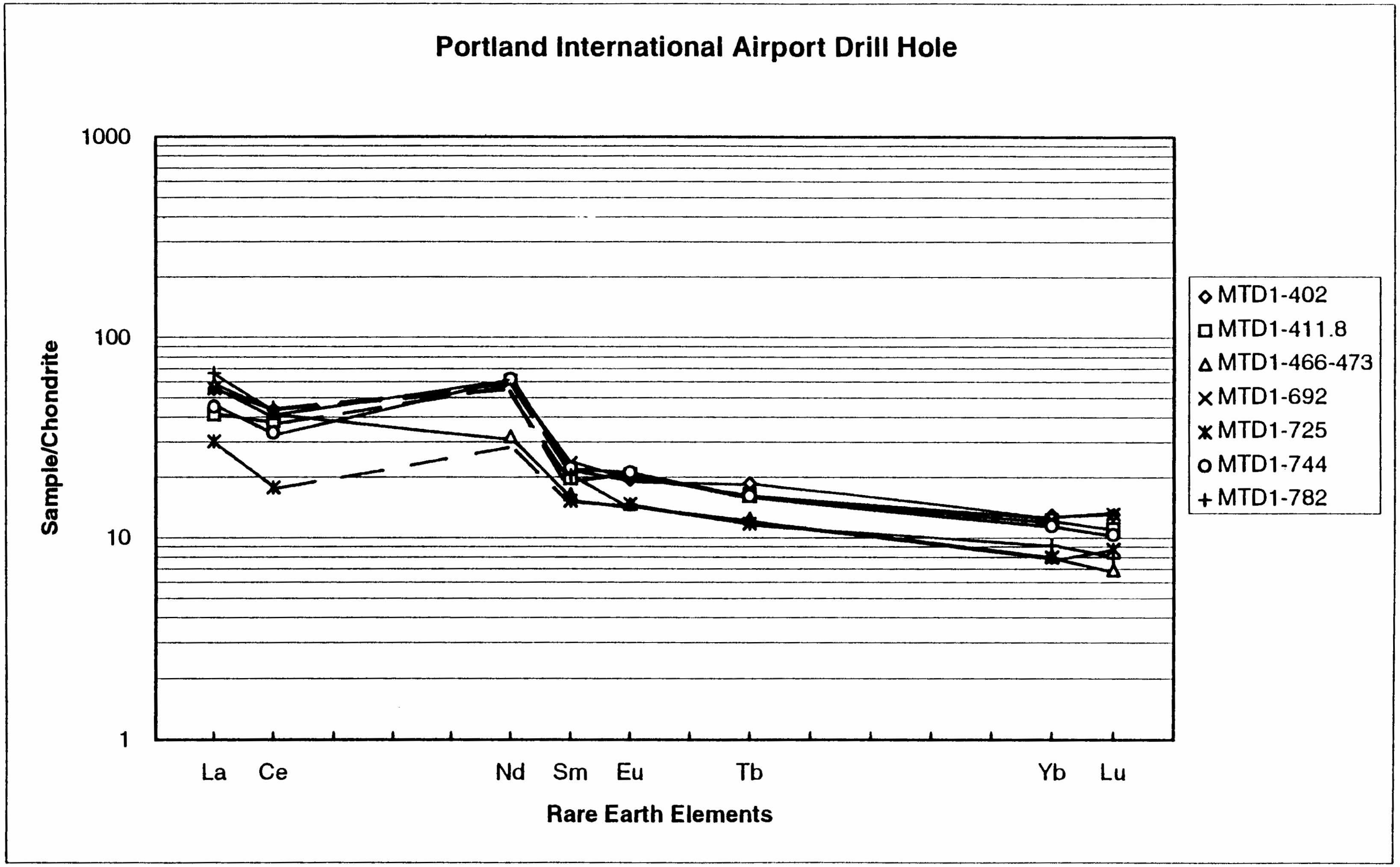

Figure 30. Portland International Airport Drill Hole Chondrite Plot (Episodic Cascadian Volcanic Sediments).

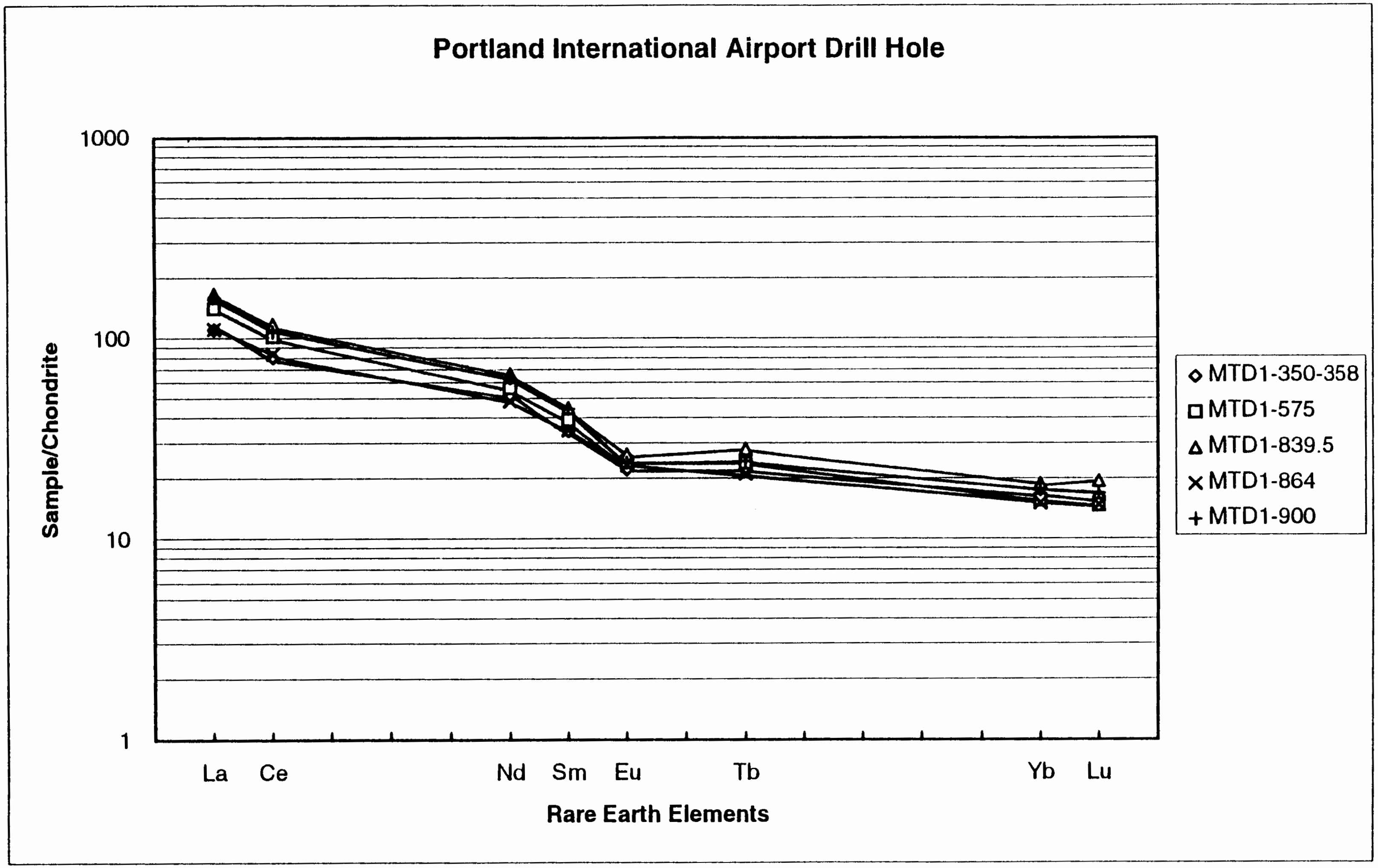

Figure 31. Portland International Airport Drill Hole Chondrite Plot (Lower Troutdale Formation).

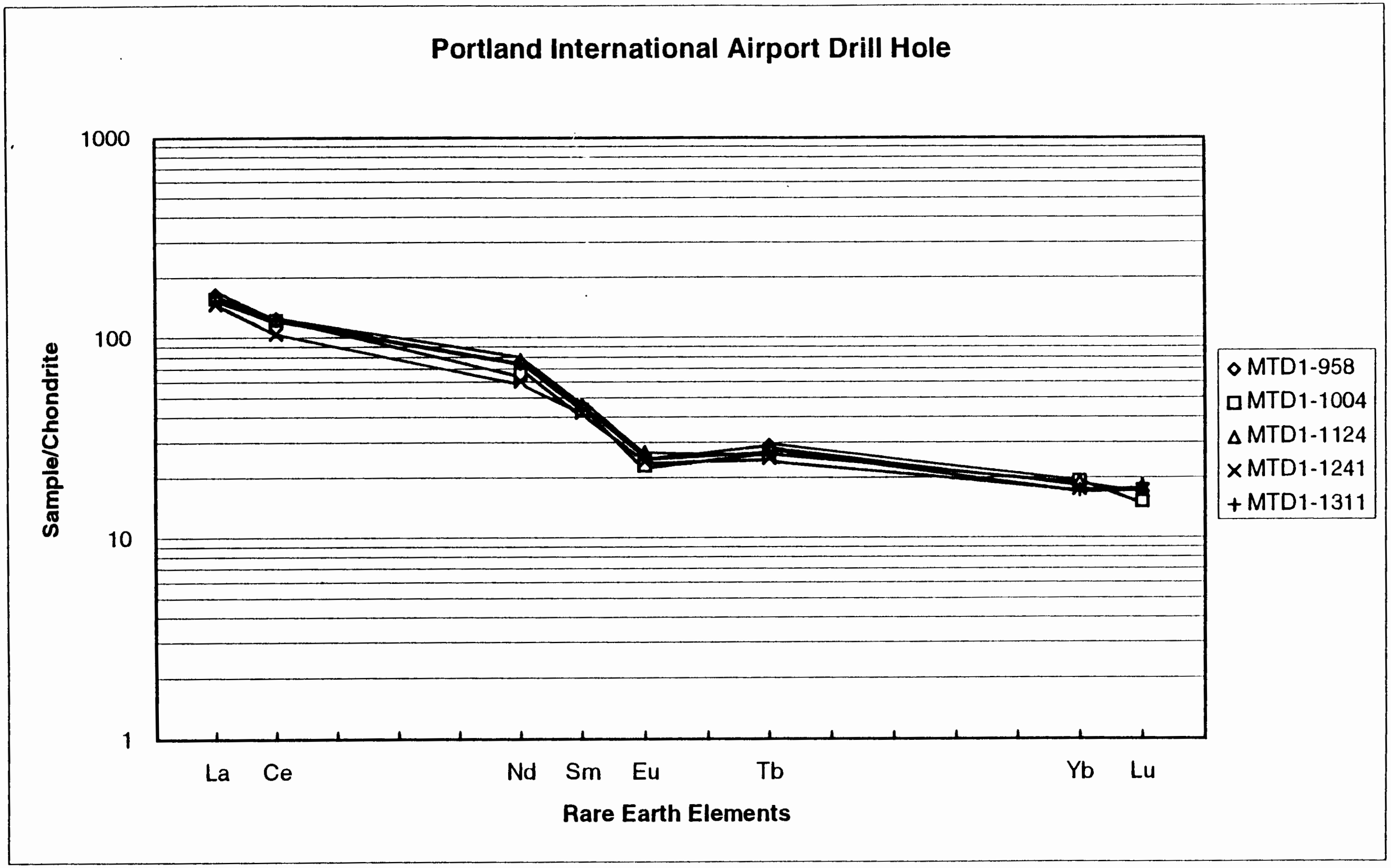

Figure 32. Portland International Airport Drill Hole Chondrite Plot (Lower Troutdale Formation).

Beeson (1984): "...quartzite-bearing, basaltic conglomerates and micaceous arkosic sandstones." Scatter plots for the lower Troutdale Formation show that the samples generally fall within the range of the Columbia River source sediments group. However, on several plots, they seem to be concentrated in one area of the Columbia River source sediment group (Figures 33-35).

HILLSBORO AIRPORT DEEP DRILL HOLE

Sediment samples were collected from the Hillsboro Airport Drill Hole (HBD1, 1095 feet). The source(s) of these sediments is currently unknown. The potential contributors include the Columbia River (both normal depositional material and flood deposits), rivers having source areas in the Coast Range, the Willamette River, and materials eroded from the nearby Tualatin Mountains, including the Boring Lava, CRBG, and loess.

Hand sample examination and geochemistry were unsuccessful in delineating distinct, consistent groups, with two exceptions. The first exception includes two samples collected from approximately 760 feet. They are lightweight, fine-grained, pale green ashy samples that do not visually compare with other samples collected from HBD1. They have a texture distinct from the other sediment samples, and contain no visible mica. Scatter

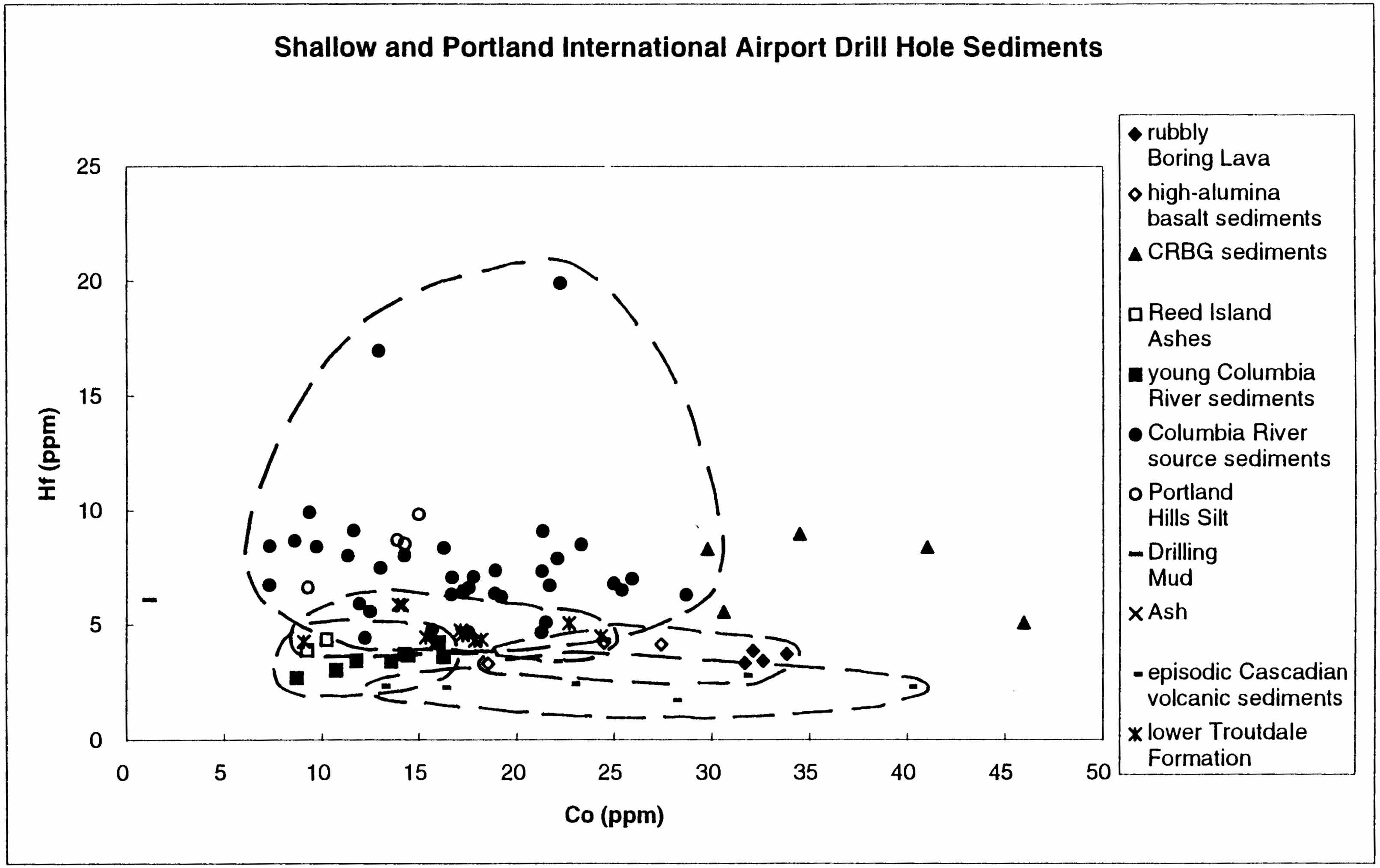

Figure 33. Shallow and Portland International Airport Drill Hole Sediments Scatter Plot (Cobalt vs. Hafnium).

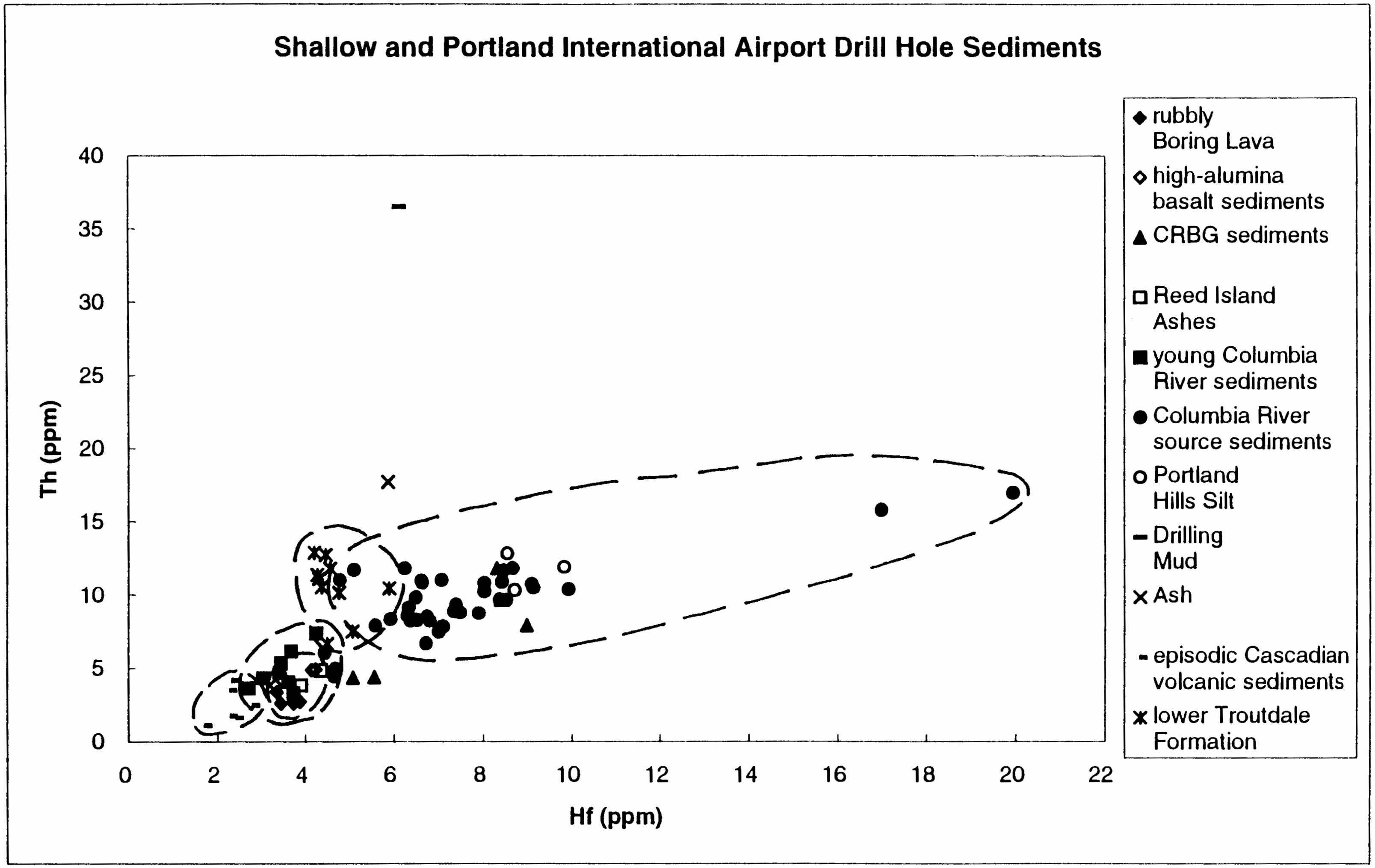

Figure 34. Shallow and Portland International Airport Drill Hole Sediments Scatter Plot (Hafnium vs. Thorium).

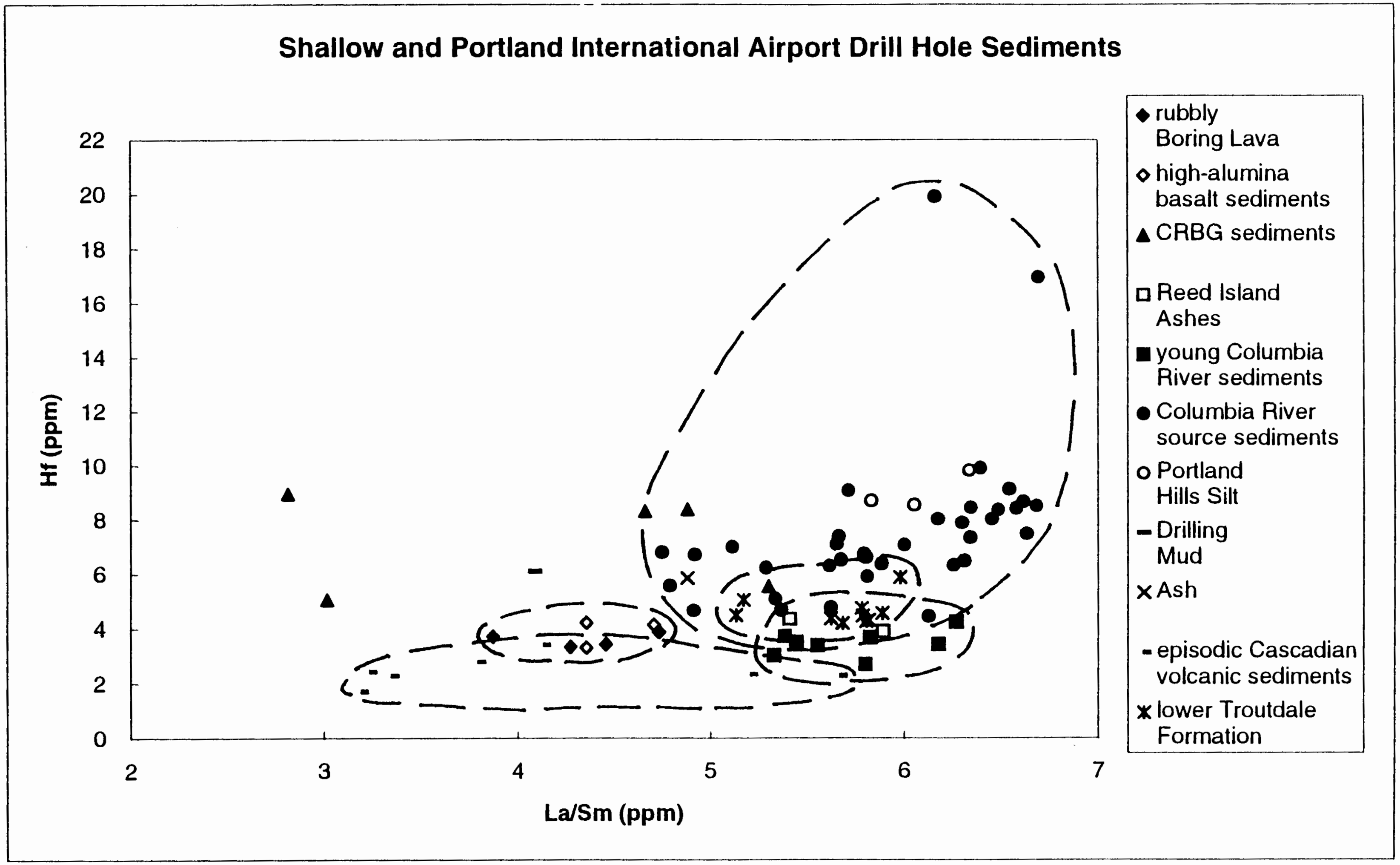

Figure 35. Shallow and Portland International Airport Drill Hole Sediments Scatter Plot (Lanthanum/Samarium vs. Hafnium).

plots show the geochemical differences between these two samples and the other samples from HBD1 (Figures 36 and 37). A chondrite plot also shows unique patterns for these two samples (Figure 38).

The second exception is that samples collected from near the sediment-CRBG contact plotted in widespread positions on the scatter plots in comparison to the majority of the other sediment samples. This widespread scatter is interpreted to indicate that weathering processes have begun to affect the sediments overlying the CRBG (Figures 36 and 37).

The remainder of the samples plotted in one large, broad group. No trends or consistent patterns could be determined from the geochemistry of the Tualatin basin sediments. Visual examination did not identify anything other than fine-grained, micaceous silts, clayey silts, or sandy silts. The samples also do not appear to have the same geochemistry as the Columbia River source sediments (Figures 39, 40, and 41).

These three scatter plots (Figure 39, 40, and 41) compare samples representing some of the key geochemical groups. On Figure 39, the Tualatin basin sediments from HBD1 fall within nearly every geochemical group shown. On Figure 40, the Tualatin basin sediment samples from HBD1 fall within the Columbia River source sediment geochemical

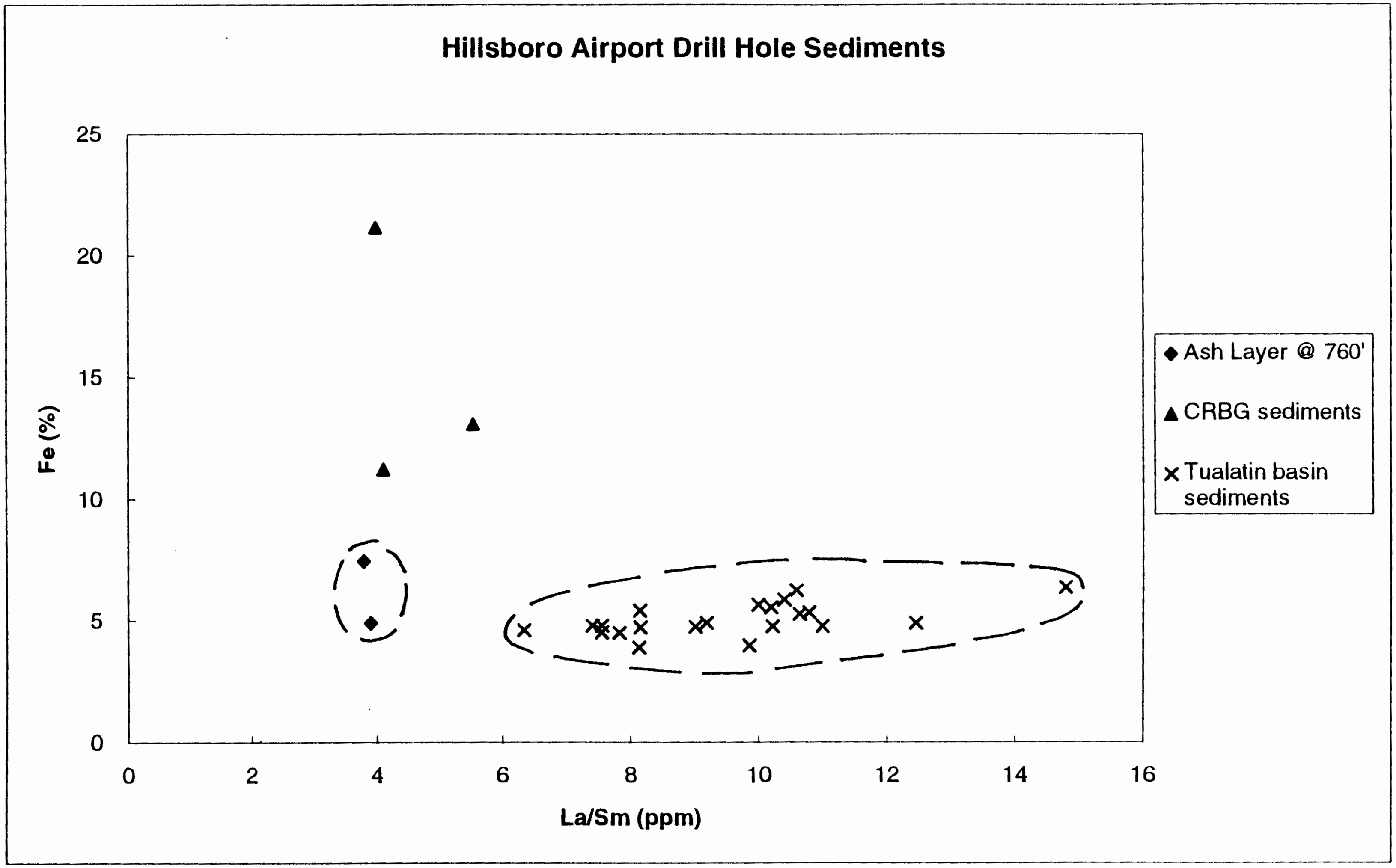

Figure 36. Hillsboro Airport Drill Hole Sediments Scatter Plot (Lanthanum/Samarium vs. Iron).

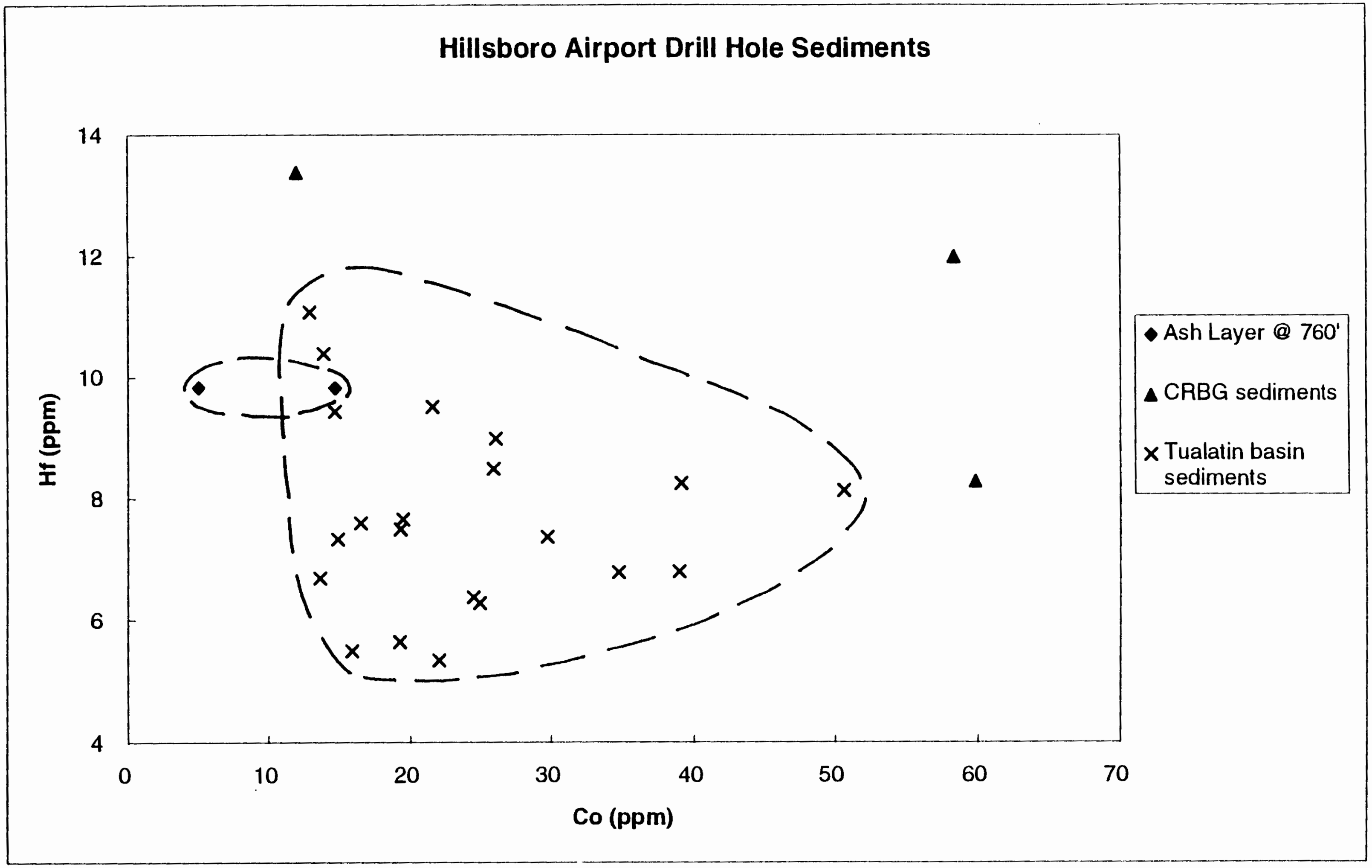

Figure 37. Hillsboro Airport Drill Hole Sediments Scatter Plot (Cobalt vs. Hafnium).

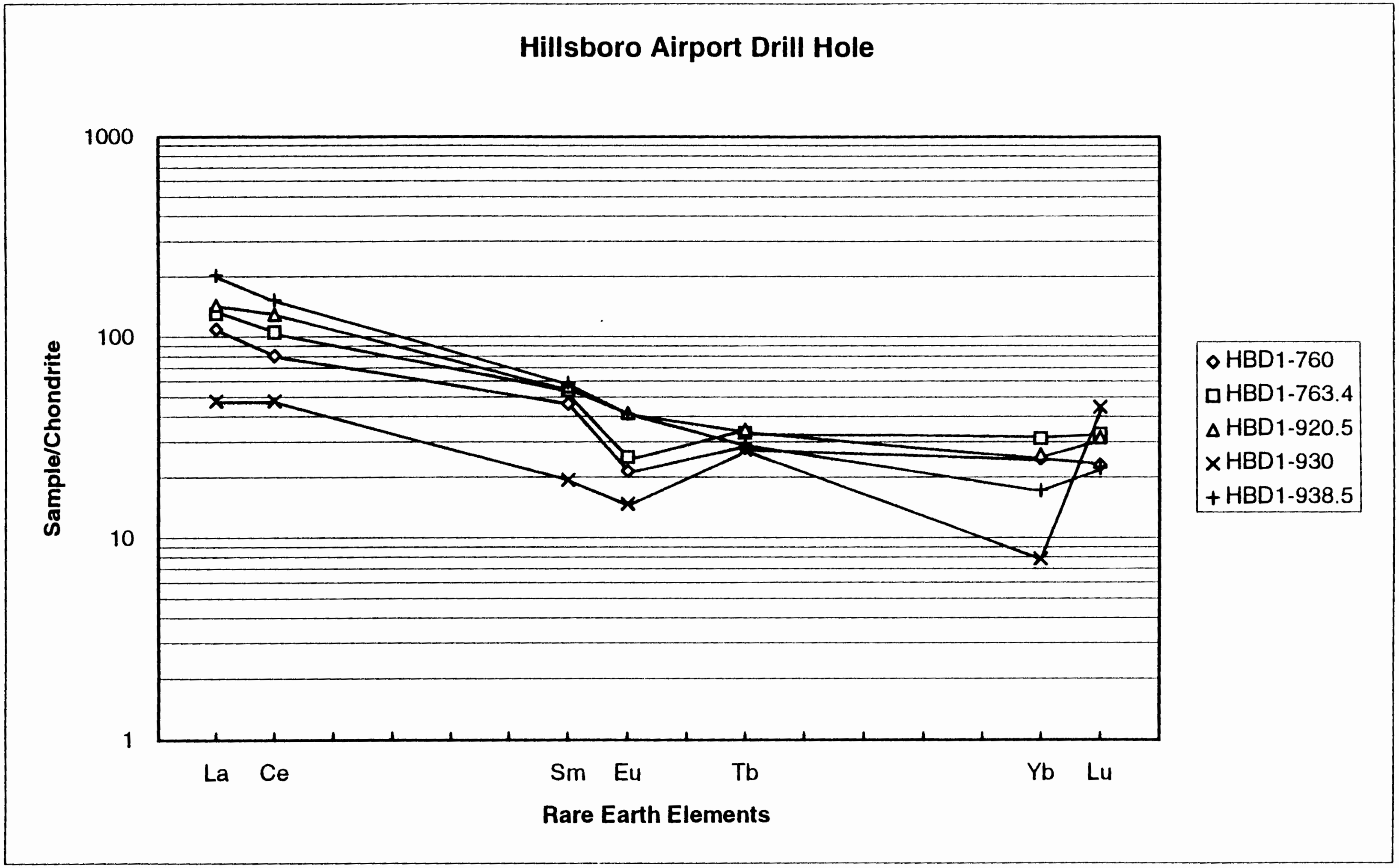

<u>Figure 38.</u> Hillsboro Airport Drill Hole Sediments Chondrite Plot (CRBG Sediments and the ash layer @ 760 feet).

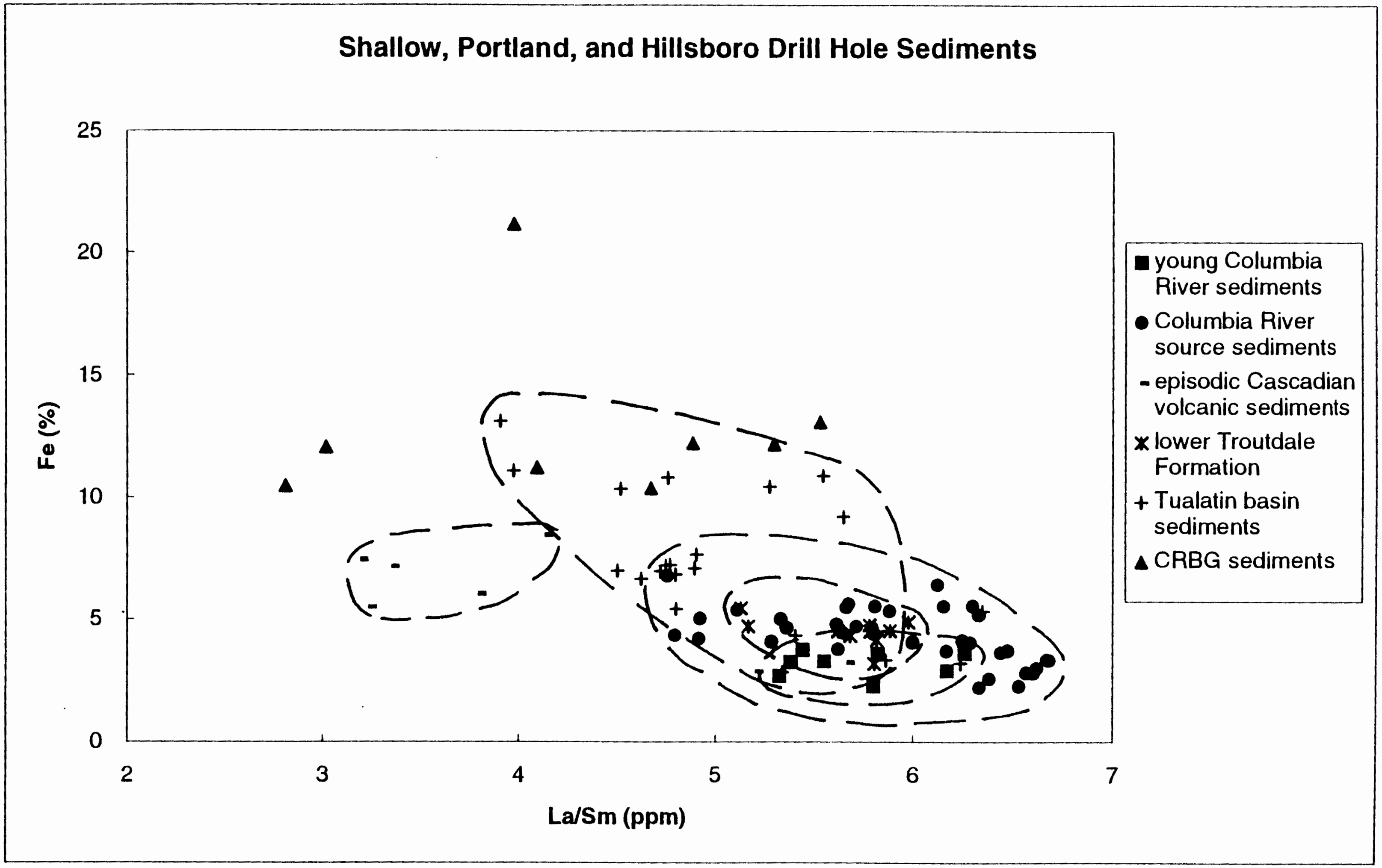

Figure 39. Shallow, Portland, and Hillsboro Drill Hole Sediments Scatter Plot (Lanthanum/Samarium vs. Iron).

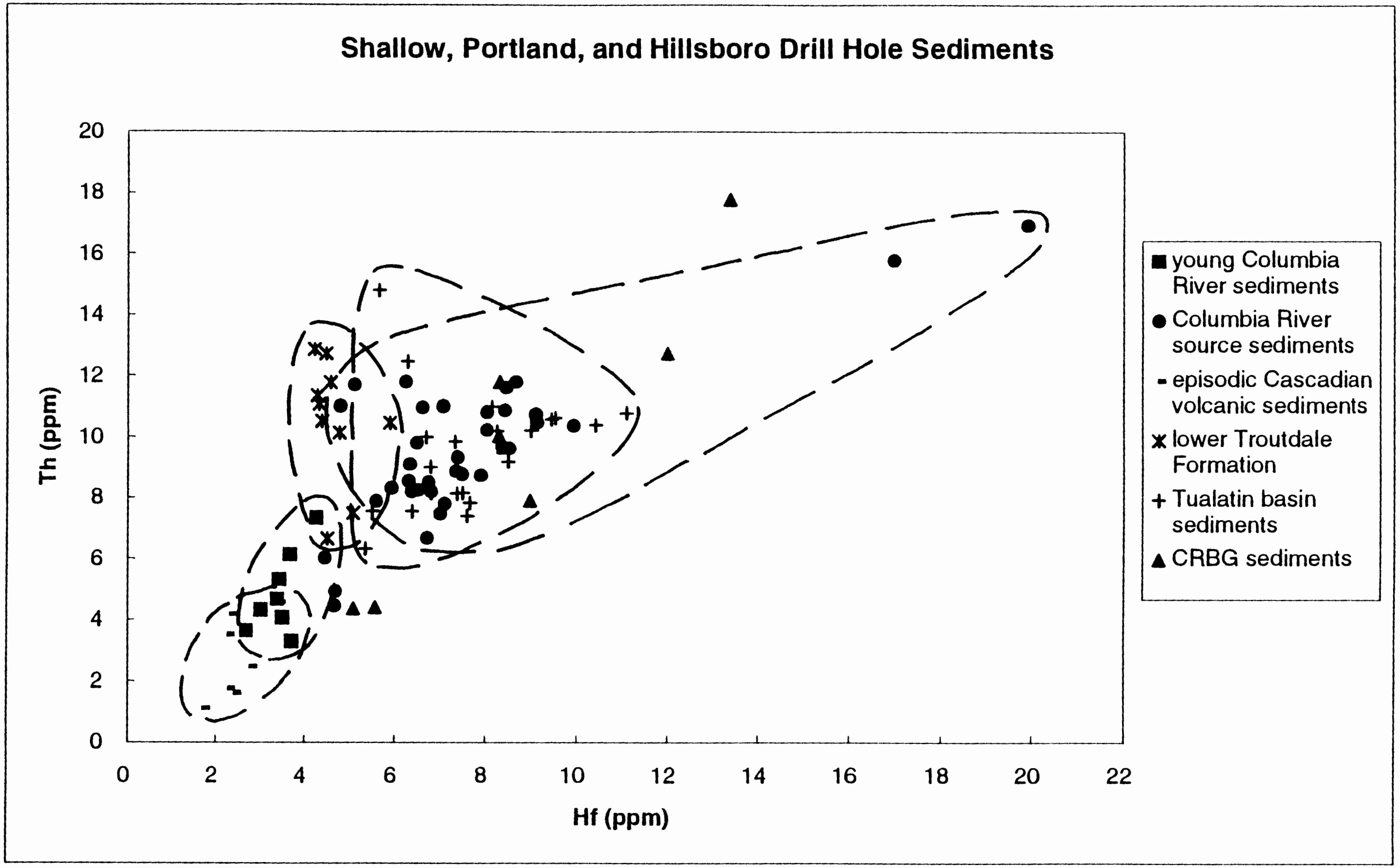

Figure 40. Shallow, Portland, and Hillsboro Drill Hole Sediments Scatter Plot (Hafnium vs. Thorium).

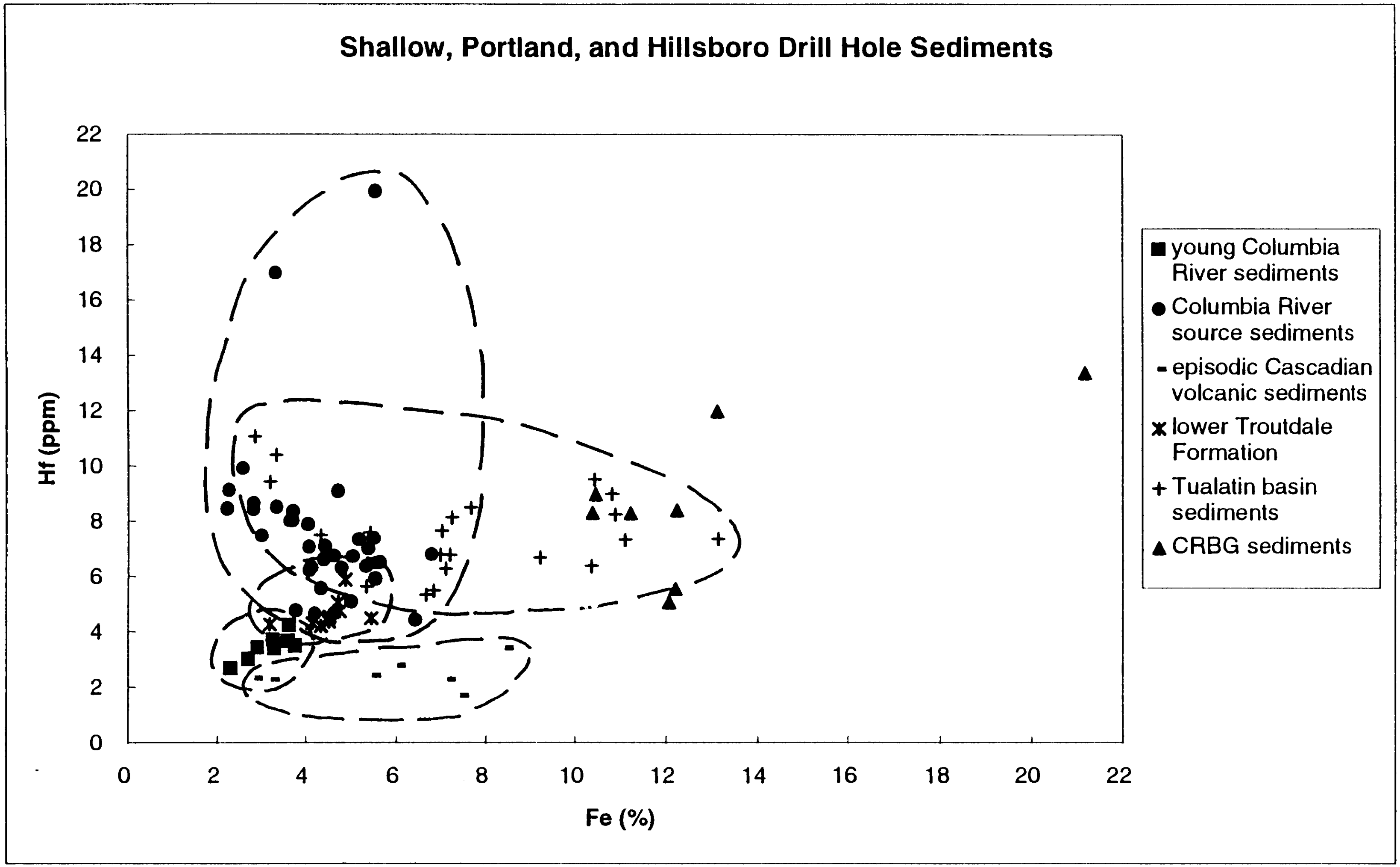

Figure 41. Shallow, Portland, and Hillsboro Drill Hole Sediments Scatter Plot (Iron vs. Hafnium).

group, however, they do not generally occur within the lower Troutdale Formation geochemical group. On Figure 41, the Tualatin basin sediment samples from HBD1 are found within the boundaries of the Columbia River source sediment geochemical and CRBG sediment groups. Although the Tualatin basin sediment samples collected from HBD1 and the Columbia River source sediments may have similar concentrations of some elements, overall, they do not appear to be the same.

The geologic history of the Tualatin basin is currently under investigation (Wilson, 1994; personal communication). The geochemical data generated for the Tualatin basin for this study will be one of numerous additional data sets being collected to examine the stratigraphy and structure of the Tualatin basin.

STATISTICAL ANALYSIS

Basic statistical analyses were completed for the seven identified geochemical groups, which were chosen based on geochemistry, geology, and location. The statistical analyses were completed to show that the chosen geochemical groups are indeed distinguishable from one another. F tests were completed initially to examine the equality of the variances between the groups. Where the F test failed to reject the equality of the variances, T tests were conducted to compare the means of the groups. Statistical analysis is presented in Appendix F.

Complete data sets were not available for all of the analyzed samples. As a result, only those samples having complete data sets were used to calculate the mean for that group. In addition, not all elements that had geochemical data available were used in the comparisons. Element choice was based on the counting error and the completeness of the data. In general, those elements having less than ten percent counting error and complete data sets were used in the statistical analysis. The elements used were Na, Cs, Ba, Fe, Sc, Cr, Co, Hf, Th, La, Ce, Sm, Eu, and Tb.

A total of 24 F tests were performed for the seven geochemical groups, using a 5% significance level. In 16 cases, the equality of the variance was rejected for each set of sediment groups compared. In 8 cases, the equality of the variances was not rejected, and a T test was conducted for that set of sediment groups, also using a 5% significance level. The equality of the means was rejected for each set of sediment groups compared. Thus, the seven, previously discussed groups, can be considered separate, distinct geochemical groups, as listed: (1) Columbia River source sediments, (2) Lower Troutdale Formation, (3) CRBG sediments, (4) Reed Island ashes,

(5) Young Columbia River sediments, (6) High-alumina basalt sediments, and (7) Episodic Cascadian volcanic sediments.

As shown previously in the discussion of the Columbia River source sediments, the Portland Hills Silt did not appear to be distinguishable from the main Columbia River source sediment group on scatter plots, and statistically, it is not. Both F and T tests were conducted comparing these two groups. The equality of the variance and the equality of the mean was not rejected. The primary basis for the identification of the Portland Hills Silt is its distribution, generally located on hilltops at shallow depths.

Also previously considered to be a likely part of the Columbia River source sediment, is the lower Troutdale Formation. The equality of the variance of these two groups was rejected in the F test, resulting in the distinction of the lower Troutdale formation from the Columbia River source sediments. It should be noted that all of the lower Troutdale Formation samples were collected from MTD1. In order to confirm that the lower Troutdale Formation is conclusively a distinct geochemical group, samples from other locations should be collected and analyzed to increase the geographic distribution over which the statistical analyses are conducted.

DISCUSSION

The seven previously discussed groups can be placed into three major geochemical categories as follows:

1. Columbia River or continental source

    * Columbia River source sediments
    * lower Troutdale Formation

2. Cascadian or local volcanic source

    * young Columbia River sediments
    * Reed Island ashes
    * high-alumina basalt sediments
    * episodic Cascadian volcanic sediments

3. Soils/sediments developed on a given rock type

    * CRBG sediments

These three major geochemical categories, and the groups listed under them as identified in this study, can be placed into the current understanding of Portland area stratigraphy.

Materials deposited from the Columbia River or continental source include the Sandy River Mudstone, the lower Troutdale Formation, the Portland Hills Silt, and the Missoula Flood deposits. As stated previously, the Columbia River source sediment group defined in this study, includes the Sandy River Mudstone, the Portland Hills Silt, and the Missoula Flood deposits. In addition, those samples of sediment collected along the tunnel alignment from the TriMet drill core, are included in this group. In particular, the two sediment layers between the

Boring Lava units could represent a Portland Hills Silt-type depositional material (i.e. wind-blown), based on radiometric ages of the Boring Lavas and the fine grained, massive nature of the sediments. Geochemically, the Columbia River source sediments and lower Troutdale Formation are all very similar.

Materials representing a Cascadian or local source include the Clackamas River terraces and alluvium of Madin (1990), and the upper Troutdale Formation, the fluvial deposits and debris flows, and alluvium of Tolan and Beeson (1993).

The Reed Island ashes and the young Columbia River sediment are considered to be a part of the alluvium unit described by both Madin (1990) and Tolan and Beeson (1993). Both geochemical groups are interpreted to be relatively young sediments based on their stratigraphic positions. The Reed Island ashes are geochemically similar to the young Columbia River sediments because the Reed Island ashes have likely been reworked by the Columbia River (Figures 15-20 and 33-35). The young Columbia River sediments are geochemically distinct from the Columbia River source sediments, as shown on Figures 16 and 17. The probable reason for this is the contribution of Cascadian-type materials to the Columbia River, introduced during the uplift of the Cascades within the last 2-3 Ma

(Beeson and Tolan, 1990). The beginning of the uplift of the Cascades is considered to mark the end of Troutdale Formation deposition (Tolan and Beeson, 1984). The young Columbia River sediments, deposited during the uplift of the Cascades represent post-Troutdale deposition.

The high-alumina basalt sediments are considered a part of the Clackamas River terraces of Madin (1990) and/or the fluvial deposits and debris flows of Tolan and Beeson (1993). As stated previously, two of the three samples in this geochemical group are located near rivers (the Columbia and Clackamas Rivers) that would be carrying Cascadian material. The third sample is located at the base of Mt. Scott, on its west side, and is representative of the erosion of Boring Lava from Mt. Scott.

The episodic Cascadian volcanic sediments may represent the portions of the hyaloclastite layers observed in the upper Troutdale Formation by Tolan and Beeson (1984), and Swanson (1986). Hoffstetter (1984) also notes the presence of hyaloclastite beds in the hydrogeologic units that he presents. The episodic Cascadian volcanic sediments occur in the Portland International Airport Drill Hole (MTD1) at approximately 400 to 800 feet, with a non-volcanic unit occurring at 575 feet. The hyaloclastite beds examined by Swanson (1986), occur in the Portland well field exploratory wells, nearest to MTD1, at approximately 300 to 700 feet, with non-hyaloclastite material beginning between 500 to 550 feet and ending between 550 to 700 feet. The hyaloclastite beds observed by Hoffstetter (1984), occur in the Portland well field wells, nearest to MTD1, at approximately 350 to 600 feet (600 feet is the maximum depth shown on the cross section by Hoffstetter, 1984), and include the Troutdale Sandstone Aquifer and the Rose City Aquifer. A confining unit that contains no hyaloclastite material, the Rose City Aquitard, separates the two aquifers at approximately 400 to 500 feet. Table VII compares the approximate depths of volcanic or hyaloclastite materials in the wells examined for each study.

Table VII. Comparison of the depth of occurrence of volcanic or hyaloclastite materials in wells examined by Hoffstetter (1984) and Swanson (1986) near MTD1.

Author	Hoffstetter (1984)	Swanson (1986)	Barnes (1995)
Hyaloclastite /Volcanic Unit	350 to 400 feet	300 to 500-550 feet	400 to 575 feet
Non-hyaloclastite Unit	400 to 500 feet	500-550 to 550-700 feet	575 feet
Hyaloclastite /Volcanic Unit	500 to 600 feet	550 to 700 feet	575 to 800 feet

The depths at which the volcanic materials occur, as determined in each study, show a good correlation. This would seem to indicate that the episodic Cascadian volcanic sediments identified in this study are indeed correlative to the hyaloclastite units described by Hoffstetter (1984) and Swanson (1986). If this is the case, then that makes the episodic Cascadian volcanic sediments a part of the upper Troutdale Formation.

The last of the three major geochemical groups represents soils and/or sediments located directly on top of solid rock units. In particular, several sediment samples collected overlying CRBG rock have been shown, geochemically, to represent weathered or residual CRBG material.

Having discussed the geochemistry of the collected samples, and placed the units defined in this study into the current stratigraphic framework, it is apparent that the sediment packages of the Portland and Tualatin basins are quite different. Finer grained volcanic sediments were identified in the Tualatin basin, while both fine and coarse grained volcanic sediments were identified in the Portland basin. This would seem logical as the Portland basin is geographically closer to the Cascades than is the Tualatin basin. The variable appearance of the sediments in the Portland International Airport Drill Hole (MTD1), compared to the generally uniform appearance of the sediments in the Hillsboro Airport Drill Hole (HBD1), can be attributed to the proximity of MTD1 to an active river channel and volcanic arc.

The differences in the grain size of the sediments observed in each basin might also be attributed to the difference in the types of source rock that contribute to the load carried by rivers draining into the two basins. The materials being transported by the Columbia River (before dams) tend to be of larger grain sizes due to the plutonic/granitic-type rock over which the Columbia River flows. Plutonic or granitic types of rock generally break down to sand-sized grains. The Tualatin basin does not currently receive depositional materials from the Columbia River, and no plutonic/granitic-type source rocks are present in the drainages that empty into the Tualatin basin.

In addition, the rise of the Tualatin Mountains would have effectively separated the basins, and likely routed an ancestral Columbia River around them to the north, much as it flows today. The result of the new path of the Columbia River would prevent the distribution of similar depositional materials throughout the two basins. It is possible that the rise of the Tualatin Mountains took place early on in the history of the two basins. As stated before, the two basins are lithilogically distinct. As shown previously on the scatter plots (Figure 39-41) and in the Hillsboro Airport Drill Hole discussion, the sediments from the Hillsboro Airport Drill Hole do not tend to plot consistently with the other geochemical groups identified in the Portland basin.

Several large differences in the sediment packages of the two basins are obvious. First, the volcanic ash unit identified at 760 feet in HBD1 is not identified in MTD1. The volcanic ash layer in HBD1 is approximately 3 feet thick, and likely represents a large volcanic eruption, that should be observed throughout the Portland area. However, because MTD1 is located so close to the Columbia River channel, it is likely that the Columbia River had a direct affect on what materials would be preserved in the area of MTD1. It is entirely possible that the Columbia River eroded away the record, in MTD1, of the volcanic ash observed at 760 feet in HBD1.

Likewise, the young Columbia River sediment and episodic Cascadian volcanic sediments are present only in the Portland basin. Again, the proximity of MTD1 to the Columbia River channel is the likely reason. Both units were deposited by the Columbia River, and if the Tualatin Mountains did rise early, then the sediments deposited by the Columbia River would not have been transported into the Tualatin basin.

It is also possible that the volcanic ash layer in HBD1, and the episodic Cascadian volcanic sediments in the MTD1 different phases or stages in one or more volcanic periods of the Cascades. The volcanic ash may be a distal deposit of a large explosive eruption, while the episodic Cascadian volcanic sediments may represent more proximal materials deposited and eroded nearer the river, or deposited directly in the river. Even though both basins may have been separate basins early on during post-CRBG time, their stratigraphy may be tied together by one or more of these types of large-scale events.

CONCLUSIONS

The purpose of this study was to analyze volcanic rock and sediment samples using INAA to produce geochemical data useful in better understanding the geologic history of the Portland area. In the case of the volcanic rock, the INAA geochemistry was used in conjunction with three other data sets to identify the distribution of Boring Lava along the west side of the Tualatin Mountains, near Highway 26. Three flows were identified: the Boring Lava of Barnes Road, the Boring Lava of Sylvan Hill, and the Boring Lava of Cornell Mountain. Geochemistry, radiometric age, and magnetic polarity data allowed a surface map and a cross section to be presented for portions of that area.

In the case of the sediment samples, INAA geochemistry allowed the identification of seven geochemical sediment groups. These seven groups can be placed into three major geochemical categories:

Columbia River or continental source

1. Columbia River source sediments
2. lower Troutdale Formation

Cascadian or local source

3. young Columbia River sediments
4. Reed Island ashes
5. high-alumina basalt sediments
6. episodic Cascadian volcanic sediments

Soils/sediments developed on a given rock type

7. CRBG sediments

All seven of the groups were identified in the Portland basin. Only one of the seven groups (CRBG sediments) was identified at the base of the Hillsboro Airport Drill Hole (lower 200 feet) in the Tualatin basin. Data obtained for the additional Hillsboro Airport Drill Hole samples showed no trends or patterns, with the exception of the volcanic ash layer at 760 feet. This volcanic ash layer was not observed in the Portland basin.

Two main conclusions can be suggested about the history of the Portland and Tualatin basins. The first is that the two basins are distinct, and have been since early in post-CRBG time. Visually and geochemically, their sediment packages are very different. The second conclusion is that the position of MTD1 in relation to the current and ancestral Columbia River channels, and in relation to the Cascades (an active volcanic arc) would provide the opportunity for a more varied sediment record to be preserved over time. The Tualatin basin is located farther from the Cascades, and is not cut by the river that is the channel through which all the waters of the

Columbia River drainage basin must eventually flow to reach the Pacific Ocean.

Finally, each of the seven sediment groups was able to be placed into the current stratigraphic framework of Madin (1990) and Tolan and Beeson (1993). The Columbia River source sediment group includes the Portland Hills Silt, Sandy River Mudstone, and Missoula Flood deposits. The lower Troutdale Formation is clearly a part of the Troutdale Formation. The young Columbia River sediments and the Reed Island ashes are considered a part of the recent alluvium described by both Madin (1990) and Tolan and Beeson (1993). The high-alumina basalt sediments are interpreted to represent the Clackamas River terraces of Madin (1990) and/or the fluvial deposits and debris flows of Tolan and Beeson (1993). The episodic Cascadian volcanic sediments are believed to be a part of the upper Troutdale Formation.

Based on the identification of the seven geochemical groups and their locations within the Portland basin, it has been demonstrated that INAA is an effective tool for working out stratigraphy in the Portland area. Based on the placement of those seven groups into three broad geochemical categories, it has been demonstrated that INAA is also an effective tool for addressing questions regarding Portland area geologic history.

FUTURE WORK

In general, more questions seem to be generated from research than are answered. This study is no different. Many additional areas of study would further our understanding of the geology and geologic history of the Portland area. Several projects are listed below:

1. Increasing the number of samples analyzed for the sediment groups. Now that the groundwork has been laid, additional sampling based on the results of this study would aid in more precisely defining the positions, vertically and horizontally, of geochemical units.

2. The Tualatin basin sediments seem to remain a mystery. Additional analyses of Tualatin basin sediments and possible source areas may clarify the situation.

3. The shallow sediments in the Portland and Tualatin basins have been generally characterized. However, those samples primarily represent the upper 300 feet of material, and in many cases much less. Also, in

most cases, only one sample per shallow drill hole was analyzed. A more complete sampling of the shallow drill holes would provide additional information in studying basin stratigraphy.

4. The grain size of the analyzed samples could be determined to identify any relation between grain size and geochemistry. In addition, the percentage of volcanic material could be quantified to determine at approximately what percentage a sediment will indicate a volcanic source area (provenance).

5. Additional samples of Boring Lava should be collected along the western side of the Tualatin Mountains to determine the extent of the oldest reverse flow of Cornell Mountain, and to identify what type of Boring Lava lies to the northwest.

REFERENCES CITED

Allen, J. E., 1975, Volcanoes of Portland, Oregon: The Ore Bin, v. 37, n. 9, p. 145-157.

Balsillie, J. H. and Benson, G. T., 1971, Evidence for the Portland Hills Fault: The Ore Bin, v. 33, n. 6, p. 109-118.

Beeson, M. H., 1993, personal communication.

Beeson, M. H., Johnson, A. G., and Moran, M. R., 1975, Portland environmental geology--fault identification: United States Geological Survey Earthquakes Hazards Reduction Program Final Technical Report, 107p.

Beeson, M. H., Fecht, K. R., Reidel, S. P., and Tolan, T. L., 1985, Regional Correlations within the Frenchmen Springs member of the Columbia River Basalt Group; New insights into the middle Miocene tectoncis of northwestern Oregon: Oregon Geology, v. 47, n. 8, p. 87-96.

Beeson, M. H., Tolan, T. L., and Anderson, J.L., 1989, The Columbia River Basalt Group in western Oregon; Geologic structures and other factors that controlled flow emplacement patterns: Geological Society of America Special Paper 239, p. 223-246.

Beeson, M. H. and Tolan, T. L., 1990, The Columbia River Basalt Group in the Cascade Range: A middle Miocene reference datum for structural analysis: Journal of Geophysical Research, v. 95, n. B12, p. 19,547-19,559.

Beeson, M. H., Tolan, T. L., and Madin, I. P., 1991, Geologic map of the Portland Quadrangle, Multnomah and Washington Counties, Oregon, and Clark County, Washington: Oregon Department of Geology and Mineral Industries Map GMS 75, 1:24,000.

Bhatia, M. R. and Taylor, S. R., 1981, Trace-element geochemistry and sedimentary provinces: A study from the Tasman Geosyncline, Australia: Chemical Geology, v. 33, p. 115-125.

Blakely, R. J., Wells, R. E., Yelin, T. S., Madin, I. P., and Beeson, M. H., 1995, Tectonic setting of the Portland-Vancouver area, Oregon and Washington: Constraints from low-altitude aeromagnetic data: Geological Society of America Bulletin, v.107, n. 9, p. 1051-1062.

Conrey, R., 1995, personal communication.

Ekambarum, V., Kawabe, I., Tanaka, T., Davis, A. M., and Grossman, L., 1984, Chemical compositions of refractory inclusions in the Murchison C2 chondrite: Geochimica et Cosmochima Acta, v. 48, p. 2089-2105.

Frank, F. J. and Collins, C. A., 1978, Groundwater in the Newberg area, Northern Willamette Valley, Oregon: United States Geological Survey Groundwater Report No. 27.

Hart, D. H. and Newcomb, R. C., 1965, Geology and ground water of the Tualatin Valley, Oregon: United States Geological Survey Water-Supply Paper 1697, 169p.

Hoffstetter, W. H., 1984, Geology of the Portland Well Field: Oregon Geology, v. 46, n. 6, p. 63-67.

Hogenson, G. M. and Foxworthy, B. L., 1965, Ground water in the east Portland area, Oregon: United States Geological Survey Water-Supply Paper 1793, 78p.

Hooper, P. R., 1982, The Columbia River basalts: Science, v. 215, no. 4539, p. 1463-1468.

Kadri, M. M., Beeson, M. H., and Van Atta, R. O., 1983, Geochemical evidence for changing provenance of Tertiary formations in northwestern Oregon: Oregon Geology, v. 45, p. 20-22.

Madin, I. P., 1990, Earthquake-hazard geology maps of the Portland metropolitan area, Oregon: Oregon Department of Geology and Mineral Industries Open-File Report 0-90-2, 21p.

Madin, I. P., Priest, G. R. , Mabey, M. A., Malone, S., Yelin, T. S., and Meier, D., 1993, March 25, 1993, Scotts Mills earthquake - western Oregon's wake-up call: Oregon Geology, v. 55, n. 3, p. 51-57.

McLennan, S. M. and Taylor, S. R., 1980, Th and U in sedimentary rocks: crustal evolution and sedimentary recycling: Nature, v. 285, p. 621-624.

Muecke, G. K., ed., 1980, Short Course in Neutron Activation Analysis in the Geosciences: Mineralogical Society of Canada, Halifax, Nova Scotia, 279p.

Piper, D., 1974, Rare earth elements in the sedimentary cycle: A summary: Chemical Geology, v.14, p.285-304.

PSU, 1987, Portland State University radiation safety program: Portland State University, Portland, Oregon, 15p.

PSU, 1993, Advanced Geochemistry Class (G519): Portland State University, Portland, Oregon.

Schlicker, H. G., Deacon, R. J., and Twelker, N. H., 1964, Earthquake geology of the Portland area, Oregon: The Ore Bin, v. 26, n. 112, p. 209-230.

Schlicker, H. G. and Deacon, R. J., 1967, Engineering geology of the Tualatin Valley Region, Oregon: Oregon Department of Geology and Mineral Industries Bulletin 60, 87p.

Squier Associates, 1992, Westside Light Rail Tunnel Geotechnical Interpretive Report: Prepared for Tri-county Metropolitan Transport District Oregon.

Swanson, R. D., 1986, A stratigraphic-geochemical study of the Troutdale Formation and Sandy River Mudstone in the Portland Basin and lower Columbia River Gorge: Portland, Oregon, Portland State University master's thesis, 103p.

Tolan, T. L. and Beeson, M. H., 1984, Intracanyon flows of the Columbia River Basalt Group in the lower Columbia River Gorge and their relationship to the Troutdale Formation: Geological Society of America, v. 95, p. 463-477.

Tolan, T. L. and Beeson, M. H., 1993, Overview of the stratigraphy and structure of the Portland area: Association of Engineering Geologists Field Trip Guide, 26p.

Tolan, T. L. and Reidel, S. P., 1989, Structure map of a portion of the Columbia River flood basalt province, *in* Reidel, S. P. and Hooper, P. R., eds., Volcanism and tectonism in the Columbia River flood-basalt province: Geological Society of America Special Paper 239, Plate 1.

Treasher, R. C., 1942, Geologic History of the Portland area: Oregon Department of Geology and Mineral Industries Short Paper 7.

Trimble, D. E., 1963, Geology of Portland, Oregon and Adjacent area: United States Geological Survey Bulletin 1119, 119p.

Wilson, D., 1994, personal communication.

Yeats, R. S., Graven, E. P., Werner, K. S., Goldfinger, C., and Popowski, T., 1991, Tectonics of the Willamette Valley, Oregon: United States Geological Survey Open File Report 91-441-P, 47p.

Yelin, T. D. and Patton, H. J., 1991, Seismotectonics of the Portland, Oregon region: Bulletin of the Seismological Society of America, v. 81, n. 1, p. 109-130.

APPENDIX A

GEOCHEMICAL DATA FOR THE BORING LAVA

BORING LAVA -- IRRADIATIONS 93D, 93E, AND 94A

Samples collected from outcrops and TriMet drill core.
* Concentrations in ppm except Na, K, and Fe

Irrad. Number	Sample Number	Na%	K%	Rb	Cs	Sr	Ba
D1	b557-38-52			30	5.54	930	390
D2	b557-80-94			666	4.40	770	330
D3	b541-27			25	10.47	720	440
D4	b556-57	3.08	1.09	625	3.20	730	64
D5	b556-95	3.04	1.18	22	2.84	780	430
D6	b557-165	2.98	1.30	39	7.66	1103	436
D7	b540-213	3.09	1.17	759		817	91
D8	b564-115	2.91	1.30	42	7.20	920	380
D9	b564-170	3.04	1.30	710	4.33	640	430
D10	b538-176	2.96	1.20	589	6.67	870	380
D11	b538-28.5	2.95	1.30	14	7.02	810	370
D12	b539-42	3.09	1.50	619	3.33	620	450
D13	b539-167.7	2.86	1.00	503	5.42	590	310
D14	b555-95	3.07	0.96	485	1.11	763	335
D15	b555-190	3.12	1.40	456	9.21	696	328
D16	b561-98	2.80	1.40	36	6.98	849	74
D17	b561-166	3.12	1.20	547	10.37	548	311
D28T	b540-34	2.84	1.50	675	7.10	660	330
D29T	b540-90	3.06	1.40	629	10.90	730	440
D22	b561-172	2.64	0.66			881	313
D23	b561-135	1.97	0.91	18	1.59	921	296
D26	b557-211	2.77	0.89	271	21.18	1163	531
D27	b557-213	2.67	1.22			1040	546
E1	KA1	2.25	2.05	23	2.22	416	599
E2	SS2	2.72	0.88	556	1.46	866	554
E3	CR3	2.90	1.05	516	2.26	967	607
E4	CY5	2.92		28	1.41	958	640
E5	CY6	3.18	1.01	666	0.58	798	454
E6	BA7	2.99	1.60	531	0.81	778	472
E7	BU8	2.87	1.78	30	1.16	1016	652
E8	SH9	2.86	0.92	23	1.12	847	491
E9	HWY26-2	3.08	1.62	620	1.38	891	584
E10	HWY26-3	3.04	1.46	21	0.71	775	434
E11	HWY26-4	2.92	1.31	12	0.44	776	417
E12	ODOT-K108-48-49	3.06	1.32	18	0.39	858	463
E13	CLAR-110-120	1.38	1.12	36	2.38	621	711
E14	B541-27	3.03	1.08	28	5.23	784	646
E15	B557-32	2.96	1.43	619	3.33	800	511
E16	B557-93.5	3.04	0	36	0.76	830	470
E17	B14-37.5	3.08	1.31	485	0.46	788	434
E18	B537-155	3.06	1.07	27	1.52	789	487
E19	B12-94	2.91	1.52	31	2.13	1005	498
E20	B12-119	2.94	0.95	547	0.75	860	461

Irrad. Number	Sample Number	Fe%	Sc	Cr	Co	Zr	Hf
D1	b557-38-52	6.25	19.1	173	31	17	3.40
D2	b557-80-94	5.26	16.5	141	26	11	3.00
D3	b541-27	6.12	19.1	169	30	8	3.60
D4	b556-57	6.18	19.3	159	29	11	3.60
D5	b556-95	5.86	18.5	161	28	350	3.50
D6	b557-165	5.76	16.7	205	32	240	3.61
D7	b540-213	6.03	22.9	190	34	15	3.36
D8	b564-115	5.54	16.5	267	34	9	3.60
D9	b564-170	6.54	22.9	210	35	8	3.60
D10	b538-176	6.57	21.9	205	35	240	3.70
D11	b538-28.5	6.09	18.2	178	30	8	3.70
D12	b539-42	6.14	18.0	185	30	250	3.50
D13	b539-167.7	6.24	24.3	179	34	230	3.20
D14	b555-95	6.37	25.3	166	35	256	3.28
D15	b555-190	5.96	22.0	175	32	210	3.06
D16	b561-98	6.20	20.6	253	36	8	3.58
D17	b561-166	5.59	21.4	155	32		3.05
D28T	b540-34	5.09	15.6	142	24	330	3.20
D29T	b540-90	5.94	17.6	179	29	370	4.00
D22	b561-172	6.43	24.2	178	34	258	3.72
D23	b561-135	5.70	18.8	255	32	231	3.34
D26	b557-211	6.35	17.4	224	33		3.43
D27	b557-213	6.21	16.3	231	32		3.88
E1	KA1	7.44	22.2	321	44	183	4.31
E2	SS2	6.72	18.5	201	33	134	3.87
E3	CR3	6.26	22.3	184	34	194	3.15
E4	CY5	6.92	18.4	165	33	269	3.85
E5	CY6	6.22	20.4	247	35	135	3.41
E6	BA7	6.35	16.3	168	30	137	3.76
E7	BU8	6.48	18.2	227	36	249	3.45
E8	SH9	6.50	20.4	193	33	118	4.02
E9	HWY26-2	6.60	18.6	194	32	264	3.74
E10	HWY26-3	5.67	17.0	165	28	177	3.61
E11	HWY26-4	6.32	17.2	195	30	127	4.09
E12	ODOT-K108-48-49	5.83	16.0	153	28	140	3.37
E13	CLAR-110-120	6.91	19.3	136	38	385	8.82
E14	B541-27	6.76	18.8	210	34	181	3.83
E15	B557-32	6.36	17.5	191	32	159	3.59
E16	B557-93.5	6.31	17.6	188	32	157	3.33
E17	B14-37.5	6.33	15.3	205	30	102	4.12
E18	B537-155	6.79	19.1	217	36	110	3.48
E19	B12-94	6.80	17.1	319	41	155	3.64
E20	B12-119	6.69	21.5	205	37	213	3.13

Irrad. Number	Sample Number	Ta	Th	U	Zn	As	Sb
D1	b557-38-52	0.46	1.6	0.8	100		11.3
D2	b557-80-94	0.47	1.8	1.2	93		7.2
D3	b541-27	0.47	1.6		100		13.6
D4	b556-57	0.47	1.6	0.7	100	42.0	7.0
D5	b556-95	0.46	1.6		93	45.6	8.4
D6	b557-165	0.75	2.4	1.7	110	25.6	5.6
D7	b540-213	0.55	1.7	0.5	112	40.6	7.6
D8	b564-115	0.28	3.2		79	43.0	9.0
D9	b564-170	0.49	1.5	1.0	110	30.0	5.9
D10	b538-176	0.50	1.4	1.4	110		5.2
D11	b538-28.5		1.7	4.8	99	26.1	5.9
D12	b539-42	0.49	2.1	0.9	96	41.4	6.5
D13	b539-167.7	0.42	1.6		100	26.1	5.9
D14	b555-95	0.44	1.3		114	28.5	6.6
D15	b555-190	0.62	1.4		99		3.8
D16	b561-98	0.73	3.3	2.8	100	64.5	7.0
D17	b561-166	0.47	1.8		101	38.6	7.9
D28T	b540-34	0.38	1.3	2.5	82	44.8	8.6
D29T	b540-90	0.45	1.6		100	42.4	7.8
D22	b561-172	0.53	2.6	10.6	106	45.3	
D23	b561-135	0.67	3.4	2.1	84	6.4	12.0
D26	b557-211	0.62	2.6	1.2	93	85.7	2.8
D27	b557-213	0.67	2.7		83		
E1	KA1	5.19	2.6	11.9	102	24.5	7.7
E2	SS2	3.63	2.0	8.0	107	37.5	6.5
E3	CR3	3.74	1.6	0.8	100	20.5	6.6
E4	CY5	3.00	2.1	8.1	103	25.7	11.3
E5	CY6	3.40	1.5	11.8	99	31.0	7.2
E6	BA7	5.64	1.7	1.3	93	14.5	2.3
E7	BU8	3.36	2.9	10.4	100	13.3	7.0
E8	SH9	0.57	2.1	1.7	114	5.3	8.4
E9	HWY26-2	2.90	1.9	1.7	107	25.6	5.6
E10	HWY26-3	2.11	1.6	2.4	87	32.6	7.6
E11	HWY26-4	4.47	1.8	9.0	96	46.0	2.0
E12	ODOT-K108-48-49	3.41	1.6	3.2	90	12.7	6.2
E13	CLAR-110-120	5.09	9.0	3.8	90	7.5	5.2
E14	B541-27	3.85	1.7	10.6	119	26.1	8.3
E15	B557-32	3.57	1.6	14.9	100	41.4	6.5
E16	B557-93.5	3.41	1.5	10.3	103	26.1	6.0
E17	B14-37.5	6.55	1.9	20.4	98	133.7	6.6
E18	B537-155	8.35	1.8	10.0	103	74.4	3.8
E19	B12-94	7.52	3.7	1.8	95	27.2	7.0
E20	B12-119	8.52	1.6	16.1	101	38.6	5.1

Irrad. Number	Sample Number	La	Ce	Nd	Sm	Eu	Tb
D1	b557-38-52		38.3	5		1.70	0.57
D2	b557-80-94		32.4	3		1.50	
D3	b541-27		39.6	32		1.70	0.63
D4	b556-57	17.7	41.4	36	5.15	1.80	0.62
D5	b556-95	17.4	38.3	25	4.63	1.70	0.58
D6	b557-165	26.4	57.9	33	5.61	1.69	0.61
D7	b540-213	16.5	35.6	20	4.42	1.48	0.60
D8	b564-115	25.9	49.5	29	5.39	1.60	
D9	b564-170	15.7	35.0	3	4.39	1.50	0.70
D10	b538-176	14.8	33.0	3	4.15	1.50	0.60
D11	b538-28.5	17.3	39.0	3	4.94	1.70	0.66
D12	b539-42	18.3	40.0	3	4.80	1.70	0.80
D13	b539-167.7	16.7	31.0	3	4.59	1.70	0.60
D14	b555-95	15.7	34.0	30	4.11	1.50	
D15	b555-190	16.7	34.8	29	4.23	1.50	0.57
D16	b561-98	25.0	54.5	39	5.13	1.80	0.65
D17	b561-166	16.1	31.8	3	4.32	1.40	0.85
D28T	b540-34	16.2	33.0	4	4.40	1.40	0.53
D29T	b540-90	17.3	38.0	22	4.60	1.70	0.57
D22	b561-172	19.1	39.5	27	4.94	1.75	
D23	b561-135	19.4	42.4		4.54	1.30	0.54
D26	b557-211	32.3	62.2	40	7.23	2.18	0.79
D27	b557-213	31.3	61.0		6.60	2.02	0.65
E1	KA1	30.0	51.3	27	6.70	2.01	0.84
E2	SS2	19.5	43.2	3	5.30	1.85	0.68
E3	CR3	27.8	35.9	3	7.00	2.03	0.87
E4	CY5	25.7	53.5	110	6.20	2.10	0.76
E5	CY6	20.5	42.6	3	4.90	1.60	0.59
E6	BA7	20.8	45.0	18	5.70	1.76	0.62
E7	BU8	32.0	66.3	3	6.80	2.03	0.69
E8	SH9	21.6	45.7	3	5.50	1.82	0.69
E9	HWY26-2	20.4	46.8	3	5.40	1.90	0.68
E10	HWY26-3	20.1	37.4	24	5.20	1.56	0.57
E11	HWY26-4	19.5	43.1	25	5.30	1.71	0.60
E12	ODOT-K108-48-49	21.8	42.6	3	5.70	1.71	0.59
E13	CLAR-110-120	41.3	84.6	3	7.90	2.05	1.12
E14	B541-27	20.5	45.2	3	5.47	1.87	0.67
E15	B557-32	19.0	40.6	3	4.87	1.67	0.62
E16	B557-93.5	18.6	38.6	3	5.00	1.74	0.63
E17	B14-37.5	20.6	43.5	25	5.18	1.70	0.63
E18	B537-155	18.0	35.4	2	4.49	1.53	0.65
E19	B12-94	28.4	62.5	3	5.94	1.92	0.65
E20	B12-119	16.3	35.7	60	4.34	1.58	0.67

Irrad. Number	Sample Number	Yb	Lu
D1	b557-38-52	1.50	0.21
D2	b557-80-94	1.50	0.25
D3	b541-27	1.80	0.22
D4	b556-57	1.80	0.26
D5	b556-95	1.70	0.31
D6	b557-165	1.41	0.19
D7	b540-213	2.09	0.31
D8	b564-115	1.40	0.12
D9	b564-170	2.10	0.36
D10	b538-176	2.20	0.31
D11	b538-28.5	1.80	0.33
D12	b539-42	1.60	0.41
D13	b539-167.7	2.30	0.34
D14	b555-95	2.33	0.31
D15	b555-190	2.09	0.29
D16	b561-98	1.43	0.23
D17	b561-166	1.83	0.28
D28T	b540-34	1.50	0.20
D29T	b540-90	1.60	0.25
D22	b561-172	2.32	0.38
D23	b561-135	1.32	0.22
D26	b557-211	1.81	0.24
D27	b557-213	1.78	0.22
E1	KA1	2.35	0.46
E2	SS2	1.68	0.35
E3	CR3	2.61	0.49
E4	CY5	1.67	0.36
E5	CY6	1.63	0.43
E6	BA7	1.54	0.28
E7	BU8	1.67	0.30
E8	SH9	1.60	0.34
E9	HWY26-2	1.76	0.28
E10	HWY26-3	1.65	0.29
E11	HWY26-4	1.62	0.31
E12	ODOT-K108-48-49	1.48	0.22
E13	CLAR-110-120	3.17	0.65
E14	B541-27	1.98	0.37
E15	B557-32	1.61	0.25
E16	B557-93.5	1.63	0.24
E17	B14-37.5	1.44	0.28
E18	B537-155	1.77	0.39
E19	B12-94	1.41	0.25
E20	B12-119	2.13	0.50

Irrad. Number	Sample Number	Na%	K%	Rb	Cs	Sr	Ba
E21	B13-76.2	2.85	1.62	36	1.90	940	520
E22	B13-104.7	2.75	1.57	34	1.31	986	558
E23	B13-155	3.03	0.96	12	0.47	874	371
E24	B19-46	3.07	1.15	727	4.10	876	587
E25	B535-105	2.86	2.18	29	1.57	1017	508
E26	B535-209	3.05	0.94	799	3.75	697	376
E27	B537-40.3	2.84	1.08	553	0.49	759	442
E28	B538-91	3.08	1.65	28	0.88	879	474
E29	B555-70	3.08	0.92	687	1.36	1086	553
E30	B555-119.5	3.07	1.28	568	1.55	1095	465
E31	B561-71.7	2.82	1.35	38	1.00	1262	537
E32	B561-90	2.75	1.29	29	0.75	1085	426
E33	B561-123.5	2.80	1.56	27	0.81	964	479
E34	B562-74.3	2.42	1.13	30	1.70	834	505
E35	B562-198.5	2.84	1.93	39	2.96	1094	471
E36	B565-63	3.35	0.94	22	1.08	1172	553
E37	B565-154	2.96			1.06	699	379
A14T	MB88-186	3.10				895	385
A15T	MB88-190	2.78			1.22	750	229
A16T	92TB-5	2.43			0.95	480	240

Irrad. Number	Sample Number	Fe%	Sc	Cr	Co	Zr	Hf
E21	B13-76.2	6.58	17.4	355	41	173	4.35
E22	B13-104.7	6.48	17.0	300	38	218	3.97
E23	B13-155	6.39	20.4	199	34	95	3.55
E24	B19-46	6.53	16.5	224	32	153	4.41
E25	B535-105	6.32	17.8	267	37	96	3.82
E26	B535-209	6.68	21.7	215	36	157	3.78
E27	B537-40.3	6.82	22.7	218	36	165	3.87
E28	B538-91	6.31	19.8	203	30	143	4.24
E29	B555-70	6.76	21.8	192	35	148	3.75
E30	B555-119.5	6.61	21.8	198	34	184	3.99
E31	B561-71.7	6.78	18.9	329	42	202	4.62
E32	B561-90	6.78	18.9	342	40	135	4.36
E33	B561-123.5	6.48	17.8	331	39	130	3.93
E34	B562-74.3	6.62	18.9	278	38	172	3.77
E35	B562-198.5	6.45	18.4	318	40	203	3.90
E36	B565-63	6.64	17.7	234	37	109	4.14
E37	B565-154	6.79	26.6	198	38		3.37
A14T	MB88-186	5.15	20.7	294	31	245	2.75
A15T	MB88-190	4.19	17.1	218	25	140	2.15
A16T	92TB-5	7.07	24.4	223	41	218	2.28

Irrad. Number	Sample Number	Ta	Th	U	Zn	As	Sb
E21	B13-76.2	7.15	4.0	14.8	85	1.1	8.6
E22	B13-104.7	6.65	3.6	1.8	104	42.4	7.8
E23	B13-155	7.89	1.5	9.5	96	82.4	7.9
E24	B19-46	5.94	2.1	2.6	104	23.8	5.5
E25	B535-105	6.17	3.7	1.0	91	196.8	6.8
E26	B535-209	6.94	1.5	12.5	102	36.4	7.9
E27	B537-40.3	7.03	1.5	17.7	120	112.5	5.8
E28	B538-91	0.54	1.8	1.5	101	63.7	12.0
E29	B555-70	8.44	1.6	11.8	118		8.1
E30	B555-119.5	7.60	1.6		99	11.4	2.1
E31	B561-71.7	6.42	4.7	20.1	103	85.7	2.8
E32	B561-90	6.58	3.9	8.3	105	39.6	8.6
E33	B561-123.5	6.12	3.4	10.3	103	23.2	6.2
E34	B562-74.3	6.56	3.8	2.9	109	35.1	7.1
E35	B562-198.5	5.64	3.5	9.1	95	70.7	6.8
E36	B565-63	4.08	3.0	6.8	94	99.1	
E37	B565-154	3.59	1.7	11.6	124	22.9	
A14T	MB88-186	0.52	2.0	6.1	84	45.1	3.6
A15T	MB88-190	0.34	1.9	1.5	75		
A16T	92TB-5	0.40	1.1	4.5	100	34.9	2.0

Irrad. Number	Sample Number	La	Ce	Nd	Sm	Eu	Tb
E21	B13-76.2	2.7	58.9	35	5.91	1.82	1.02
E22	B13-104.7	26.9	59.2	40	5.67	1.79	0.69
E23	B13-155	17.0	34.2	19	4.49	1.48	0.59
E24	B19-46	19.5	42.7	22	5.07	1.91	0.82
E25	B535-105	27.9	59.6	4	5.86	1.82	0.64
E26	B535-209	16.4	35.2	25	4.51	1.64	0.68
E27	B537-40.3	19.7	36.4	28	4.95	1.71	0.72
E28	B538-91	19.6	41.4	25	5.21	1.80	0.67
E29	B555-70	17.9	36.1	4	4.65	1.64	0.72
E30	B555-119.5	17.3	36.2	20	4.65	1.65	0.61
E31	B561-71.7	28.0	62.5	38	6.02	1.93	1.03
E32	B561-90	29.3	63.7	33	6.38	1.82	0.67
E33	B561-123.5	26.4	56.9	31	5.57	1.81	0.59
E34	B562-74.3	30.3	61.9	46	6.42	1.97	0.68
E35	B562-198.5	27.0	60.1	32	5.74	1.87	0.69
E36	B565-63	31.4	67.7	38	6.65	2.08	0.69
E37	B565-154	16.9	35.9		4.48	1.68	0.67
A14T	MB88-186	21.3	42.4	46	4.32	1.39	0.54
A15T	MB88-190	14.0	20.8		3.00	1.06	0.47
A16T	92TB-5	8.9	17.8		2.84	1.13	0.55

Irrad. Number	Sample Number	Yb	Lu
E21	B13-76.2	1.62	0.25
E22	B13-104.7	1.44	0.34
E23	B13-155	1.90	0.35
E24	B19-46	1.80	0.25
E25	B535-105	1.63	0.25
E26	B535-209	1.97	0.32
E27	B537-40.3	2.33	0.30
E28	B538-91	1.67	0.32
E29	B555-70	2.02	0.41
E30	B555-119.5	2.17	0.36
E31	B561-71.7	1.94	0.29
E32	B561-90	1.47	0.26
E33	B561-123.5	1.54	0.30
E34	B562-74.3	1.64	0.31
E35	B562-198.5	1.83	0.28
E36	B565-63	1.54	0.23
E37	B565-154	2.13	0.37
A14T	MB88-186	1.55	0.28
A15T	MB88-190	1.19	0.23
A16T	92TB-5	1.86	0.33

APPENDIX B

GEOCHEMICAL DATA FOR SHALLOW SEDIMENT AND OTHER MISCELLANEOUS SAMPLES

SHALLOW DRILL HOLE SEDIMENTS AND MISCELLANEOUS SAMPLES -- IRRADIATIONS 93D, 93G, AND 94A

Samples collected from TriMet drill core, DOGAMI shallow drill holes, David's Hill Well, several volcanic ash samples, and standard drilling mud.
* Concentrations in ppm except Na, K, and Fe

Irrad. Number	Sample Number	Na%	K%	Rb	Cs	Sr	Ba
D18	b563-152	1.27	1.78	80	2.88	192	582
D19	b563-172.2	3.27	0.13				451
D20	b563-212	3.85	0.70		1.11	577	
D21	b563-259	0.09	0.44	51	3.56	422	
D22	b561-172	2.64	0.66			881	313
D23	b561-135	1.97	0.91	18	1.59	921	296
D24	b561-222	1.13	1.24	71	2.68	321	553
D25	b557-114	1.33	1.14	76	3.09	310	595
D26	b557-211	2.77	0.89	271	21.18	1163	531
D27	b557-213	2.67	1.22			1040	546
D28	b540-161	1.19	1.17	70	3.36	240	618
D29	b541-54	1.53	1.56	51	2.64	301	608
D30	b538-128	1.40	1.76	72	3.19	276	639
D31	b538-148	0.78	1.09	73	2.30	206	559
D32	b539-121	1.69	1.19	58	2.22	418	539
D33	b539-146	0.69	0.97	58	2.66	162	439
D34	b564-241	1.17	1.45	72	2.60	621	
D35	b564-261	1.35	1.53	57	2.90	285	607
D36	b564-286	1.61	1.71	77	3.06	281	671
G1	B535-12	1.11	1.37	51	3.36	311	564
G2	B535-280.2	1.75	2.11	64	2.40	285	659
G3	B562-19.6	1.25	1.87	81	3.41	299	663
G4	B563-159	1.32	2.31	78	3.63	220	662
G5	B563-169	1.35	2.13	71	3.50	171	549
G6	B564-38	1.37	1.64	54	3.51	352	556
G7	B565-170	1.17	1.56	85	3.27	291	516
G8	B565-205	1.13	1.50	62	1.86	183	599
G9	B565-214	1.22	1.84	76	3.38	257	666
G10	B565-226	0.29	0.40	49	1.29	642	531
A24	BVD2-93.5	2.54	1.03	35	1.71	316	456
A25	BVD3-19.8	1.85	1.81	65	3.36	367	670
A26	BVD4-36.5	0.35	0.82	67	3.88	614	
A27	BVD4-59.9	0.11	0.35	40	3.89	277	256
A28	BVD4-91.4	0.76	1.85	77	5.62	588	
A29	BVD5-55	1.90	1.98	83	4.38	359	722
A30	BVD6-25	2.33	1.57	46	1.82	452	610
A31	BVD6-47	1.36	1.24	42	3.06	493	653
A32	GSD2-10-15	2.26	1.27	43	2.47	411	634
A33	GSD3-35-65	1.09	2.13	86	5.45	274	721
A34	GSD5-75-95	2.66	1.48	41	1.82	502	568

Irrad. Number	Sample Number	Fe%	Sc	Cr	Co	Zr	Hf
D18	b563-152	3.71	12.7	52	11	231	8.03
D19	b563-172.2	12.06	57.4	42	46		5.07
D20	b563-212	12.20	45.3	56	31	220	5.56
D21	b563-259	12.23	43.4	59	41	528	8.39
D22	b561-172	6.43	24.2	178	34	258	3.72
D23	b561-135	5.70	18.8	255	32	231	3.34
D24	b561-222	4.63	16.0	70	7	272	6.74
D25	b557-114	4.05	11.3	83	22	201	7.90
D26	b557-211	6.35	17.4	224	33		3.43
D27	b557-213	6.21	16.3	231	32		3.88
D28	b540-161	5.17	12.8	145	21	319	7.35
D29	b541-54	3.01	8.8	64	13	308	7.48
D30	b538-128	3.65	12.5	71	14	227	8.03
D31	b538-148	5.63	17.0	136	25	282	6.52
D32	b539-121	4.80	15.1	108	29		6.31
D33	b539-146	5.34	16.5	87	19	220	6.38
D34	b564-241	3.35	11.5	85	23	264	8.52
D35	b564-261	3.32	10.7	74	13	448	16.98
D36	b564-286	2.81	9.8	72	10	308	8.43
G1	B535-12	4.78	16.8	87	9	172	6.64
G2	B535-280.2	2.58	10.9	66	9	154	9.92
G3	B562-19.6	4.37	16.0	75	14	212	8.54
G4	B563-159	4.71	17.0	55	21	219	9.10
G5	B563-169	2.22	13.1	68	7	170	8.45
G6	B564-38	4.24	15.0	80	15	217	9.83
G7	B565-170	2.26	15.8	79	12	205	9.13
G8	B565-205	5.54	18.9	65	22	364	19.93
G9	B565-214	4.40	16.1	64	18	196	6.62
G10	B565-226	10.47	55.5	26	35	415	8.97
A24	BVD2-93.5	4.20	17.4	164	21	127	4.66
A25	BVD3-19.8	5.50	17.2	134	19	335	7.39
A26	BVD4-36.5	10.39	37.3	70	30	407	8.31
A27	BVD4-59.9	6.42	22.4	71	12	340	4.44
A28	BVD4-91.4	3.82	14.2	39	14	298	5.87
A29	BVD5-55	4.06	14.8	90	17	183	7.07
A30	BVD6-25	4.64	13.8	64	18	198	4.68
A31	BVD6-47	5.04	20.1	82	22	319	6.72
A32	GSD2-10-15	5.14	18.4	64	24	149	4.22
A33	GSD3-35-65	5.01	18.0	80	21	261	5.10
A34	GSD5-75-95	6.18	18.6	64	27	328	4.14

Irrad. Number	Sample Number	Ta	Th	U	Zn	As	Sb
D18	b563-152	0.97	10.2	3.0	68	5.8	1.4
D19	b563-172.2	0.86	4.4	1.9	221	28.0	1.8
D20	b563-212	0.93	4.4	1.2	229		
D21	b563-259	1.50	9.7	2.8	179	4.3	7.9
D22	b561-172	0.53	2.6	10.6	106	45.3	
D23	b561-135	0.67	3.4	2.1	84	6.4	12.0
D24	b561-222	0.91	8.5	3.0	67	4.2	
D25	b557-114	0.82	8.7	2.5	63	6.6	8.3
D26	b557-211	0.62	2.6	1.2	93	85.7	2.8
D27	b557-213	0.67	2.7		83		
D28	b540-161	0.90	8.9	2.7	77	5.4	
D29	b541-54	0.95	8.8	0.7	38	5.6	7.1
D30	b538-128	0.88	10.8	2.8	72	5.6	
D31	b538-148	0.97	8.3	2.9	111	3.9	
D32	b539-121	0.86	8.5		134	7.1	
D33	b539-146	0.90	8.2	2.5	79	6.0	1.1
D34	b564-241	0.96	9.6	2.8	55	4.4	
D35	b564-261	1.22	15.8	4.2	52	7.0	0.8
D36	b564-286	1.02	10.9		59	1.3	
G1	B535-12	0.65	10.8	3.3	76	8.7	1.0
G2	B535-280.2	0.57	10.4	4.2	55	10.3	1.3
G3	B562-19.6	0.75	12.8	2.8	242	8.8	1.0
G4	B563-159	0.78	10.7	3.2	81	6.2	1.3
G5	B563-169	0.54	11.6	2.9	68		0.5
G6	B564-38	0.52	11.9	3.8	70	9.8	
G7	B565-170	0.62	10.5	2.9	88	2.3	0.8
G8	B565-205	0.62	17.0	5.2	88	5.8	0.8
G9	B565-214	0.58	11.0	3.6	81	5.9	1.2
G10	B565-226	1.61	7.9	3.3	211	2.3	
A24	BVD2-93.5	0.56	4.5	1.6	85	8.7	0.8
A25	BVD3-19.8	1.12	9.3	2.2	95	16.0	1.0
A26	BVD4-36.5	1.33	11.8	4.2	145	14.8	
A27	BVD4-59.9	0.84	6.0	1.9	99	3.4	0.7
A28	BVD4-91.4	2.27	17.7	5.0	106	2.0	1.1
A29	BVD5-55	1.21	11.0	4.3	80	10.6	1.4
A30	BVD6-25	0.63	4.9	2.1	75	4.9	0.5
A31	BVD6-47	1.12	6.7	2.3	102	8.0	
A32	GSD2-10-15	0.58	4.9	0.7	86	9.4	1.6
A33	GSD3-35-65	1.15	11.7	4.0	119	8.6	2.5
A34	GSD5-75-95	0.72	4.9	1.2	97	3.2	1.5

Irrad. Number	Sample Number	La	Ce	Nd	Sm	Eu	Tb
D18	b563-152	38.2	70.9	35	6.19	1.35	0.86
D19	b563-172.2	31.4	56.2		10.42	3.05	1.64
D20	b563-212	51.6	30.8		9.73	3.07	1.41
D21	b563-259	48.9	95.1	50	10.02	2.68	
D22	b561-172	19.1	39.5	27	4.94	1.75	
D23	b561-135	19.4	42.4		4.54	1.30	0.54
D24	b561-222	26.7	47.5	28	4.60	1.13	0.69
D25	b557-114	34.6	68.3	30	5.49	1.29	0.77
D26	b557-211	32.3	62.2	40	7.23	2.18	0.79
D27	b557-213	31.3	61.0		6.60	2.02	0.65
D28	b540-161	37.1	67.2		5.86	1.55	0.91
D29	b541-54	36.5	65.7	32	5.51	1.27	0.82
D30	b538-128	41.3	78.0	40	6.40	1.48	0.91
D31	b538-148	34.4	73.0	50	6.06	1.53	0.79
D32	b539-121	40.1	71.8	47	7.14	1.81	0.96
D33	b539-146	22.1	54.8	33	3.75	0.92	0.78
D34	b564-241	37.7	69.5	29	5.65	1.30	0.81
D35	b564-261	59.1	117.1	46	8.84	1.81	1.14
D36	b564-286	41.9	73.7	34	6.38	1.37	0.87
G1	B535-12	33.3	69.5		5.75	1.38	0.74
G2	B535-280.2	46.6	81.8		7.29	1.42	0.87
G3	B562-19.6	47.5	87.0	42	7.85	1.75	1.04
G4	B563-159	40.2	85.8		7.03	1.69	0.95
G5	B563-169	49.1	82.8	35	7.75	1.56	1.00
G6	B564-38	41.0	82.9		6.48	1.47	0.92
G7	B565-170	43.2	81.4	35	6.61	1.39	0.83
G8	B565-205	69.3	119.2	55	11.25	2.14	1.39
G9	B565-214	41.7	78.4	40	7.18	1.61	0.97
G10	B565-226	38.2	159.2	52	13.59	3.76	1.65
A24	BVD2-93.5	20.7	38.4	24	4.21	1.11	0.67
A25	BVD3-19.8	35.8	69.1		6.32	1.51	0.94
A26	BVD4-36.5	40.5	82.6		8.68	2.32	1.80
A27	BVD4-59.9	13.5	22.6		2.20	0.65	0.49
A28	BVD4-91.4	31.9	64.8	29	6.54	1.20	1.14
A29	BVD5-55	40.4	78.4		6.73	1.56	0.98
A30	BVD6-25	23.0	44.4		4.29	1.22	0.66
A31	BVD6-47	31.4	58.1	29	6.37	1.62	0.94
A32	GSD2-10-15	24.4	46.0	28	5.59	1.66	0.80
A33	GSD3-35-65	38.9	79.7	41	7.29	1.68	1.10
A34	GSD5-75-95	24.4	50.4		5.18	1.63	0.80

Irrad. Number	Sample Number	Yb	Lu
D18	b563-152	2.86	0.44
D19	b563-172.2	7.67	1.14
D20	b563-212	4.56	0.64
D21	b563-259	3.41	0.53
D22	b561-172	2.32	0.38
D23	b561-135	1.32	0.22
D24	b561-222	2.45	0.35
D25	b557-114	2.40	0.37
D26	b557-211	1.81	0.24
D27	b557-213	1.78	0.22
D28	b540-161	3.04	0.48
D29	b541-54	2.35	0.34
D30	b538-128	2.68	0.42
D31	b538-148	2.65	0.37
D32	b539-121	2.53	0.39
D33	b539-146	1.95	0.32
D34	b564-241	2.46	0.37
D35	b564-261	4.29	0.56
D36	b564-286	2.76	0.38
G1	B535-12	2.32	0.44
G2	B535-280.2	2.90	0.51
G3	B562-19.6	3.09	0.54
G4	B563-159	2.95	0.56
G5	B563-169	3.10	0.49
G6	B564-38	2.89	0.54
G7	B565-170	2.53	0.49
G8	B565-205	4.55	0.79
G9	B565-214	3.04	0.56
G10	B565-226	3.74	0.68
A24	BVD2-93.5	2.22	0.34
A25	BVD3-19.8	2.86	0.42
A26	BVD4-36.5	3.50	0.59
A27	BVD4-59.9	1.67	0.26
A28	BVD4-91.4	2.94	0.47
A29	BVD5-55	2.92	0.47
A30	BVD6-25	2.14	0.31
A31	BVD6-47	3.02	0.43
A32	GSD2-10-15	2.51	0.42
A33	GSD3-35-65	3.16	0.55
A34	GSD5-75-95	2.24	0.37

Irrad. Number	Sample Number	Na%	K%	Rb	Cs	Sr	Ba
A35	GSD5-195-215	1.33	1.62	82	4.02	244	722
A36	Drill Mud	1.57	0.59	16	0.73	284	316
A1T	LOD1-53	1.80	2.01	58	2.95	421	628
A2T	LOD3-22	1.61	1.88	71	3.99	300	576
A3T	LOD4-100	1.00	1.26	40	2.59	310	609
A4T	LOD5-29.6	1.49	2.73	94	6.99	234	674
A5T	LOD6-95-110	0.11	0.26				
A6T	LOD9-41.7	1.38	1.26	48	2.89	389	683
A7T	LTD4-11.6	1.87	1.84	79	3.33	348	690
A8T	MTD2-145-155	2.23	2.03	60	1.95	324	656
A9T	MTD5-95-115	0.76	1.37	46	2.27	78	399
A10T	ORD1-19.6	1.63	3.46	123	2.30	269	700
A11T	VND1-25-30	2.33	2.13	59	1.82	323	592
A12T	DHW-330	1.53	1.31	73	4.24	273	579
A17T	Sample #7-JS	3.38		29	1.02	472	444
A18T	SR-3-JS	2.77		31	2.16	376	533
MF	LE-50 Missoula Floods	1.60	1.70	57	2.70	380	540
BLUE	LE-186 Willamette Blue Mud	0.59	1.40	44	3.50	110	390
PHS	Portland Hills Silt	1.83	1.73	65	2.70	338	628
SRM	Sandy River Mudstone	0.96	1.89	90	5.00	243	676

Irrad. Number	Sample Number	Fe%	Sc	Cr	Co	Zr	Hf
A35	GSD5-195-215	5.56	15.6	114	17	408	6.48
A36	Drill Mud	3.10	5.0	4	1	155	6.11
A1T	LOD1-53	2.82	10.7	52	9	235	8.67
A2T	LOD3-22	5.53	11.9	53	12	310	5.92
A3T	LOD4-100	5.38	17.3	71	26	234	7.00
A4T	LOD5-29.6	3.77	14.5	63	16	148	4.78
A5T	LOD6-95-110						
A6T	LOD9-41.7	6.79	26.8	92	25	362	6.81
A7T	LTD4-11.6	3.72	12.2	60	16	276	8.37
A8T	MTD2-145-155	3.29	10.9	42	14	141	3.40
A9T	MTD5-95-115	4.12	14.2	56	17	203	6.33
A10T	ORD1-19.6	3.62	12.5	46	16	236	4.24
A11T	VND1-25-30	4.70	17.2	38	19	152	3.31
A12T	DHW-330	4.34	15.7	59	13	224	5.58
A17T	Sample #7-JS	2.26	8.0	23	9	227	3.90
A18T	SR-3-JS	2.57	9.1	22	10	97	4.36
MF	LE-50 Missoula Floods	4.43	15.1	61	18	270	7.10
BLUE	LE-186 Willamette Blue Mud	4.50	18.9	72	9	140	3.80
PHS	Portland Hills Silt	3.66	13.0	59	14		8.71
SRM	Sandy River Mudstone	4.08	16.4	76	19		6.24

Irrad. Number	Sample Number	Ta	Th	U	Zn	As	Sb
A35	GSD5-195-215	1.01	9.8	2.5	83	7.1	0.9
A36	Drill Mud	3.62	36.5	16.9	58	10.6	1.1
A1T	LOD1-53	0.97	11.8	2.4	61	4.1	1.1
A2T	LOD3-22	0.75	8.3	2.9	74	3.3	1.8
A3T	LOD4-100	0.81	7.5	3.9	74	5.0	1.2
A4T	LOD5-29.6	0.89	11.0	3.9	96	13.2	1.8
A5T	LOD6-95-110			1.3		4.5	
A6T	LOD9-41.7	0.99	8.2	2.5	120	7.3	
A7T	LTD4-11.6	0.96	9.7	2.7	76	7.1	0.7
A8T	MTD2-145-155	0.57	4.7	1.2	57	2.5	0.5
A9T	MTD5-95-115	0.99	9.1	2.4	61	7.4	0.6
A10T	ORD1-19.6	0.86	7.4	2.5	59	1.7	
A11T	VND1-25-30	0.56	3.8	1.1	81	6.4	2.3
A12T	DHW-330	0.81	7.9	2.6	88	10.9	2.8
A17T	Sample #7-JS	0.56	3.8	2.1	46	5.5	
A18T	SR-3-JS	0.64	4.8	1.6	46	4.4	0.5
MF	LE-50 Missoula Floods	0.78	7.8	2.6	82	9.3	1.1
BLUE	LE-186 Willamette Blue Mud	0.71	5.6		84	6.7	0.80
PHS	Portland Hills Silt	0.94	10.3		70	6.0	
SRM	Sandy River Mudstone	1.15	11.8		87	4.5	

Irrad. Number	Sample Number	La	Ce	Nd	Sm	Eu	Tb
A35	GSD5-195-215	32.6	68.4		5.18	1.27	0.76
A36	Drill Mud	45.1	87.3	41	11.03	0.68	1.72
A1T	LOD1-53	45.6	78.5	31	6.90	1.46	0.95
A2T	LOD3-22	30.4	57.0		5.23	1.21	0.74
A3T	LOD4-100	39.9	75.5	38	7.81	1.97	1.09
A4T	LOD5-29.6	35.6	70.8	39	6.33	1.36	0.91
A5T	LOD6-95-110	36.0			10.99		
A6T	LOD9-41.7	35.4	65.4		7.44	2.07	1.09
A7T	LTD4-11.6	38.1	72.6	33	5.87	1.39	0.83
A8T	MTD2-145-155	21.2	38.7	20	3.81	1.02	0.57
A9T	MTD5-95-115	29.5	67.4	26	4.72	1.00	0.64
A10T	ORD1-19.6	27.9	52.1		4.45	1.20	0.63
A11T	VND1-25-30	18.5	35.6	22	4.25	1.22	0.67
A12T	DHW-330	28.4	54.9		5.92	1.36	0.83
A17T	Sample #7-JS	21.4	35.4		3.62	1.04	0.47
A18T	SR-3-JS	23.2	45.0	21	4.29	1.07	0.58
MF	LE-50 Missoula Floods	32.0	61.0		5.67	1.35	0.78
BLUE	LE-186 Willamette Blue Mud	22.5	42.0	22	5.53	1.23	0.64
PHS	Portland Hills Silt	37.9	78.0		6.50	1.36	1.06
SRM	Sandy River Mudstone	40.7	91.0		7.70	1.53	1.14

Irrad. Number	Sample Number	Yb	Lu
A35	GSD5-195-215	2.37	0.41
A36	Drill Mud	4.59	0.66
A1T	LOD1-53	2.94	0.49
A2T	LOD3-22	2.53	0.38
A3T	LOD4-100	3.60	0.57
A4T	LOD5-29.6	3.35	0.50
A5T	LOD6-95-110		
A6T	LOD9-41.7	3.50	0.54
A7T	LTD4-11.6	2.81	0.44
A8T	MTD2-145-155	1.74	0.33
A9T	MTD5-95-115	1.85	0.32
A10T	ORD1-19.6	2.31	0.40
A11T	VND1-25-30	1.75	0.37
A12T	DHW-330	2.83	0.50
A17T	Sample #7-JS	1.72	0.24
A18T	SR-3-JS	1.76	0.25
MF	LE-50 Missoula Floods	2.50	0.41
BLUE	LE-186 Willamette Blue Mud	2.10	0.33
PHS	Portland Hills Silt	2.63	0.53
SRM	Sandy River Mudstone	3.08	0.55

APPENDIX C

GEOCHEMICAL DATA FOR THE HILLSBORO AIRPORT DRILL HOLE (HBD1)

HILLSBORO AIRPORT DRILL HOLE (1095 FEET) --
IRRADIATION 93G

Samples collected from DOGAMI drill hole (HBD1) at the Hillsboro Airport.
* Concentrations in ppm except Na, K, and Fe

Irrad. Number	Sample Number	Na%	K%	Rb	Cs	Sr	Ba
G11	HBD1-60.5	1.51	1.90	59	2.49	333	625
G12	HBD1-84	1.03	1.64	51	3.06		555
G13	HBD1-131	0.70	1.06	42	4.00	194	620
G14	HBD1-206.5	1.38	2.52	101	4.84	326	759
G15	HBD1-230	1.15	1.55	83	3.31	287	753
G16	HBD1-257	1.54	1.48	69	2.95	286	710
G17	HBD1-303.5	0.92	1.46	43	3.47	333	589
G18	HBD1-349	0.91	1.59	39	4.24	439	512
G19	HBD1-405.5	2.63	2.99	51	3.88	639	619
G20	HBD1-436.3	1.01	1.29	55	3.13	388	503
G21	HBD1-492.5	0.32		47	3.11	226	485
G22	HBD1-545.6	0.53	1.23	57	3.79	198	456
G23	HBD1-553	0.86	1.95	61	3.86	219	744
G24	HBD1-565.7	0.68	1.23	49	3.69		547
G25	HBD1-602.3	0.61	2.22	101	6.98	343	675
G26	HBD1-659	0.30		36	4.41	403	629
G27	HBD1-714.8	0.52	1.06	35	2.86	466	537
G28	HBD1-755	0.54	1.49	49	4.27	551	727
G29	HBD1-760	1.05			1.53	630	
G30	HBD1-763.4	2.00	2.74	44	2.50	200	799
G31	HBD1-790.7	0.25	1.06	45	3.56	553	
G32	HBD1-822	0.24		40	3.60	680	
G33	HBD1-871	0.71	1.90	93	5.19	489	687
G34	HBD1-920.5	0.23		31	3.30	567	568
G35	HBD1-930	0.00			1.77	271	
G36	HBD1-938.5	0.01	0.21	28	2.97	208	477

Irrad. Number	Sample Number	Fe%	Sc	Cr	Co	Zr	Hf
G11	HBD1-60.5	3.20	11.6	64	15	224	9.44
G12	HBD1-84	2.84	14.9	46	13	332	11.09
G13	HBD1-131	7.66	25.0	61	26	202	8.49
G14	HBD1-206.5	5.34	16.4	91	19	202	5.64
G15	HBD1-230	7.20	17.3	165	35	220	6.79
G16	HBD1-257	4.33	12.9	93	19	228	7.50
G17	HBD1-303.5	6.67	15.0	88	22	163	5.34
G18	HBD1-349	7.02	16.6	88	19	201	7.66
G19	HBD1-405.5	3.33	12.9	71	14	323	10.40
G20	HBD1-436.3	5.42	12.1	59	17	198	7.60
G21	HBD1-492.5	11.11	21.1	69	15	182	7.33
G22	HBD1-545.6	9.21	21.1	68	14	200	6.69
G23	HBD1-553	6.98	19.7	74	39	208	6.80
G24	HBD1-565.7	10.37	24.8	51	24	258	6.38
G25	HBD1-602.3	7.10	17.0	81	25	246	6.28
G26	HBD1-659	10.90	27.3	56	39	371	8.25
G27	HBD1-714.8	13.14	23.6	49	30	203	7.37
G28	HBD1-755	6.84	19.4	93	16	189	5.49
G29	HBD1-760	7.45	7.4	8	15	224	9.83
G30	HBD1-763.4	4.91	7.1	4	5	293	9.84
G31	HBD1-790.7	10.83	27.1	61	26	184	9.00
G32	HBD1-822	10.44	36.0	65	22	373	9.52
G33	HBD1-871	7.24	22.7	65	51	171	8.13
G34	HBD1-920.5	11.23	35.4	50	60	382	8.29
G35	HBD1-930	21.18	32.9	90	12	293	13.38
G36	HBD1-938.5	13.11	45.6	61	58	364	12.00

Irrad. Number	Sample Number	Ta	Th	U	Zn	As	Sb
G11	HBD1-60.5	0.55	10.6	3.4	59		0.7
G12	HBD1-84	0.68	10.8	2.8	63	5.0	
G13	HBD1-131	1.13	9.2	2.7	114	11.2	1.7
G14	HBD1-206.5	0.91	14.8	2.3	101	6.8	0.5
G15	HBD1-230	3.03	9.0	4.8	108	5.2	
G16	HBD1-257	2.24	8.2	2.4	84	8.4	1.0
G17	HBD1-303.5	2.52	6.3	3.5	82	10.0	1.4
G18	HBD1-349	2.82	7.8	2.6	82	23.1	4.8
G19	HBD1-405.5	2.29	10.4	2.3	71	20.2	0.9
G20	HBD1-436.3	2.01	7.4	3.6	70	13.3	
G21	HBD1-492.5	3.29	9.8	6.7	122	6.3	
G22	HBD1-545.6	3.33	10.0	3.8	99	2.1	
G23	HBD1-553	3.02	8.2	3.4	109	5.0	2.8
G24	HBD1-565.7	3.67	7.6	3.1	113	9.2	
G25	HBD1-602.3	2.63	12.5	3.8	98	6.8	2.5
G26	HBD1-659	4.11	10.2	3.8	146	6.6	
G27	HBD1-714.8	3.42	8.1	2.6	121	8.5	1.1
G28	HBD1-755	2.78	7.6	3.0	103	5.8	1.5
G29	HBD1-760	1.16	7.2	2.9	64	8.3	1.0
G30	HBD1-763.4	1.13	7.1	3.3	55	11.4	
G31	HBD1-790.7	3.89	10.2	3.7	118	9.9	10.6
G32	HBD1-822	5.03	10.6	3.8	160	15.9	2.2
G33	HBD1-871	3.17	11.0	3.8	122	11.2	3.4
G34	HBD1-920.5	4.69	10.0	2.9	156	7.9	
G35	HBD1-930	4.23	17.8	5.5	103	20.4	1.2
G36	HBD1-938.5	5.50	12.8	3.8	182	3.2	8.3

Irrad. Number	Sample Number	La	Ce	Nd	Sm	Eu	Tb
G11	HBD1-60.5	43.8	2.5	42	7.01	1.49	0.90
G12	HBD1-84	44.7	91.8	46	8.37	1.92	1.15
G13	HBD1-131	27.3	56.7	26	5.57	1.45	0.85
G14	HBD1-206.5	48.5	92.4	41	7.62	1.63	1.06
G15	HBD1-230	42.8	107.8	43	9.01	2.46	1.37
G16	HBD1-257	32.2	63.2	30	5.95	1.53	0.87
G17	HBD1-303.5	24.1	45.2		5.21	1.40	0.79
G18	HBD1-349	26.4	48.3	26	5.88	1.49	0.82
G19	HBD1-405.5	38.2	91.3	41	6.52	1.76	0.96
G20	HBD1-436.3	28.4	49.9	26	5.92	1.35	0.70
G21	HBD1-492.5	26.3	65.4	28	6.62	1.99	1.09
G22	HBD1-545.6	21.3	36.4		3.77	1.05	0.69
G23	HBD1-553	32.8	66.9	64	6.96	1.83	0.98
G24	HBD1-565.7	35.5	64.8	39	7.88	1.96	1.05
G25	HBD1-602.3	42.2	85.5	45	8.62	1.99	1.22
G26	HBD1-659	43.2	123.0	42	7.78	2.19	1.08
G27	HBD1-714.8	30.8	70.8	38	7.88	2.22	1.23
G28	HBD1-755	26.4	49.3	28	5.50	1.46	0.86
G29	HBD1-760	25.7	49.1		6.79	1.18	1.01
G30	HBD1-763.4	30.6	64.3	36	7.86	1.38	1.20
G31	HBD1-790.7	38.4	80.1	45	8.06	2.23	1.47
G32	HBD1-822	63.1	118.6	64	11.96	3.17	1.76
G33	HBD1-871	38.5	77.4		8.08	2.02	1.21
G34	HBD1-920.5	33.8	78.8	38	8.26	2.30	1.25
G35	HBD1-930	11.2	29.2	86	2.83	0.81	0.99
G36	HBD1-938.5	47.8	93.6		8.64	2.28	1.06

Irrad. Number	Sample Number	Yb	Lu
G11	HBD1-60.5	2.85	0.49
G12	HBD1-84	3.24	0.56
G13	HBD1-131	2.87	0.53
G14	HBD1-206.5	2.94	0.51
G15	HBD1-230	4.77	0.79
G16	HBD1-257	2.66	0.42
G17	HBD1-303.5	2.52	0.44
G18	HBD1-349	2.91	0.57
G19	HBD1-405.5	2.91	0.49
G20	HBD1-436.3	2.80	0.48
G21	HBD1-492.5	3.31	0.62
G22	HBD1-545.6	2.36	0.39
G23	HBD1-553	2.93	0.56
G24	HBD1-565.7	3.23	0.60
G25	HBD1-602.3	3.54	0.65
G26	HBD1-659	3.15	0.64
G27	HBD1-714.8	4.18	0.78
G28	HBD1-755	2.65	0.51
G29	HBD1-760	3.93	0.55
G30	HBD1-763.4	4.95	0.78
G31	HBD1-790.7	4.04	0.70
G32	HBD1-822	5.22	0.84
G33	HBD1-871	4.01	0.70
G34	HBD1-920.5	4.11	0.75
G35	HBD1-930	1.25	1.07
G36	HBD1-938.5	2.73	0.53

APPENDIX D

GEOCHEMICAL DATA FOR THE PORTLAND INTERNATIONAL AIRPORT DRILL HOLE (MTD1)

PORTLAND INTERNATIONAL AIRPORT DRILL HOLE (1523 FEET) -- IRRADIATION 94A

Samples collected from DOGAMI drill hole (MTD1) at the Portland International Airport.

* No Potassium concentrations were obtained for these samples.
* Concentrations in ppm except Na, K, and Fe

Irrad. Number	Sample Number	Na%	Rb	Cs	Sr	Ba	Fe%
A1	MTD1-30-40	3.15	34	1.75	531	400	3.75
A2	MTD1-50-55	3.44	26	1.08	501	344	3.26
A3	MTD1-105-110	2.64	49	1.82	389	597	2.90
A4	MTD1-155-165	2.64	69	2.20	464	662	2.69
A5	MTD1-225	2.67	58	1.74	412	604	2.29
A6	MTD1-295-300	1.68		2.75	334	642	3.59
A7	MTD1-350-358	2.56	66	2.31	376	527	4.72
A8	MTD1-402	0.18	48	2.33	423	338	8.46
A9	MTD1-411.8	0.91		2.60		423	7.17
A10	MTD1-466-473	1.90	53	1.69	260	452	3.25
A11	MTD1-575	1.17	72	4.76	277	605	4.76
A12	MTD1-692	2.27	34	0.66		325	6.05
A13	MTD1-725	1.53	26	0.84	308	248	7.46
A14	MTD1-744	2.46	28	1.44	408	337	5.50
A15	MTD1-782	2.02	43	1.59	331	536	2.87
A16	MTD1-839.5	1.55	89	4.30	224	713	4.88
A17	MTD1-864	2.11	54	3.37	276	508	5.44
A18	MTD1-900	1.22	89	5.18	150	643	4.15
A19	MTD1-958	0.81	111	6.37	155	644	4.50
A20	MTD1-1004	1.69	84	4.90	312	720	3.18
A21	MTD1-1124	0.83	108	7.29	311	641	4.34
A22	MTD1-1241	1.26	92	5.04		586	4.51
A23	MTD1-1311	1.00	84	6.12	247	616	4.53

Irrad. Number	Sample Number	Sc	Cr	Co	Zr	Hf	Ta
A1	MTD1-30-40	10.3	39	16	270	3.61	0.64
A2	MTD1-50-55	9.9	29	14	182	3.72	0.65
A3	MTD1-105-110	9.4	46	12	165	3.44	0.62
A4	MTD1-155-165	9.2	35	11		3.03	0.59
A5	MTD1-225	8.2	32	9	106	2.70	0.62
A6	MTD1-295-300	11.7	51	14	181	3.67	0.79
A7	MTD1-350-358	15.3	45	23	158	5.06	0.78
A8	MTD1-402	26.3	198	22	280	3.42	0.56
A9	MTD1-411.8	20.0	114	40	203	2.30	0.35
A10	MTD1-466-473	10.7	77	16	165	2.29	0.49
A11	MTD1-575	16.7	67	17	198	4.76	1.01
A12	MTD1-692	21.2	127	32	187	2.80	0.47
A13	MTD1-725	15.4	113	28	239	1.72	0.29
A14	MTD1-744	20.3	128	23	168	2.44	0.39
A15	MTD1-782	9.6	83	13	102	2.34	0.44
A16	MTD1-839.5	12.6	69	14	229	5.89	1.08
A17	MTD1-864	17.4	78	24	181	4.49	0.74
A18	MTD1-900	14.4	74	18	237	4.31	1.01
A19	MTD1-958	15.6	77	15	395	4.47	1.03
A20	MTD1-1004	9.9	41	9	245	4.27	1.17
A21	MTD1-1124	15.4	74	16	217	4.21	1.04
A22	MTD1-1241	15.6	63	18	181	4.37	1.02
A23	MTD1-1311	15.4	71	17	223	4.56	1.09

Irrad. Number	Sample Number	Th	U	Zn	As	Sb	La
A1	MTD1-30-40	4.1	1.7	61	93.6	0.4	20.3
A2	MTD1-50-55	3.3	1.1	60	9.1	20.3	
A3	MTD1-105-110	5.3	1.4	50	7.7	0.9	24.1
A4	MTD1-155-165	4.3	1.8	63	5.8	0.7	17.9
A5	MTD1-225	3.6	1.8	45	2.4	0.4	18.7
A6	MTD1-295-300	6.2	2.1	56	4.2	1.4	25.5
A7	MTD1-350-358	7.5	2.0	93	10.9	1.9	26.0
A8	MTD1-402	4.6	23.5	111	12.3	13.0	
A9	MTD1-411.8	1.8	21.6	83	3.6	313.0	9.7
A10	MTD1-466-473	3.5	2.3	111	1.9	4.1	13.6
A11	MTD1-575	10.1	3.9	81	14.2	2.1	33.1
A12	MTD1-692	2.5	2.3	98	4.5	2.3	13.1
A13	MTD1-725	1.1	21.5	70			7.1
A14	MTD1-744	1.6	13.0	92	2.8	267.1	10.6
A15	MTD1-782	4.2	1.3	101	3.5	0.5	15.6
A16	MTD1-839.5	10.4	3.4	78		1.1	39.1
A17	MTD1-864	6.6	2.4	98	17.3	11.9	26.1
A18	MTD1-900	11.1	3.8	91	6.9	2.4	37.7
A19	MTD1-958	12.7	3.9	91	9.0	1.6	38.7
A20	MTD1-1004	11.4	4.3	71	4.6	2.9	36.9
A21	MTD1-1124	12.9	4.7	98	10.3	9.0	38.3
A22	MTD1-1241	10.5	2.9	92	7.7	1.4	34.6
A23	MTD1-1311	11.8	3.3	107	8.4	10.5	37.9

Irrad. Number	Sample Number	Ce	Nd	Sm	Eu	Tb	Yb
A1	MTD1-30-40	39.4	16	3.73	1.10	0.51	1.44
A2	MTD1-50-55	35.3	19	3.77	1.05	0.48	1.42
A3	MTD1-105-110	38.2		3.91	0.91	0.54	1.76
A4	MTD1-155-165	34.5		3.36	0.95	0.51	1.53
A5	MTD1-225	30.8	13	3.22	0.83	0.42	1.40
A6	MTD1-295-300	44.0	20	4.38	1.15	0.64	1.85
A7	MTD1-350-358	49.0	23	5.04	1.22	0.79	2.59
A8	MTD1-402	26.6		3.15	1.07	0.68	2.06
A9	MTD1-411.8	23.3		2.89	1.13	0.58	1.96
A10	MTD1-466-473	25.5	14	2.39	0.81	0.45	1.29
A11	MTD1-575	62.1	25	5.72	1.33	0.86	2.46
A12	MTD1-692	25.1	27	3.45	1.14	0.60	1.95
A13	MTD1-725	10.9		2.23	0.81	0.43	1.27
A14	MTD1-744	20.4	28	3.27	1.16	0.58	1.82
A15	MTD1-782	27.2		3.00	0.80	0.43	1.45
A16	MTD1-839.5	71.6	30	6.55	1.45	1.01	2.98
A17	MTD1-864	50.9	22	5.09	1.27	0.76	2.38
A18	MTD1-900	65.7	28	6.47	1.31	0.88	2.76
A19	MTD1-958	76.5	34	6.70	1.37	1.05	2.91
A20	MTD1-1004	74.6	29	6.35	1.26	0.95	3.06
A21	MTD1-1124	76.0	35	6.74	1.47	1.03	3.01
A22	MTD1-1241	63.7	27	6.15	1.33	0.90	2.78
A23	MTD1-1311	74.4	33	6.43	1.43	0.98	2.74

Irrad. Number	Sample Number	Lu
A1	MTD1-30-40	0.21
A2	MTD1-50-55	0.21
A3	MTD1-105-110	0.24
A4	MTD1-155-165	0.23
A5	MTD1-225	0.20
A6	MTD1-295-300	0.27
A7	MTD1-350-358	0.38
A8	MTD1-402	0.31
A9	MTD1-411.8	0.26
A10	MTD1-466-473	0.17
A11	MTD1-575	0.35
A12	MTD1-692	0.31
A13	MTD1-725	0.21
A14	MTD1-744	0.25
A15	MTD1-782	0.19
A16	MTD1-839.5	0.46
A17	MTD1-864	0.35
A18	MTD1-900	0.40
A19	MTD1-958	0.41
A20	MTD1-1004	0.36
A21	MTD1-1124	0.43
A22	MTD1-1241	0.41
A23	MTD1-1311	0.44

APPENDIX E

GEOCHEMICAL DATA FOR STANDARDS USED IN IRRADIATIONS 93D, 93E, 93G, AND 94A

STANDARDS USED IN IRRADIATIONS 93D, 93E, 93G, AND 94A

BRC1 -- Columbia River basalt (Grande Ronde)
CFA -- Coal Fly Ash (1633a)
MAG-1 -- Marine Mud
* Concentrations in ppm except Na, K, and Fe

Irrad. Number	Sample Number	Na%	K%	Rb	Cs	Sr	Ba
D38	BCR1	2.37	1.31	44	1.10	326	625
E38	BCR1	2.42	1.73	73	1.93	387	744
G37	BCR1	2.42		45	1.45	543	632
A39	BCR1	2.98	1.57	59	1.83	401	654
E39	CFA(1633a)	0.17	1.80				
G39	CFA(1633a)	0.17	1.88	122	9.91	875	1272
A38	CFA(1633a)	0.20	1.88	131	10.42	830	1320
A13T	CFA(1633a)	0.20		134	10.00	933	1333
D39	MAG-1	2.80	2.84		6.49	172	465
G38	MAG-1	2.79	3.58	128	7.58		511
A37	MAG-1	2.77	2.48	125	7.46	138	436

Irrad. Number	Sample Number	Fe%	Sc	Cr	Co	Zr	Hf
D38	BCR1	9.04	30.0	10	35	168	4.25
E38	BCR1	9.79	32.4	8	39	236	4.87
G37	BCR1	9.34	24.2	12	35	123	4.83
A39	BCR1	10.36	34.7	15	40	158	5.15
E39	CFA(1633a)	9.84	38.6	223	45		6.88
G39	CFA(1633a)	9.30	33.1	208	43	226	7.27
A38	CFA(1633a)	9.41	38.6	196	44	240	7.29
A13T	CFA(1633a)	9.11	37.9	192	43	338	7.09
D39	MAG-1	4.41	14.7	95	20	105	3.44
G38	MAG-1	4.59	13.5	10	20	132	3.61
A37	MAG-1	4.26	15.0	86	19	193	3.20

Irrad. Number	Sample Number	Ta	Th	U	Zn	As	Sb
D38	BCR1	0.56	5.5		146		
E38	BCR1	2.25	6.4	2.0	158	2.4	2.0
G37	BCR1	3.44	5.8	1.8	129	2.6	
A39	BCR1	0.78	6.4	1.4	166	2.2	
E39	CFA(1633a)		24.2	10.6	146		
G39	CFA(1633a)	3.46	24.7	10.2	211	145.0	6.0
A38	CFA(1633a)	1.93	24.7	10.2	220	145.0	6.8
A13T	CFA(1633a)	1.79	24.4	9.9	221	138.9	6.8
D39	MAG-1	0.95	10.8		102	13.4	1.1
G38	MAG-1	1.58	11.4	2.8	102	10.6	0.7
A37	MAG-1	1.07	10.4	1.9	108	9.2	1.3

Irrad. Number	Sample Number	La	Ce	Nd	Sm	Eu	Tb
D38	BCR1	23.4	48.2	26	5.60	1.79	0.90
E38	BCR1	26.3	55.5	32	6.62	2.09	1.03
G37	BCR1	24.9	50.3	27	6.21	1.88	0.96
A39	BCR1	27.0	57.2	33	6.94	2.12	1.15
E39	CFA(1633a)	79.5			16.91		
G39	CFA(1633a)	79.1	166.7	71	16.83	3.53	2.53
A38	CFA(1633a)	79.1	168.3	76	16.83	3.58	2.53
A13T	CFA(1633a)	77.2	166.6	77	16.51	3.42	2.60
D39	MAG-1	40.2	76.5	32	6.75	1.35	0.87
G38	MAG-1	41.0	80.6	35	7.07	1.38	0.94
A37	MAG-1	37.0	75.4	34	6.32	1.34	0.93

Irrad. Number	Sample Number	Yb	Lu
D38	BCR1	2.83	0.45
E38	BCR1	3.18	0.56
G37	BCR1	2.97	0.51
A39	BCR1	3.68	0.53
E39	CFA(1633a)	7.92	0.92
G39	CFA(1633a)	7.13	1.13
A38	CFA(1633a)	7.50	1.08
A13T	CFA(1633a)	7.24	1.05
D39	MAG-1	2.40	0.35
G38	MAG-1	2.53	0.41
A37	MAG-1	2.45	0.34

APPENDIX F

STATISTICAL DATA FOR GEOCHEMICAL GROUPS

Comparison of Boring Lava Flows
on the West Side of the Tualatin Mountains

Barnes Road (BR) vs. Sylvan Hill (SH)

** F TESTS **

Label		N	Mean	Std Dev	Var	F	C-Value	Ho:V1=V2 H1:V1<>V2 Ho OR H1?
Na%	BR	21	2.96	0.25	0.06	1.7905	2.39	cannot
	SH	15	2.85	0.19	0.03			reject Ho
Cs	BR	21	2.74	2.79	7.81	3.6140	2.20	reject Ho
	SH	15	3.57	5.31	28.22			
Ba	BR	21	446	120.01	14403.10	1.2084	2.20	cannot
	SH	15	493	131.93	17404.41			reject Ho
Fe%	BR	21	6.18	0.40	0.16	1.9036	2.39	cannot
	SH	15	6.51	0.29	0.08			reject Ho
Sc	BR	21	17.9	1.46	2.14	2.1478	2.39	cannot
	SH	15	18.1	1.00	1.00			reject Ho
Cr	BR	21	190	28.74	825.93	3.9102	2.20	reject Ho
	SH	15	276	56.83	3229.52			
Co	BR	21	30	2.47	6.12	1.5835	2.20	cannot
	SH	15	37	3.11	9.69			reject Ho
Hf	BR	21	3.73	0.33	0.11	1.1203	2.20	cannot
	SH	15	3.89	0.35	0.12			reject Ho
Th	BR	21	1.8	0.42	0.18	2.5834	2.20	reject Ho
	SH	15	3.4	0.67	0.46			
La	BR	21	19.3	1.51	2.29	21.430	2.20	reject Ho
	SH	15	26.6	7.00	49.00			
Ce	BR	21	41.5	3.28	10.76	1.4550	2.20	cannot
	SH	15	60.5	3.96	15.65			reject Ho
Sm	BR	21	5.09	0.37	0.14	2.1945	2.20	cannot
	SH	15	6.07	0.55	0.30			reject Ho
Eu	BR	21	1.71	0.15	0.023	1.1624	2.39	cannot
	SH	15	1.91	0.14	0.019			reject Ho
Tb	BR	21	0.64	0.07	0.01	3.2874	2.20	reject Ho
	SH	15	0.72	0.13	0.02			

Comparison of Boring Lava Flows
on the West Side of the Tualatin Mountains

Barnes Road (BR) vs. Cornell Mountain (CM)

** F TESTS **

Label		N	Mean	Std Dev	Var	F	C-Value	Ho:V1=V2 H1:V1<>V2 Ho OR H1?
Na%	BR	21	2.96	0.25	0.06	1.2699	2.20	cannot
	CM	15	2.93	0.28	0.08			reject Ho
Cs	BR	21	2.74	2.79	7.81	1.3117	2.20	cannot
	CM	15	3.39	3.20	10.24			reject Ho
Ba	BR	21	446	120.01	14403.10	1.7379	2.39	cannot
	CM	15	413	91.04	8287.86			reject Ho
Fe%	BR	21	6.18	0.40	0.156	1.0232	2.20	cannot
	CM	15	6.43	0.40	0.160			reject Ho
Sc	BR	21	17.9	1.46	2.14	1.6612	2.20	cannot
	CM	15	21.9	1.89	3.56			reject Ho
Cr	BR	21	190	28.74	825.93	1.5533	2.39	cannot
	CM	15	200	23.06	531.71			reject Ho
Co	BR	21	30	2.47	6.12	1.7498	2.39	cannot
	CM	15	35	1.87	3.50			reject Ho
Hf	BR	21	3.73	0.33	0.11	1.1240	2.39	cannot
	CM	15	3.47	0.31	0.10			reject Ho
Th	BR	21	1.8	0.42	0.18	1.3185	2.20	cannot
	CM	15	1.7	0.48	0.23			reject Ho
La	BR	21	19.3	1.51	2.29	4.092	2.20	reject Ho
	CM	15	17.8	3.06	9.36			
Ce	BR	21	41.5	3.28	10.76	1.6467	2.39	cannot
	CM	15	35.3	2.56	6.53			reject Ho
Sm	BR	21	5.09	0.37	0.14	3.3904	2.20	reject Ho
	CM	15	4.65	0.68	0.46			
Eu	BR	21	1.71	0.15	0.02	1.2554	2.20	cannot
	CM	15	1.59	0.17	0.03			reject Ho
Tb	BR	21	0.64	0.07	0.005	1.6610	2.20	cannot
	CM	15	0.67	0.09	0.009			reject Ho

Comparison of Boring Lava Flows
on the West Side of the Tualatin Mountains

Sylvan Hill (SH) vs. Cornell Mountain (CM)

** F TESTS **

Label		N	Mean	Std Dev	Var	F	C-Value	Ho:V1=V2 H1:V1<>V2 Ho OR H1?
Na%	SH	15	2.85	0.19	0.03	2.2738	2.46	cannot
	CM	15	2.93	0.28	0.08			reject Ho
Cs	SH	15	3.57	5.31	28.22	2.7553	2.46	reject Ho
	CM	15	3.39	3.20	10.24			
Ba	SH	15	493	131.93	17404.41	2.1000	2.46	cannot
	CM	15	413	91.04	8287.86			reject Ho
Fe%	SH	15	6.51	0.29	0.082	1.9478	2.46	cannot
	CM	15	6.43	0.40	0.160			reject Ho
Sc	SH	15	18.1	1.00	1.00	3.5679	2.46	reject Ho
	CM	15	21.9	1.89	3.56			
Cr	SH	15	276	56.83	3229.52	6.0738	2.46	reject Ho
	CM	15	200	23.06	531.71			
Co	SH	15	37	3.11	9.69	2.7707	2.46	reject Ho
	CM	15	35	1.87	3.50			
Hf	SH	15	3.89	0.35	0.12	1.2592	2.46	cannot
	CM	15	3.47	0.31	0.10			reject Ho
Th	SH	15	3.4	0.67	0.46	1.9593	2.46	cannot
	CM	15	1.7	0.48	0.23			reject Ho
La	SH	15	26.6	7.00	49.00	5.2370	2.46	reject Ho
	CM	15	17.8	3.06	9.36			
Ce	SH	15	60.5	3.96	15.65	2.3959	2.46	cannot
	CM	15	35.3	2.56	6.53			reject Ho
Sm	SH	15	6.07	0.55	0.30	1.5449	2.46	cannot
	CM	15	4.65	0.68	0.46			reject Ho
Eu	SH	15	1.91	0.14	0.02	1.4593	2.46	cannot
	CM	15	1.59	0.17	0.03			reject Ho
Tb	SH	15	0.72	0.13	0.018	1.9792	2.46	cannot
	CM	15	0.67	0.09	0.009			reject Ho

Comparison of Columbia River Source Sediments (CRSS)
and
Lower Troutdale Formation (LTFM)

** F TESTS **

Label		N	Mean	Std Dev	Var	F	C-Value	Ho:V1=V2 H1:V1<>V2 Ho OR H1?
Na%	CRSS	30	1.41	0.48	0.23	1.3898	2.22	cannot
	LTFM	10	1.42	0.57	0.32			reject Ho
Cs	CRSS	30	3.28	1.06	1.13	1.8584	2.22	cannot
	LTFM	10	4.96	1.45	2.10			reject Ho
Ba	CRSS	30	594	103.13	10636.03	2.2359	2.90	cannot
	LTFM	10	620	68.97	4756.96			reject Ho
Fe%	CRSS	30	6.21	1.09	1.18	3.5018	2.90	reject Ho
	LTFM	10	4.50	0.58	0.34			
Sc	CRSS	30	14.5	3.07	9.41	2.0507	2.90	cannot
	LTFM	10	14.8	2.14	4.59			reject Ho
Cr	CRSS	30	82	29.59	875.77	5.2325	2.90	reject Ho
	LTFM	10	66	12.94	167.37			
Co	CRSS	30	16	5.55	30.76	1.6862	2.90	cannot
	LTFM	10	17	4.27	18.24			reject Ho
Hf	CRSS	30	7.04	1.48	2.18	8.4768	2.90	reject Ho
	LTFM	10	4.64	0.51	0.26			
Th	CRSS	30	9.2	1.90	3.59	1.1512	2.22	cannot
	LTFM	10	10.5	2.03	4.13			reject Ho
La	CRSS	30	35.2	8.18	66.85	2.6822	2.90	cannot
	LTFM	10	34.8	4.99	24.92			reject Ho
Ce	CRSS	30	67.0	14.43	208.23	2.0331	2.90	cannot
	LTFM	10	66.5	10.12	102.42			reject Ho
Sm	CRSS	30	5.88	1.22	1.49	3.7506	2.90	reject Ho
	LTFM	10	6.12	0.63	0.40			
Eu	CRSS	30	1.37	0.25	0.060	8.3745	2.90	reject Ho
	LTFM	10	1.35	0.08	0.007			
Tb	CRSS	30	0.84	0.13	0.02	1.6659	2.90	cannot
	LTFM	10	0.92	0.10	0.01			reject Ho

Comparison of Columbia River Source Sediments (CRSS)
and
Portland Hills Silt (PHS)

** F TESTS **

Label		N	Mean	Std Dev	Var	F	C-Value	Ho:V1=V2 H1:V1<>V2 Ho OR H1?
Na%	CRSS	30	1.41	0.48	0.23	2.3784	8.64	cannot
	PHS	4	1.39	0.31	0.10			reject Ho
Cs	CRSS	30	3.28	1.06	1.13	8.3052	8.64	cannot
	PHS	4	3.25	0.37	0.14			reject Ho
Ba	CRSS	30	594	103.13	10636.03	4.0175	8.64	cannot
	PHS	4	603	51.45	2647.46			reject Ho
Fe%	CRSS	30	6.21	1.09	1.18	5.4912	8.64	cannot
	PHS	4	4.26	0.46	0.21			reject Ho
Sc	CRSS	30	14.5	3.07	9.41	3.5435	8.64	cannot
	PHS	4	15.2	1.63	2.66			reject Ho
Cr	CRSS	30	82	29.59	875.77	5.9593	8.64	cannot
	PHS	4	75	12.12	146.96			reject Ho
Co	CRSS	30	16	5.55	30.76	4.5294	8.64	cannot
	PHS	4	13	2.61	6.79			reject Ho
Hf	CRSS	30	7.04	1.48	2.18	1.2411	8.64	cannot
	PHS	4	8.43	1.33	1.76			reject Ho
Th	CRSS	30	9.2	1.90	3.59	2.9120	8.64	cannot
	PHS	4	11.5	1.11	1.23			reject Ho
La	CRSS	30	35.2	8.18	66.85	1.8834	8.64	cannot
	PHS	4	39.9	5.96	35.49			reject Ho
Ce	CRSS	30	67.0	14.43	208.23	3.6796	8.64	cannot
	PHS	4	79.3	7.52	56.59			reject Ho
Sm	CRSS	30	5.88	1.22	1.49	1.9407	8.64	cannot
	PHS	4	6.65	0.88	0.77			reject Ho
Eu	CRSS	30	1.37	0.25	0.060	1.8565	8.64	cannot
	PHS	4	1.49	0.18	0.032			reject Ho
Tb	CRSS	30	0.84	0.13	0.017	1.3500	2.92	cannot
	PHS	4	0.94	0.15	0.022			reject Ho

Comparison of Columbia River Source Sediments (CRSS)
and
Portland Hills Silt (PHS)

** T TESTS **

Label		N	Mean	Std Dev	Sp	Se	T	C-Value	Ho:X1=X2 H1:X1<>X2 Ho OR H1?
Na%	CRSS	30	1.41	0.48				+/-	cannot
	PHS	4	1.39	0.31	0.47	0.25	0.06	2.042	reject Ho
Cs	CRSS	30	3.28	1.06				+/-	cannot
	PHS	4	3.25	0.37	1.02	0.54	0.06	2.042	reject Ho
Ba	CRSS	30	594	103.13				+/-	cannot
	PHS	4	603	51.45	99.43	52.93	-0.16	2.042	reject Ho
Fe%	CRSS	30	4.23	1.09				+/-	cannot
	PHS	4	4.26	0.46	1.04	0.56	-0.05	2.042	reject Ho
Sc	CRSS	30	14.5	3.07				+/-	cannot
	PHS	4	15.2	1.63	2.96	1.58	-0.42	2.042	reject Ho
Cr	CRSS	30	82	29.59				+/-	cannot
	PHS	4	75	12.12	28.42	15.13	0.42	2.042	reject Ho
Co	CRSS	30	16	5.55				+/-	cannot
	PHS	4	13	2.61	5.34	2.84	1.15	2.042	reject Ho
Hf	CRSS	30	7.04	1.48				+/-	cannot
	PHS	4	8.43	1.33	1.46	0.78	-1.79	2.042	reject Ho
Th	CRSS	30	9.2	1.90				+/-	
	PHS	4	11.5	1.11	1.84	0.98	-2.26	2.042	reject Ho
La	CRSS	30	35.2	8.18				+/-	cannot
	PHS	4	39.9	5.96	7.99	4.26	-1.12	2.042	reject Ho
Ce	CRSS	30	67.0	14.43				+/-	cannot
	PHS	4	79.3	7.52	13.93	7.41	-1.66	2.042	reject Ho
Sm	CRSS	30	5.88	1.22				+/-	cannot
	PHS	4	6.65	0.88	1.19	0.64	-1.20	2.042	reject Ho
Eu	CRSS	30	1.37	0.25				+/-	cannot
	PHS	4	1.49	0.18	0.24	0.13	-0.96	2.042	reject Ho
Tb	CRSS	30	0.84	0.13				+/-	cannot
	PHS	4	0.94	0.15	0.13	0.07	-1.41	2.042	reject Ho

Comparison of Columbia River Source Sediments (CRSS)
and
Columbia River Basalt Group Sediments (CRBS)

** F TESTS **

Label		N	Mean	Std Dev	Var	F	C-Value	Ho:V1=V2 H1:V1<>V2 Ho OR H1?
Na%	CRSS	30	1.41	0.48	0.23	18.011	3.32	reject Ho
	CRBS	3	1.50	2.04	4.16			
Cs	CRSS	30	3.28	1.06	1.13	2.1372	3.32	cannot
	CRBS	3	2.09	1.55	2.41			reject Ho
Ba	CRSS	30	594	103.13	10636.03	6.1419	19.45	cannot
	CRBS	3	574	41.61	1731.72			reject Ho
Fe%	CRSS	30	6.21	1.09	1.18	1.1253	19.45	cannot
	CRBS	3	11.0	1.02	1.05			reject Ho
Sc	CRSS	30	14.5	3.07	9.41	8.7987	3.32	reject Ho
	CRBS	3	46.0	9.10	82.83			
Cr	CRSS	30	82	29.59	875.77	1.7515	19.45	cannot
	CRBS	3	50	22.36	500.00			reject Ho
Co	CRSS	30	16	5.55	30.76	4.8739	19.45	cannot
	CRBS	3	32	2.51	6.31			reject Ho
Hf	CRSS	30	7.04	1.48	2.18	1.5027	3.32	cannot
	CRBS	3	7.61	1.81	3.27			reject Ho
Th	CRSS	30	9.2	1.90	3.59	3.7976	3.32	reject Ho
	CRBS	3	8.0	3.69	13.64			
La	CRSS	30	35.2	8.18	66.85	1.3103	19.45	cannot
	CRBS	3	43.4	7.14	51.02			reject Ho
Ce	CRSS	30	67.0	14.43	208.23	20.038	3.32	reject Ho
	CRBS	3	90.9	64.60	4172.58			
Sm	CRSS	30	5.88	1.22	1.49	4.4815	3.32	reject Ho
	CRBS	3	10.7	2.59	6.68			
Eu	CRSS	30	1.37	0.25	0.060	8.6465	3.32	reject Ho
	CRBS	3	3.05	0.72	0.522			
Tb	CRSS	30	0.84	0.13	0.02	2.2791	3.32	cannot
	CRBS	3	1.62	0.19	0.04			reject Ho

Comparison of Columbia River Source Sediments (CRSS)
and
Reed Island Ashes (RIA)

** F TESTS **

Label		N	Mean	Std Dev	Var	F	C-Value	Ho:V1=V2 H1:V1<>V2 Ho OR H1?
Na%	CRSS	30	1.41	0.48	0.23	1.2700	249.05	cannot
	RIA	2	3.07	0.43	0.18			reject Ho
Cs	CRSS	30	3.28	1.06	1.13	1.7440	249.05	cannot
	RIA	2	1.59	0.80	0.65			reject Ho
Ba	CRSS	30	594	103.13	10636.03	2.6976	249.05	cannot
	RIA	2	489	62.79	3942.72			reject Ho
Fe%	CRSS	30	6.21	1.09	1.18	23.633	249.05	cannot
	RIA	2	2.41	0.22	0.05			reject Ho
Sc	CRSS	30	14.5	3.07	9.41	16.250	249.05	cannot
	RIA	2	8.5	0.76	0.58			reject Ho
Cr	CRSS	30	82	29.59	875.77	616.18	249.05	reject Ho
	RIA	2	23	1.19	1.42			
Co	CRSS	30	16	5.55	30.76	60.193	249.05	cannot
	RIA	2	10	0.71	0.51			reject Ho
Hf	CRSS	30	7.04	1.48	2.18	20.607	249.05	cannot
	RIA	2	4.13	0.33	0.11			reject Ho
Th	CRSS	30	9.2	1.90	3.59	7.1099	249.05	cannot
	RIA	2	4.3	0.71	0.51			reject Ho
La	CRSS	30	35.2	8.18	66.85	40.275	249.05	cannot
	RIA	2	22.3	1.29	1.66			reject Ho
Ce	CRSS	30	67.0	14.43	208.23	4.5340	249.05	cannot
	RIA	2	40.2	6.78	45.93			reject Ho
Sm	CRSS	30	5.88	1.22	1.49	6.8156	249.05	cannot
	RIA	2	3.96	0.47	0.22			reject Ho
Eu	CRSS	30	1.37	0.25	0.0603	131.42	249.05	cannot
	RIA	2	1.05	0.02	0.0005			reject Ho
Tb	CRSS	30	0.84	0.13	0.02	2.6203	249.05	cannot
	RIA	2	0.52	0.08	0.01			reject Ho

Comparison of Columbia River Source Sediments (CRSS)
and
Reed Island Ashes (RIA)

** T TESTS **

Label		N	Mean	Std Dev	Sp	Se	T	C-Value	Ho:X1=X2 H1:X1<>X2 Ho OR H1?
Na%	CRSS	30	1.41	0.48				+/-	
	RIA	2	3.07	0.43	0.48	0.35	-4.77	2.042	reject Ho
Cs	CRSS	30	3.28	1.06				+/-	
	RIA	2	1.59	0.80	1.05	0.77	2.19	2.042	reject Ho
Ba	CRSS	30	594	103.13				+/-	cannot
	RIA	2	489	62.79	102.04	74.52	1.42	2.042	reject Ho
Fe%	CRSS	30	6.21	1.09				+/-	
	RIA	2	2.41	0.22	1.07	0.78	4.86	2.042	reject Ho
Sc	CRSS	30	14.5	3.07				+/-	
	RIA	2	8.5	0.76	3.02	2.21	2.72	2.042	reject Ho
Cr	CRSS	30	82	29.59				+/-	
	RIA	2	23	1.19	29.10	21.25	2.78	2.042	reject Ho
Co	CRSS	30	16	5.55				+/-	cannot
	RIA	2	10	0.71	5.45	3.98	1.67	2.042	reject Ho
Hf	CRSS	30	7.04	1.48				+/-	
	RIA	2	4.13	0.33	1.45	1.06	2.74	2.042	reject Ho
Th	CRSS	30	9.2	1.90				+/-	
	RIA	2	4.3	0.71	1.87	1.36	3.59	2.042	reject Ho
La	CRSS	30	35.2	8.18				+/-	
	RIA	2	22.3	1.29	8.04	5.87	2.20	2.042	reject Ho
Ce	CRSS	30	67.0	14.43				+/-	
	RIA	2	40.2	6.78	14.24	10.40	2.58	2.042	reject Ho
Sm	CRSS	30	5.88	1.22				+/-	
	RIA	2	3.96	0.47	1.20	0.88	2.19	2.042	reject Ho
Eu	CRSS	30	1.37	0.25				+/-	cannot
	RIA	2	1.05	0.02	0.24	0.18	1.79	2.042	reject Ho
Tb	CRSS	30	0.84	0.13				+/-	
	RIA	2	0.52	0.08	0.13	0.09	3.41	2.042	reject Ho

Comparison of Columbia River Source Sediments (CRSS)
and
Young Columbia River Sediments (YCRS)

** F TESTS **

Label		N	Mean	Std Dev	Var	F	C-Value	Ho:V1=V2 H1:V1<>V2 Ho OR H1?
Na%	CRSS	30	1.41	0.48	0.23	1.7786	2.35	cannot
	YCRS	8	2.51	0.64	0.41			reject Ho
Cs	CRSS	30	3.28	1.06	1.13	4.7045	3.41	reject Ho
	YCRS	8	1.95	0.49	0.24			
Ba	CRSS	30	594	103.13	10636.03	1.6096	2.35	cannot
	YCRS	8	575	130.84	17119.87			reject Ho
Fe%	CRSS	30	6.21	1.09	1.18	4.5483	3.41	reject Ho
	YCRS	8	3.17	0.51	0.26			
Sc	CRSS	30	14.5	3.07	9.41	4.7937	3.41	reject Ho
	YCRS	8	10.2	1.40	1.96			
Cr	CRSS	30	82	29.59	875.77	15.055	3.41	reject Ho
	YCRS	8	40	7.63	58.17			
Co	CRSS	30	16	5.55	30.76	4.3969	3.41	reject Ho
	YCRS	8	13	2.65	7.00			
Hf	CRSS	30	7.04	1.48	2.18	10.081	3.41	reject Ho
	YCRS	8	3.48	0.46	0.22			
Th	CRSS	30	9.2	1.90	3.59	1.9432	3.41	cannot
	YCRS	8	4.9	1.36	1.85			reject Ho
La	CRSS	30	35.2	8.18	66.85	5.4746	3.41	reject Ho
	YCRS	8	22.0	3.49	12.21			
Ce	CRSS	30	67.0	14.43	208.23	4.8953	3.41	reject Ho
	YCRS	8	39.1	6.52	42.54			
Sm	CRSS	30	5.88	1.22	1.49	8.0682	3.41	reject Ho
	YCRS	8	3.83	0.43	0.18			
Eu	CRSS	30	1.37	0.25	0.06	3.9434	3.41	reject Ho
	YCRS	8	1.03	0.12	0.02			
Tb	CRSS	30	0.84	0.13	0.02	2.9842	3.41	cannot
	YCRS	8	0.54	0.07	0.01			reject Ho

Comparison of Columbia River Source Sediments (CRSS)
and
High-Alumina Basalt Sediments (HABS)

** F TESTS **

Label		N	Mean	Std Dev	Var	F	C-Value	Ho:V1=V2 H1:V1<>V2 Ho OR H1?
Na%	CRSS	30	1.41	0.48	0.23	5.0309	19.45	cannot
	HABS	3	2.42	0.21	0.05			reject Ho
Cs	CRSS	30	3.28	1.06	1.13	8.0245	19.45	cannot
	HABS	3	2.03	0.37	0.14			reject Ho
Ba	CRSS	30	594	103.13	10636.03	9.5650	19.45	cannot
	HABS	3	598	33.35	1111.98			reject Ho
Fe%	CRSS	30	6.21	1.09	1.18	2.0543	19.45	cannot
	HABS	3	5.34	0.76	0.57			reject Ho
Sc	CRSS	30	14.5	3.07	9.41	14.998	19.45	cannot
	HABS	3	18.1	0.79	0.63			reject Ho
Cr	CRSS	30	82	29.59	875.77	3.7712	19.45	cannot
	HABS	3	55	15.24	232.23			reject Ho
Co	CRSS	30	16	5.55	30.76	1.4967	19.45	cannot
	HABS	3	23	4.53	20.55			reject Ho
Hf	CRSS	30	7.04	1.48	2.18	8.5560	19.45	cannot
	HABS	3	3.89	0.50	0.25			reject Ho
Th	CRSS	30	9.2	1.90	3.59	9.5771	19.45	cannot
	HABS	3	4.5	0.61	0.37			reject Ho
La	CRSS	30	35.2	8.18	66.85	5.9004	19.45	cannot
	HABS	3	22.4	3.37	11.33			reject Ho
Ce	CRSS	30	67.0	14.43	208.23	3.6216	19.45	cannot
	HABS	3	44.0	7.58	57.50			reject Ho
Sm	CRSS	30	5.88	1.22	1.49	3.1878	19.45	cannot
	HABS	3	5.01	0.68	0.47			reject Ho
Eu	CRSS	30	1.37	0.25	0.060	1.0225	19.45	cannot
	HABS	3	1.50	0.24	0.059			reject Ho
Tb	CRSS	30	0.84	0.13	0.02	2.8640	19.45	cannot
	HABS	3	0.76	0.08	0.01			reject Ho

Comparison of Columbia River Source Sediments (CRSS) and High-Alumina Basalt Sediments (HABS)

** T TESTS **

Label		N	Mean	Std Dev	Sp	Se	T	C-Value	Ho:X1=X2 H1:X1<>X2 Ho OR H1?
Na%	CRSS	30	1.41	0.48				+/-	
	HABS	3	2.42	0.21	0.47	0.28	-3.57	2.042	reject Ho
Cs	CRSS	30	3.28	1.06				+/-	cannot
	HABS	3	2.03	0.37	1.03	0.62	1.99	2.042	reject Ho
Ba	CRSS	30	594	103.13				+/-	cannot
	HABS	3	598	33.35	100.11	60.62	-0.06	2.042	reject Ho
Fe%	CRSS	30	6.21	1.09				+/-	cannot
	HABS	3	5.34	0.76	1.07	0.65	1.34	2.042	reject Ho
Sc	CRSS	30	14.5	3.07				+/-	cannot
	HABS	3	18.1	0.79	2.97	1.80	-1.98	2.042	reject Ho
Cr	CRSS	30	82	29.59				+/-	cannot
	HABS	3	55	15.24	28.88	17.49	1.58	2.042	reject Ho
Co	CRSS	30	16	5.55				+/-	
	HABS	3	23	4.53	5.49	3.32	-2.14	2.042	reject Ho
Hf	CRSS	30	7.04	1.48				+/-	
	HABS	3	3.89	0.50	1.43	0.87	3.62	2.042	reject Ho
Th	CRSS	30	9.2	1.90				+/-	
	HABS	3	4.5	0.61	1.84	1.11	4.22	2.042	reject Ho
La	CRSS	30	35.2	8.18				+/-	
	HABS	3	22.4	3.37	7.95	4.82	2.64	2.042	reject Ho
Ce	CRSS	30	67.0	14.43				+/-	
	HABS	3	44.0	7.58	14.09	8.53	2.67	2.042	reject Ho
Sm	CRSS	30	5.88	1.22				+/-	cannot
	HABS	3	5.01	0.68	1.19	0.72	1.21	2.042	reject Ho
Eu	CRSS	30	1.37	0.25				+/-	cannot
	HABS	3	1.50	0.24	0.25	0.15	-0.90	2.042	reject Ho
Tb	CRSS	30	0.84	0.13				+/-	cannot
	HABS	3	0.76	0.08	0.13	0.08	1.09	2.042	reject Ho

Comparison of Columbia River Source Sediments (CRSS)
and
Episodic Cascadian Volcanic Sediments (ECVS)

** F TESTS **

Label		N	Mean	Std Dev	Var	F	C-Value	Ho:V1=V2 H1:V1<>V2 Ho OR H1?
Na%	CRSS	30	1.41	0.48	0.23	2.8408	2.43	reject Ho
	ECVS	7	1.61	0.81	0.66			
Cs	CRSS	30	3.28	1.06	1.13	2.2461	3.84	cannot reject Ho
	ECVS	7	1.59	0.71	0.50			
Ba	CRSS	30	594	103.13	10636.03	1.1477	3.84	cannot reject Ho
	ECVS	7	380	96.27	9267.60			
Fe%	CRSS	30	6.21	1.09	1.18	3.8009	2.43	reject Ho
	ECVS	7	5.82	2.12	4.48			
Sc	CRSS	30	14.5	3.07	9.41	3.8790	2.43	reject Ho
	ECVS	7	17.6	6.04	36.52			
Cr	CRSS	30	82	29.59	875.77	1.8052	2.43	cannot reject Ho
	ECVS	7	120	39.76	1580.94			
Co	CRSS	30	16	5.55	30.76	2.7843	2.43	reject Ho
	ECVS	7	25	9.25	85.65			
Hf	CRSS	30	7.04	1.48	2.18	7.9531	3.84	reject Ho
	ECVS	7	2.47	0.52	0.27			
Th	CRSS	30	9.2	1.90	3.59	1.9635	3.84	cannot reject Ho
	ECVS	7	2.8	1.35	1.83			
La	CRSS	30	35.2	8.18	66.85	8.2025	3.84	reject Ho
	ECVS	7	11.8	2.85	8.15			
Ce	CRSS	30	67.0	14.43	208.23	6.4226	3.84	reject Ho
	ECVS	7	22.7	5.69	32.42			
Sm	CRSS	30	5.88	1.22	1.49	7.3160	3.84	reject Ho
	ECVS	7	2.91	0.45	0.20			
Eu	CRSS	30	1.37	0.25	0.060	2.0450	3.84	cannot reject Ho
	ECVS	7	0.99	0.17	0.029			
Tb	CRSS	30	0.84	0.13	0.02	1.7013	3.84	cannot reject Ho
	ECVS	7	0.53	0.10	0.01			

Comparison of Columbia River Basalt Group Sediments (CRBS)
and
Reed Island Ashes (RIA)

** F TESTS **

Label		N	Mean	Std Dev	Var	F	C-Value	Ho:V1=V2 H1:V1<>V2 Ho OR H1?
Na%	CRBS	3	1.50	2.04	4.16	22.875	199.50	cannot reject Ho
	RIA	2	3.07	0.43	0.18			
Cs	CRBS	3	2.09	1.55	2.41	3.7274	199.50	cannot reject Ho
	RIA	2	1.59	0.80	0.65			
Ba	CRBS	3	574	41.61	1731.72	2.2768	18.51	cannot reject Ho
	RIA	2	489	62.79	3942.72			
Fe%	CRBS	3	11.0	1.02	1.05	21.002	199.50	cannot reject Ho
	RIA	2	2.41	0.22	0.05			
Sc	CRBS	3	46.0	9.10	82.83	142.98	199.50	cannot reject Ho
	RIA	2	8.5	0.76	0.58			
Cr	CRBS	3	50	22.36	500.00	351.79	199.50	reject Ho
	RIA	2	23	1.19	1.42			
Co	CRBS	3	32	2.51	6.31	12.350	199.50	cannot reject Ho
	RIA	2	10	0.71	0.51			
Hf	CRBS	3	7.61	1.81	3.27	30.966	199.50	cannot reject Ho
	RIA	2	4.13	0.33	0.11			
Th	CRBS	3	8.0	3.69	13.64	27.000	199.50	cannot reject Ho
	RIA	2	4.3	0.71	0.51			
La	CRBS	3	43.4	7.14	51.02	30.736	199.50	cannot reject Ho
	RIA	2	22.3	1.29	1.66			
Ce	CRBS	3	90.9	64.60	4172.58	90.853	199.50	cannot reject Ho
	RIA	2	40.2	6.78	45.93			
Sm	CRBS	3	10.7	2.59	6.68	30.544	199.50	cannot reject Ho
	RIA	2	3.96	0.47	0.22			
Eu	CRBS	3	3.05	0.72	0.52	1136.3	199.50	reject Ho
	RIA	2	1.05	0.02	0.0005			
Tb	CRBS	3	1.62	0.19	0.04	5.9719	199.50	cannot reject Ho
	RIA	2	0.52	0.08	0.01			

Comparison of Columbia River Basalt Group Sediments (CRBS)
and
Reed Island Ashes (RIA)

** T TESTS **

Label		N	Mean	Std Dev	Sp	Se	T	C-Value	Ho:X1=X2 H1:X1<>X2 Ho OR H1?
Na%	CRBS	3	1.50	2.04				+/-	cannot
	RIA	2	3.07	0.43	1.68	1.54	-1.03	3.182	reject Ho
Cs	CRBS	3	2.09	1.55				+/-	cannot
	RIA	2	1.59	0.80	1.35	1.23	0.41	3.182	reject Ho
Ba	CRBS	3	574	41.61				+/-	cannot
	RIA	2	489	62.79	49.69	45.36	1.88	3.182	reject Ho
Fe%	CRBS	3	11.0	1.02				+/-	
	RIA	2	2.41	0.22	0.85	0.77	11.1	3.182	reject Ho
Sc	CRBS	3	46.0	9.10				+/-	
	RIA	2	8.5	0.76	7.44	6.80	5.52	3.182	reject Ho
Cr	CRBS	3	50	22.36				+/-	cannot
	RIA	2	23	1.19	18.27	16.68	1.67	3.182	reject Ho
Co	CRBS	3	32	2.51				+/-	
	RIA	2	10	0.71	2.09	1.91	11.5	3.182	reject Ho
Hf	CRBS	3	7.61	1.81				+/-	cannot
	RIA	2	4.13	0.33	1.49	1.36	2.56	3.182	reject Ho
Th	CRBS	3	8.0	3.69				+/-	cannot
	RIA	2	4.3	0.71	3.04	2.78	1.33	3.182	reject Ho
La	CRBS	3	43.4	7.14				+/-	
	RIA	2	22.3	1.29	5.88	5.37	3.94	3.182	reject Ho
Ce	CRBS	3	90.9	64.60				+/-	cannot
	RIA	2	40.2	6.78	52.89	48.28	1.05	3.182	reject Ho
Sm	CRBS	3	10.7	2.59				+/-	
	RIA	2	3.96	0.47	2.13	1.94	3.45	3.182	reject Ho
Eu	CRBS	3	3.05	0.72				+/-	
	RIA	2	1.05	0.02	0.59	0.54	3.71	3.182	reject Ho
Tb	CRBS	3	1.62	0.19				+/-	
	RIA	2	0.52	0.08	0.17	0.15	7.26	3.182	reject Ho

Comparison of Columbia River Basalt Group Sediments (CRBS)
and
Young Columbia River Sediments (YCRS)

** F TESTS **

Label		N	Mean	Std Dev	Var	F	C-Value	Ho:V1=V2 H1:V1<>V2 Ho OR H1?
Na%	CRBS	3	1.50	2.04	4.16	10.126	4.74	reject Ho
	YCRS	8	2.51	0.64	0.41			
Cs	CRBS	3	2.09	1.55	2.41	10.055	4.74	reject Ho
	YCRS	8	1.95	0.49	0.24			
Ba	CRBS	3	574	41.61	1731.72	9.8861	19.35	reject Ho
	YCRS	8	575	130.84	17119.87			
Fe%	CRBS	3	11.0	1.02	1.05	4.0420	4.74	cannot reject Ho
	YCRS	8	3.17	0.51	0.26			
Sc	CRBS	3	46.0	9.10	82.83	42.179	4.74	reject Ho
	YCRS	8	10.2	1.40	1.96			
Cr	CRBS	3	50	22.36	500.00	8.5951	4.74	reject Ho
	YCRS	8	40	7.63	58.17			
Co	CRBS	3	32	2.51	6.31	1.1085	19.35	cannot reject Ho
	YCRS	8	13	2.65	7.00			
Hf	CRBS	3	7.61	1.81	3.27	15.149	4.74	reject Ho
	YCRS	8	3.48	0.46	0.22			
Th	CRBS	3	8.0	3.69	13.64	7.3794	4.74	reject Ho
	YCRS	8	4.9	1.36	1.85			
La	CRBS	3	43.4	7.14	51.02	4.1780	4.74	cannot reject Ho
	YCRS	8	22.0	3.49	12.21			
Ce	CRBS	3	90.9	64.60	4172.58	98.092	4.74	reject Ho
	YCRS	8	39.1	6.52	42.54			
Sm	CRBS	3	10.7	2.59	6.68	36.158	4.74	reject Ho
	YCRS	8	3.83	0.43	0.18			
Eu	CRBS	3	3.05	0.72	0.52	34.097	4.74	reject Ho
	YCRS	8	1.03	0.12	0.02			
Tb	CRBS	3	1.62	0.19	0.04	6.8013	4.74	reject Ho
	YCRS	8	0.54	0.07	0.01			

Comparison of Columbia River Basalt Group Sediments (CRBS)
and
High-Alumina Basalt Sediments (HABS)

** F TESTS **

Label		N	Mean	Std Dev	Var	F	C-Value	Ho:V1=V2 H1:V1<>V2 Ho OR H1?
Na%	CRBS	3	1.50	2.04	4.16	90.614	19.00	reject Ho
	HABS	3	2.42	0.21	0.05			
Cs	CRBS	3	2.09	1.55	2.41	17.150	19.00	cannot reject Ho
	HABS	3	2.03	0.37	0.14			
Ba	CRBS	3	574	41.61	1731.72	1.5573	19.00	cannot reject Ho
	HABS	3	598	33.35	1111.98			
Fe%	CRBS	3	11.0	1.02	1.05	1.8256	19.00	cannot reject Ho
	HABS	3	5.34	0.76	0.57			
Sc	CRBS	3	46.0	9.10	82.83	131.96	19.00	reject Ho
	HABS	3	18.1	0.79	0.63			
Cr	CRBS	3	50	22.36	500.00	2.1531	19.00	cannot reject Ho
	HABS	3	55	15.24	232.23			
Co	CRBS	3	32	2.51	6.31	3.2565	19.00	cannot reject Ho
	HABS	3	23	4.53	20.55			
Hf	CRBS	3	7.61	1.81	3.27	12.857	19.00	cannot reject Ho
	HABS	3	3.89	0.50	0.25			
Th	CRBS	3	8.0	3.69	13.64	36.370	19.00	reject Ho
	HABS	3	4.5	0.61	0.37			
La	CRBS	3	43.4	7.14	51.02	4.5030	19.00	cannot reject Ho
	HABS	3	22.4	3.37	11.33			
Ce	CRBS	3	90.9	64.60	4172.58	72.570	19.00	reject Ho
	HABS	3	44.0	7.58	57.50			
Sm	CRBS	3	10.7	2.59	6.68	14.286	19.00	cannot reject Ho
	HABS	3	5.01	0.68	0.47			
Eu	CRBS	3	3.05	0.72	0.52	8.8410	19.00	cannot reject Ho
	HABS	3	1.50	0.24	0.06			
Tb	CRBS	3	1.62	0.19	0.04	6.5273	19.00	cannot reject Ho
	HABS	3	0.76	0.08	0.01			

Comparison of Columbia River Basalt Group Sediments (CRBS)
and
Episodic Cascadian Volcanic Sediments (ECVS)

** F TESTS **

Label		N	Mean	Std Dev	Var	F	C-Value	Ho:V1=V2 H1:V1<>V2 Ho OR H1?
Na%	CRBS	3	1.50	2.04	4.16	6.3402	5.14	reject Ho
	ECVS	7	1.61	0.81	0.66			
Cs	CRBS	3	2.09	1.55	2.41	4.8004	5.14	cannot reject Ho
	ECVS	7	1.59	0.71	0.50			
Ba	CRBS	3	574	41.61	1731.72	5.3517	19.33	cannot reject Ho
	ECVS	7	380	96.27	9267.60			
Fe%	CRBS	3	11.0	1.02	1.05	4.2770	19.33	cannot reject Ho
	ECVS	7	5.82	2.12	4.48			
Sc	CRBS	3	46.0	9.10	82.83	2.2683	5.14	cannot reject Ho
	ECVS	7	17.6	6.04	36.52			
Cr	CRBS	3	50	22.36	500.00	3.1619	19.33	cannot reject Ho
	ECVS	7	120	39.76	1580.94			
Co	CRBS	3	32	2.51	6.31	13.571	19.33	cannot reject Ho
	ECVS	7	25	9.25	85.65			
Hf	CRBS	3	7.61	1.81	3.27	11.951	5.14	reject Ho
	ECVS	7	2.47	0.52	0.27			
Th	CRBS	3	8.0	3.69	13.64	7.4564	5.14	reject Ho
	ECVS	7	2.8	1.35	1.83			
La	CRBS	3	43.4	7.14	51.02	6.2598	5.14	reject Ho
	ECVS	7	11.8	2.85	8.15			
Ce	CRBS	3	90.9	64.60	4172.58	128.70	5.14	reject Ho
	ECVS	7	22.7	5.69	32.42			
Sm	CRBS	3	10.7	2.59	6.68	32.787	5.14	reject Ho
	ECVS	7	2.91	0.45	0.20			
Eu	CRBS	3	3.05	0.72	0.52	17.682	5.14	reject Ho
	ECVS	7	0.99	0.17	0.03			
Tb	CRBS	3	1.62	0.19	0.04	3.8774	5.14	cannot reject Ho
	ECVS	7	0.53	0.10	0.01			

Comparison of Reed Island Ashes (RIA)
and
Young Columbia River Sediments (YCRS)

** F TESTS **

Label		N	Mean	Std Dev	Var	F	C-Value	Ho:V1=V2 H1:V1<>V2 Ho OR H1?
Na%	RIA	2	3.07	0.43	0.18	2.2589	236.77	cannot
	YCRS	8	2.51	0.64	0.41			reject Ho
Cs	RIA	2	1.59	0.80	0.65	2.6975	5.59	cannot
	YCRS	8	1.95	0.49	0.24			reject Ho
Ba	RIA	2	489	62.79	3942.72	4.3421	236.77	cannot
	YCRS	8	575	130.84	17119.87			reject Ho
Fe%	RIA	2	2.41	0.22	0.05	5.1960	236.77	cannot
	YCRS	8	3.17	0.51	0.26			reject Ho
Sc	RIA	2	8.5	0.76	0.58	3.3899	236.77	cannot
	YCRS	8	10.2	1.40	1.96			reject Ho
Cr	RIA	2	23	1.19	1.42	40.929	236.77	cannot
	YCRS	8	40	7.63	58.17			reject Ho
Co	RIA	2	10	0.71	0.51	13.690	236.77	cannot
	YCRS	8	13	2.65	7.00			reject Ho
Hf	RIA	2	4.13	0.33	0.11	2.0441	236.77	cannot
	YCRS	8	3.48	0.46	0.22			reject Ho
Th	RIA	2	4.3	0.71	0.51	3.6589	236.77	cannot
	YCRS	8	4.9	1.36	1.85			reject Ho
La	RIA	2	22.3	1.29	1.66	7.3567	236.77	cannot
	YCRS	8	22.0	3.49	12.21			reject Ho
Ce	RIA	2	40.2	6.78	45.93	1.0797	5.59	cannot
	YCRS	8	39.1	6.52	42.54			reject Ho
Sm	RIA	2	3.96	0.47	0.22	1.1838	5.59	cannot
	YCRS	8	3.83	0.43	0.18			reject Ho
Eu	RIA	2	1.05	0.02	0.0005	33.326	236.77	cannot
	YCRS	8	1.03	0.12	0.0153			reject Ho
Tb	RIA	2	0.52	0.08	0.0063	1.1389	5.59	cannot
	YCRS	8	0.54	0.07	0.0056			reject Ho

Comparison of Reed Island Ashes (RIA)
and
Young Columbia River Sediments (YCRS)

** T TESTS **

Label		N	Mean	Std Dev	Sp	Se	T	C-Value	Ho:X1=X2 H1:X1<>X2 Ho OR H1?
Na%	RIA	2	3.07	0.43				+/-	can't
	YCRS	8	2.51	0.64	0.62	0.49	1.16	2.306	reject Ho
Cs	RIA	2	1.59	0.80				+/-	can't
	YCRS	8	1.95	0.49	0.54	0.43	-0.84	2.306	reject Ho
Ba	RIA	2	489	62.79				+/-	can't
	YCRS	8	575	130.84	124.39	98.34	-0.88	2.306	reject Ho
Fe%	RIA	2	2.41	0.22				+/-	can't
	YCRS	8	3.17	0.51	0.48	0.38	-1.99	2.306	reject Ho
Sc	RIA	2	8.5	0.76				+/-	can't
	YCRS	8	10.2	1.40	1.34	1.06	-1.64	2.306	reject Ho
Cr	RIA	2	23	1.19				+/-	
	YCRS	8	40	7.63	7.15	5.65	-3.12	2.306	reject Ho
Co	RIA	2	10	0.71				+/-	can't
	YCRS	8	13	2.65	2.49	1.97	-1.78	2.306	reject Ho
Hf	RIA	2	4.13	0.33				+/-	can't
	YCRS	8	3.48	0.46	0.45	0.36	1.83	2.306	reject Ho
Th	RIA	2	4.3	0.71				+/-	can't
	YCRS	8	4.9	1.36	1.30	1.02	-0.50	2.306	reject Ho
La	RIA	2	22.3	1.29				+/-	can't
	YCRS	8	22.0	3.49	3.30	2.61	0.11	2.306	reject Ho
Ce	RIA	2	40.2	6.78				+/-	can't
	YCRS	8	39.1	6.52	6.55	5.18	0.21	2.306	reject Ho
Sm	RIA	2	3.96	0.47				+/-	
	YCRS	8	3.83	0.43	0.43	0.34	0.37	2.306	reject Ho
Eu	RIA	2	1.05	0.02				+/-	can't
	YCRS	8	1.03	0.12	0.12	0.09	0.30	2.306	reject Ho
Tb	RIA	2	0.52	0.08				+/-	can't
	YCRS	8	0.54	0.07	0.08	0.06	-0.22	2.306	reject Ho

Comparison of Reed Island Ashes (RIA)
and
High-Alumina Basalt Sediments (HABS)

** F TESTS **

Label		N	Mean	Std Dev	Var	F	C-Value	Ho:V1=V2 H1:V1<>V2 Ho OR H1?
Na%	RIA	2	3.07	0.43	0.18	3.9613	18.51	cannot
	HABS	3	2.42	0.21	0.05			reject Ho
Cs	RIA	2	1.59	0.80	0.65	4.6011	18.51	cannot
	HABS	3	2.03	0.37	0.14			reject Ho
Ba	RIA	2	489	62.79	3942.72	3.5457	18.51	cannot
	HABS	3	598	33.35	1111.98			reject Ho
Fe%	RIA	2	2.41	0.22	0.05	11.504	199.50	cannot
	HABS	3	5.34	0.76	0.57			reject Ho
Sc	RIA	2	8.5	0.76	0.58	1.0835	199.50	cannot
	HABS	3	18.1	0.79	0.63			reject Ho
Cr	RIA	2	23	1.19	1.42	163.39	199.50	cannot
	HABS	3	55	15.24	232.23			reject Ho
Co	RIA	2	10	0.71	0.51	40.218	199.50	cannot
	HABS	3	23	4.53	20.55			reject Ho
Hf	RIA	2	4.13	0.33	0.11	2.4084	199.50	cannot
	HABS	3	3.89	0.50	0.25			reject Ho
Th	RIA	2	4.3	0.71	0.51	1.3470	18.51	cannot
	HABS	3	4.5	0.61	0.37			reject Ho
La	RIA	2	22.3	1.29	1.66	6.8257	199.50	cannot
	HABS	3	22.4	3.37	11.33			reject Ho
Ce	RIA	2	40.2	6.78	45.93	1.2519	199.50	cannot
	HABS	3	44.0	7.58	57.50			reject Ho
Sm	RIA	2	3.96	0.47	0.22	2.1380	199.50	cannot
	HABS	3	5.01	0.68	0.47			reject Ho
Eu	RIA	2	1.05	0.02	0.0005	128.53	199.50	cannot
	HABS	3	1.50	0.24	0.0590			reject Ho
Tb	RIA	2	0.52	0.08	0.0063	1.0930	18.51	cannot
	HABS	3	0.76	0.08	0.0058			reject Ho

Comparison of Reed Island Ashes (RIA)
and
High-Alumina Basalt Sediments (HABS)

** T TESTS **

Label		N	Mean	Std Dev	Sp	Se	T	C-Value	Ho:X1=X2 H1:X1<>X2 Ho OR H1?
Na%	RIA	2	3.07	0.43				+/-	can't
	HABS	3	2.42	0.21	0.30	0.28	2.38	3.182	reject Ho
Cs	RIA	2	1.59	0.80				+/-	can't
	HABS	3	2.03	0.37	0.56	0.51	-0.87	3.182	reject Ho
Ba	RIA	2	489	62.79				+/-	can't
	HABS	3	598	33.35	45.34	41.39	-2.64	3.182	reject Ho
Fe%	RIA	2	2.41	0.22				+/-	
	HABS	3	5.34	0.76	0.63	0.58	-5.07	3.182	reject Ho
Sc	RIA	2	8.5	0.76				+/-	
	HABS	3	18.1	0.79	0.78	0.71	-13.4	3.182	reject Ho
Cr	RIA	2	23	1.19				+/-	can't
	HABS	3	55	15.24	12.46	11.38	-2.89	3.182	reject Ho
Co	RIA	2	10	0.71				+/-	
	HABS	3	23	4.53	3.72	3.40	-4.05	3.182	reject Ho
Hf	RIA	2	4.13	0.33				+/-	can't
	HABS	3	3.89	0.50	0.45	0.41	0.56	3.182	reject Ho
Th	RIA	2	4.3	0.71				+/-	can't
	HABS	3	4.5	0.61	0.65	0.59	-0.34	3.182	reject Ho
La	RIA	2	22.3	1.29				+/-	can't
	HABS	3	22.4	3.37	2.85	2.60	-0.06	3.182	reject Ho
Ce	RIA	2	40.2	6.78				+/-	can't
	HABS	3	44.0	7.58	7.32	6.69	-0.57	3.182	reject Ho
Sm	RIA	2	3.96	0.47				+/-	can't
	HABS	3	5.01	0.68	0.62	0.57	-1.86	3.182	reject Ho
Eu	RIA	2	1.05	0.02				+/-	can't
	HABS	3	1.50	0.24	0.20	0.18	-2.48	3.182	reject Ho
Tb	RIA	2	0.52	0.08				+/-	
	HABS	3	0.76	0.08	0.08	0.07	-3.32	3.182	reject Ho

Comparison of Reed Island Ashes (RIA)
and
Episodic Cascadian Volcanic Sediments (ECVS)

** F TESTS **

Label		N	Mean	Std Dev	Var	F	C-Value	Ho:V1=V2 H1:V1<>V2 Ho OR H1?
Na%	RIA	2	3.07	0.43	0.18	3.6079	233.99	cannot
	ECVS	7	1.61	0.81	0.66			reject Ho
Cs	RIA	2	1.59	0.80	0.65	1.2879	8.81	cannot
	ECVS	7	1.59	0.71	0.50			reject Ho
Ba	RIA	2	489	62.79	3942.72	2.3506	233.99	cannot
	ECVS	7	380	96.27	9267.60			reject Ho
Fe%	RIA	2	2.41	0.22	0.05	89.826	233.99	cannot
	ECVS	7	5.82	2.12	4.48			reject Ho
Sc	RIA	2	8.5	0.76	0.58	63.035	233.99	cannot
	ECVS	7	17.6	6.04	36.52			reject Ho
Cr	RIA	2	23	1.19	1.42	1112.3	233.99	reject Ho
	ECVS	7	120	39.76	1580.94			
Co	RIA	2	10	0.71	0.51	167.60	233.99	cannot
	ECVS	7	25	9.25	85.65			reject Ho
Hf	RIA	2	4.13	0.33	0.11	2.5910	233.99	cannot
	ECVS	7	2.47	0.52	0.27			reject Ho
Th	RIA	2	4.3	0.71	0.51	3.6211	233.99	cannot
	ECVS	7	2.8	1.35	1.83			reject Ho
La	RIA	2	22.3	1.29	1.66	4.9101	233.99	cannot
	ECVS	7	11.8	2.85	8.15			reject Ho
Ce	RIA	2	40.2	6.78	45.93	1.4165	8.81	cannot
	ECVS	7	22.7	5.69	32.42			reject Ho
Sm	RIA	2	3.96	0.47	0.22	1.0734	8.81	cannot
	ECVS	7	2.91	0.45	0.20			reject Ho
Eu	RIA	2	1.05	0.02	0.0005	64.262	233.99	cannot
	ECVS	7	0.99	0.17	0.0295			reject Ho
Tb	RIA	2	0.52	0.08	0.006	1.5402	233.99	cannot
	ECVS	7	0.53	0.10	0.010			reject Ho

Comparison of Reed Island Ashes (RIA)
and
Episodic Cascadian Volcanic Sediments (ECVS)

** T TESTS **

Label		N	Mean	Std Dev	Sp	Se	T	C-Value	Ho:X1=X2 H1:X1<>X2 Ho OR H1?
Na%	RIA	2	3.07	0.43				+/-	
	ECVS	7	1.61	0.81	0.77	0.61	2.38	2.365	reject Ho
Cs	RIA	2	1.59	0.80				+/-	can't
	ECVS	7	1.59	0.71	0.72	0.58	-0.0001	2.365	reject Ho
Ba	RIA	2	489	62.79				+/-	can't
	ECVS	7	380	96.27	92.23	73.95	1.47	2.365	reject Ho
Fe%	RIA	2	2.41	0.22				+/-	can't
	ECVS	7	5.82	2.12	1.96	1.57	-2.17	2.365	reject Ho
Sc	RIA	2	8.5	0.76				+/-	can't
	ECVS	7	17.6	6.04	5.60	4.49	-2.03	2.365	reject Ho
Cr	RIA	2	23	1.19				+/-	
	ECVS	7	120	39.76	36.81	29.52	-3.30	2.365	reject Ho
Co	RIA	2	10	0.71				+/-	can't
	ECVS	7	25	9.25	8.57	6.87	-2.21	2.365	reject Ho
Hf	RIA	2	4.13	0.33				+/-	
	ECVS	7	2.47	0.52	0.50	0.40	4.13	2.365	reject Ho
Th	RIA	2	4.3	0.71				+/-	can't
	ECVS	7	2.8	1.35	1.28	1.03	1.55	2.365	reject Ho
La	RIA	2	22.3	1.29				+/-	
	ECVS	7	11.8	2.85	2.69	2.15	4.85	2.365	reject Ho
Ce	RIA	2	40.2	6.78				+/-	
	ECVS	7	22.7	5.69	5.86	4.70	3.72	2.365	reject Ho
Sm	RIA	2	3.9	0.47				+/-	
	ECVS	7	2.91	0.45	0.45	0.36	2.87	2.365	reject Ho
Eu	RIA	2	1.05	0.02				+/-	can't
	ECVS	7	0.99	0.17	0.16	0.13	0.49	2.365	reject Ho
Tb	RIA	2	0.52	0.08				+/-	can't
	ECVS	7	0.53	0.10	0.10	0.08	-0.13	2.365	reject Ho

Comparison of Young Columbia River Sediments (YCRS)
and
High-Alumina Basalt Sediments (HABS)

** F TESTS **

Label		N	Mean	Std Dev	Var	F	C-Value	Ho:V1=V2 H1:V1<>V2 Ho OR H1?
Na%	YCRS	8	2.51	0.64	0.41	8.9480	19.35	cannot
	HABS	3	2.42	0.21	0.05			reject Ho
Cs	YCRS	8	1.95	0.49	0.24	1.7057	19.35	cannot
	HABS	3	2.03	0.37	0.14			reject Ho
Ba	YCRS	8	575	130.84	17119.87	15.396	19.35	cannot
	HABS	3	598	33.35	1111.98			reject Ho
Fe%	YCRS	8	3.17	0.51	0.26	2.2140	4.74	cannot
	HABS	3	5.34	0.76	0.57			reject Ho
Sc	YCRS	8	10.2	1.40	1.96	3.1286	19.35	cannot
	HABS	3	18.1	0.79	0.63			reject Ho
Cr	YCRS	8	40	7.63	58.17	3.9920	4.74	cannot
	HABS	3	55	15.24	232.23			reject Ho
Co	YCRS	8	13	2.65	7.00	2.9377	4.74	cannot
	HABS	3	23	4.53	20.55			reject Ho
Hf	YCRS	8	3.48	0.46	0.22	1.1783	4.74	cannot
	HABS	3	3.89	0.50	0.25			reject Ho
Th	YCRS	8	4.9	1.36	1.85	4.9286	19.35	cannot
	HABS	3	4.5	0.61	0.37			reject Ho
La	YCRS	8	22.0	3.49	12.21	1.0770	19.35	cannot
	HABS	3	22.4	3.37	11.33			reject Ho
Ce	YCRS	8	39.1	6.52	42.54	1.3517	4.74	cannot
	HABS	3	44.0	7.58	57.50			reject Ho
Sm	YCRS	8	3.83	0.43	0.18	2.5310	4.74	cannot
	HABS	3	5.01	0.68	0.47			reject Ho
Eu	YCRS	8	1.03	0.12	0.02	3.8567	4.74	cannot
	HABS	3	1.50	0.24	0.06			reject Ho
Tb	YCRS	8	0.54	0.07	0.0056	1.0420	4.74	cannot
	HABS	3	0.76	0.08	0.0058			reject Ho

Comparison of Young Columbia River Sediments (YCRS)
and
High-Alumina Basalt Sediments (HABS)

** T TESTS **

Label		N	Mean	Std Dev	Sp	Se	T	C-Value	Ho:X1=X2 H1:X1<>X2 Ho OR H1?
Na%	YCRS	8	2.51	0.64				+/-	can't
	HABS	3	2.42	0.21	0.57	0.39	0.23	2.262	reject Ho
Cs	YCRS	8	1.95	0.49				+/-	can't
	HABS	3	2.03	0.37	0.47	0.32	-0.27	2.262	reject Ho
Ba	YCRS	8	575	130.84				+/-	can't
	HABS	3	598	33.35	116.46	78.84	-0.29	2.262	reject Ho
Fe%	YCRS	8	3.17	0.51				+/-	
	HABS	3	5.34	0.76	0.57	0.39	-5.57	2.262	reject Ho
Sc	YCRS	8	10.2	1.40				+/-	
	HABS	3	18.1	0.79	1.29	0.87	-8.95	2.262	reject Ho
Cr	YCRS	8	40	7.63				+/-	
	HABS	3	55	15.24	9.84	6.66	-2.29	2.262	reject Ho
Co	YCRS	8	13	2.65				+/-	
	HABS	3	23	4.53	3.16	2.14	-4.79	2.262	reject Ho
Hf	YCRS	8	3.48	0.46				+/-	can't
	HABS	3	3.89	0.50	0.47	0.32	-1.30	2.262	reject Ho
Th	YCRS	8	4.9	1.36				+/-	can't
	HABS	3	4.5	0.61	1.23	0.83	0.37	2.262	reject Ho
La	YCRS	8	22.0	3.49				+/-	can't
	HABS	3	22.4	3.37	3.47	2.35	-0.19	2.262	reject Ho
Ce	YCRS	8	39.1	6.52				+/-	can't
	HABS	3	44.0	7.58	6.77	4.58	-1.06	2.262	reject Ho
Sm	YCRS	8	3.83	0.43				+/-	
	HABS	3	5.01	0.68	0.50	0.34	-3.50	2.262	reject Ho
Eu	YCRS	8	1.03	0.12				+/-	
	HABS	3	1.50	0.24	0.16	0.11	-4.46	2.262	reject Ho
Tb	YCRS	8	0.54	0.07				+/-	
	HABS	3	0.76	0.08	0.07	0.05	-4.36	2.262	reject Ho

Comparison of Young Columbia River Sediments (YCRS)
and
Episodic Cascadian Volcanic Sediments (ECVS)

** F TESTS **

Label		N	Mean	Std Dev	Var	F	C-Value	Ho:V1=V2 H1:V1<>V2 Ho OR H1?
Na%	YCRS	8	2.51	0.64	0.41	1.5972	3.87	cannot
	ECVS	7	1.61	0.81	0.66			reject Ho
Cs	YCRS	8	1.95	0.49	0.24	2.0945	3.87	cannot
	ECVS	7	1.59	0.71	0.50			reject Ho
Ba	YCRS	8	575	130.84	17119.87	1.8473	4.21	cannot
	ECVS	7	380	96.27	9267.60			reject Ho
Fe%	YCRS	8	3.17	0.51	0.26	17.288	3.87	reject Ho
	ECVS	7	5.82	2.12	4.48			
Sc	YCRS	8	10.2	1.40	1.96	18.595	3.87	reject Ho
	ECVS	7	17.6	6.04	36.52			
Cr	YCRS	8	40	7.63	58.17	27.177	3.87	reject Ho
	ECVS	7	120	39.76	1580.94			
Co	YCRS	8	13	2.65	7.00	12.242	3.87	reject Ho
	ECVS	7	25	9.25	85.65			
Hf	YCRS	8	3.48	0.46	0.22	1.2676	3.87	cannot
	ECVS	7	2.47	0.52	0.27			reject Ho
Th	YCRS	8	4.9	1.36	1.85	1.0104	4.21	cannot
	ECVS	7	2.8	1.35	1.83			reject Ho
La	YCRS	8	22.0	3.49	12.21	1.4983	4.21	cannot
	ECVS	7	11.8	2.85	8.15			reject Ho
Ce	YCRS	8	39.1	6.52	42.54	1.3120	4.21	cannot
	ECVS	7	22.7	5.69	32.42			reject Ho
Sm	YCRS	8	3.83	0.43	0.18	1.1028	3.87	cannot
	ECVS	7	2.91	0.45	0.20			reject Ho
Eu	YCRS	8	1.03	0.12	0.02	1.9283	3.87	cannot
	ECVS	7	0.99	0.17	0.03			reject Ho
Tb	YCRS	8	0.54	0.07	0.006	1.7541	3.87	cannot
	ECVS	7	0.53	0.10	0.010			reject Ho

Comparison of High-Alumina Basalt Sediments (HABS)
and
Episodic Cascadian Volcanic Sediments (ECVS)

** F TESTS **

Label		N	Mean	Std Dev	Var	F	C-Value	Ho:V1=V2 H1:V1<>V2 Ho OR H1?
Na%	HABS	3	2.42	0.21	0.05	14.29	19.33	cannot
	ECVS	7	1.61	0.81	0.66			reject Ho
Cs	HABS	3	2.03	0.37	0.14	3.57	19.33	cannot
	ECVS	7	1.59	0.71	0.50			reject Ho
Ba	HABS	3	598	33.35	1111.98	8.33	19.33	cannot
	ECVS	7	380	96.27	9267.60			reject Ho
Fe%	HABS	3	5.34	0.76	0.57	7.81	19.33	cannot
	ECVS	7	5.82	2.12	4.48			reject Ho
Sc	HABS	3	18.1	0.79	0.63	58.18	19.33	reject Ho
	ECVS	7	17.6	6.04	36.52			
Cr	HABS	3	55	15.24	232.23	6.81	19.33	cannot
	ECVS	7	120	39.76	1580.94			reject Ho
Co	HABS	3	23	4.53	20.55	4.17	19.33	cannot
	ECVS	7	25	9.25	85.65			reject Ho
Hf	HABS	3	3.89	0.50	0.25	1.08	19.33	cannot
	ECVS	7	2.47	0.52	0.27			reject Ho
Th	HABS	3	4.5	0.61	0.37	4.88	19.33	cannot
	ECVS	7	2.8	1.35	1.83			reject Ho
La	HABS	3	22.4	3.37	11.33	1.39	5.14	cannot
	ECVS	7	11.8	2.85	8.15			reject Ho
Ce	HABS	3	44.0	7.58	57.50	1.77	5.14	cannot
	ECVS	7	22.7	5.69	32.42			reject Ho
Sm	HABS	3	5.01	0.68	0.47	2.29	5.14	cannot
	ECVS	7	2.91	0.45	0.20			reject Ho
Eu	HABS	3	1.50	0.24	0.06	2.00	5.14	cannot
	ECVS	7	0.99	0.17	0.03			reject Ho
Tb	HABS	3	0.76	0.08	0.006	1.68	19.33	cannot
	ECVS	7	0.53	0.10	0.010			reject Ho

Comparison of High-Alumina Basalt Sediments (HABS)
and
Episodic Cascadian Volcanic Sediments (ECVS)

** T TESTS **

Label		N	Mean	Std Dev	Sp	Se	T	C-Value	Ho:X1=X2 H1:X1<>X2 Ho OR H1?
Na%	HABS	3	2.42	0.21				+/-	can't
	ECVS	7	1.61	0.81	0.71	0.49	1.65	2.306	reject Ho
Cs	HABS	3	2.03	0.37				+/-	can't
	ECVS	7	1.59	0.71	0.64	0.44	0.10	2.306	reject Ho
Ba	HABS	3	598	33.35				+/-	
	ECVS	7	380	96.27	85.02	58.67	3.72	2.306	reject Ho
Fe%	HABS	3	5.34	0.76				+/-	can't
	ECVS	7	5.82	2.12	1.87	1.29	-0.38	2.306	reject Ho
Sc	HABS	3	18.1	0.79				+/-	can't
	ECVS	7	17.6	6.04	5.25	3.62	0.12	2.306	reject Ho
Cr	HABS	3	55	15.24				+/-	
	ECVS	7	120	39.76	35.27	24.34	-2.66	2.306	reject Ho
Co	HABS	3	23	4.53				+/-	can't
	ECVS	7	25	9.25	8.33	5.75	-0.25	2.306	reject Ho
Hf	HABS	3	3.89	0.50				+/-	
	ECVS	7	2.47	0.52	0.52	0.36	3.97	2.306	reject Ho
Th	HABS	3	4.5	0.61				+/-	can't
	ECVS	7	2.8	1.35	1.21	0.84	2.14	2.306	reject Ho
La	HABS	3	22.4	3.37				+/-	
	ECVS	7	11.8	2.85	2.99	2.06	5.14	2.306	reject Ho
Ce	HABS	3	44.0	7.58				+/-	
	ECVS	7	22.7	5.69	6.22	4.29	4.96	2.306	reject Ho
Sm	HABS	3	5.01	0.68				+/-	
	ECVS	7	2.91	0.45	0.52	0.36	5.84	2.306	reject Ho
Eu	HABS	3	1.50	0.24				+/-	
	ECVS	7	0.99	0.17	0.19	0.13	3.87	2.306	reject Ho
Tb	HABS	3	0.76	0.08				+/-	
	ECVS	7	0.53	0.10	0.09	0.06	3.47	2.306	reject Ho